Study of Dosimetric Characteristics of a Flattening Filter Free Medical accelerator for its Clinical Use

By
Bibekananda Mishra

HLTH 09 2012 04 002

Tata Memorial Centre, Mumbai

A thesis submitted to the

Board of Studies in Health Sciences

In partial fulfillment of requirements

for the Degree of

DOCTOR OF PHILOSOPHY

of

HOMI BHABHA NATIONAL INSTITUTE

August, 2018

Homi Bhabha National Institute[1]

Recommendations of the Viva Voce Committee

As members of the Viva Voce Committee, we certify that we have read the dissertation prepared by Bibekananda Mishra entitled "Study of Dosimetric Characteristics of a Flattening Filter Free Medical accelerator for its Clinical Use" and recommend that it may be accepted as fulfilling the thesis requirement for the award of Degree of Doctor of Philosophy.

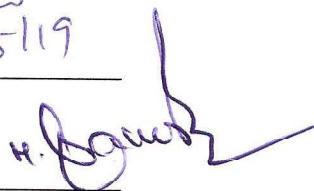Chairman - Dr. J. P. Agarwal   **Date:**
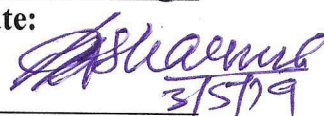
Guide / Convener -Dr. T. Palani Selvam   **Date:** 3/5/19

Examiner - Dr. K. M. Ganesh   **Date:**

Member 1- Dr. S. D. Sharma   **Date:** 3/5/19

Member 2- Dr. D. D. Deshpande   **Date:** 3/5/19

Final approval and acceptance of this thesis is contingent upon the candidate's submission of the final copies of the thesis to HBNI.

I/We hereby certify that I/we have read this thesis prepared under my/our direction and recommend that it may be accepted as fulfilling the thesis requirement.

Date: 3/5/19

Place: **Mumbai, India**

Dr. T. Palani Selvam

Guide

---

[1] This page is to be included only for final submission after successful completion of viva voce.

STATEMENT BY AUTHOR

This dissertation has been submitted in partial fulfillment of requirements for an advanced degree at Homi Bhabha National Institute (HBNI) and is deposited in the Library to be made available to borrowers under rules of the HBNI.

Brief quotations from this dissertation are allowable without special permission, provided that accurate acknowledgement of source is made. Requests for permission for extended quotation from or reproduction of this manuscript in whole or in part may be granted by the Competent Authority of HBNI when in his or her judgment the proposed use of the material is in the interests of scholarship. In all other instances, however, permission must be obtained from the author.

(Bibekananda Mishra)

DECLARATION

I, hereby declare that the investigation presented in the thesis has been carried out by me. The work is original and has not been submitted earlier as a whole or in part for a degree / diploma at this or any other Institution / University.

(Bibekananda Mishra)

CERTIFICATION ON ACADEMIC INTEGRITY

1. I Shri Bibekananda Mishra, HBNI Enrolment No. **HLTH09201204002** hereby undertake that, the Thesis titled "*Study of Dosimetric Characteristics of a Flattening Filter Free Medical accelerator for its Clinical Use*" is prepared by me and is the original work undertaken by me and free of any plagiarism. That the document has been duly checked through a plagiarism detection tool and the document is plagiarism free.

2. I am aware and undertake that if plagiarism is detected in my thesis at any stage in future, suitable penalty will be imposed as per the applicable guidelines of the Institute/UGC.

(Shri Bibekananda Mishra) 3·5·19
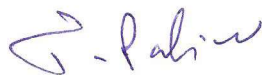
Signature of the Student

(with date)

Endorsed by the PhD Supervisor

(I certify that the work done by the Researcher is plagiarism free)

Signature:

Name: Dr. T. Palani Selvam

Designation: Assoc. Prof. HBNI;

Head, CRP&QAS

Department/Centre: RPAD, BARC

Name of the CI/OCC: TMC

List of Publications arising from the thesis

Journal

1. "Structural Shielding Design of a 6 MV Flattening Filter Free Linear Accelerator: Indian Scenario", **Bibekananda Mishra,** T. Palani Selvam and P. K. Dash Sharma,*J. Med. Phys*. **2017**, 42(1), 18-24.

2. "Comparison of measured and Monte Carlo-calculated dose distributions from indigenously developed 6 MV flattening filter free Medical Linear Accelerator", **Bibekananda Mishra,** Subhalaxmi Mishra, T. Palani Selvam, S. T. Chavan and S. N. Pethe, *J. Med. Phys*.**2018**, 43(3), 162-7.

Manuscript(s) Communicated

1. "Beam characteristics analysis of unflattened X-Rays from standard Medical Linear Accelerator: A comparison of protocols", **Bibekananda Mishra**, S. D. Sharma, A. Dinesh, T. Palani Selvam, A. Pichandi. *Int J Cancer Ther Oncol,* **2018**, (**Accepted**).

Conferences proceedings:

1. "Shielding consideration of Flattening Filter Free Medical Accelerators", **Bibekananda Mishra,** T. Palani Selvam and P.K. Dash Sharma International Conference on Medical Physics, Radiation Protection and Radiobiology (ICMPRPR2K15) 21st & 22nd Feb, **2015** SMS Medical College, Jaipur.

2. "Flattening Filter Free beam acceptance study of high energy X-Ray beam generated from Medical Linear Accelerator using AERB protocol", **Bibekananda Mishra,** 3rd National conference for Association of Medical Physicist of India-Western Chapter **2015** (AMPI-WC). 18th & 19th July, 2015, Shri H.N Reliance Foundation Hospital, Mumbai.

3. "Measurement and analysis of surface dose for flattening filter free medical accelerator using advanced markus chamber", **Bibekananda Mishra,** A. Pichandi, S. D. Sharma T. Palani Selvam, Proceedings of 39th Annual conference of the Association of Medical Physicists of India (AMPICON **2018**), November 2-4, 2018.

(Bibekananda Mishra)

DEDICATED TO

My grandfather Late Shri Nilamani Mishra

&

My grandmother Late Smt. Sulochana Mishra

ACKNOWLEDGEMENTS

necessary proprietary details of the accelerator unit for Monte Carlo simulation and his constant suggestions without which I could not have able to complete this work.

All the measurements carried out in this thesis were in close collaboration with different hospitals. I am extremely thankful to the management of Health Care Global, Enterprise Bangalore for accepting my request for technical collaboration and providing me the opportunity to work in different Medical Linear Accelerators of their facility. I am grateful to the entire medical physicist team of Health Care Global, Enterprise especially Dr. A. Pichandi, Chief Medical Physicist for their support in carrying out the measurements.

I am thankful to Shri Vaibhav Mahtre, Chief Medical Physicist Kokilaben Dhirubhai Ambani Hospital, Mumbai for his continuous support and help in measurements.

I am extremely thankful to Smt. Subhalaxmi Mishra, RP&AD, BARC for her continuous support and guidance on EGSnrc Monte Carlo Code used for this research work.

I would like to express my sincere thanks to all my colleagues of AERB especially Dr. P. Tondon, Dr. G. Sahani, Shri Amit Sen, Shri Neeraj Dixit, Shri G. K. Panda and Shri P.K. Dixit for their well wishes for completion of this research work.

I would like to thank my parents, in-laws, wife Smt. Subhalaxmi Mishra and daughters Miss Ritisha Mishra and Miss Rinisha Mishra for their long endurance and constant support. Without their help and encouragement I could never have completed this dissertation.

I would like to thank everybody who was important in the successful realization of this thesis, as well as apologize that I could not mention everyone personally. Last but not the least I thank the almighty for giving me strength to complete my thesis in time.

Bibekananda Mishra

CONTENTS

CHAPTER 4   Structural shielding design of Flattening Filter Free
Linear accelerator bunker: Indian Scenario

CHAPTER 6 Measurement and comparison of surface dose and leakage radiation for flattening filter free and flattened photon beams

CHAPTER 7 Summary, conclusion and future work

First page of Published Papers

ABSTRACT

Over the decades medical linear accelerator (Linac) are being used in Radiotherapy. The Linacs are capable of producing high energy photon and electron beams. The photon beams produced from the Linac are passed through a thick conical metallic component placed in the beam path in Linac head and is known as flattening filter (FF). Photon beams passed through the FF produce homogeneous distribution at any depth in a medium. Based on this property the radiotherapy dose delivery has been standardized and many protocols are in place for acceptance of the beam during commissioning and for further periodic checks. Due to significant advancement in technology and computer applications, Linacs operated without FF are in use. Removal the FF from the beam path has various advantages such as high dose rate, lower leakage radiation and less thickness required for the Linac bunker, etc. Introduction of this technology posed several challenges in beam dosimetry and acceptance. In view of this, dosimetric characteristics of Flattening Filter Free (FFF) Linac were investigated in this study.

An indigenously developed Linac was modeled using Monte Carlo methods and the feasibility of its use in FFF mode has been studied. Shielding adequacy of the Linac bunker was studied using the Monitoring Units (MU) delivered in the clinical cases and accordingly the workload used in the shielding was modified and found that the shielding thickness required in FFF mode is less. Several quality assurance parameters were investigated for FFF beam and a set of parameters were also suggested for acceptance of the beam. Relative surface dose (RSD) and absorbed dose due to leakage radiation (ADL) were also investigated.

SYNOPSIS

Standard medical linear accelerators (Linac) used in radiotherapy are equipped with a flattening filter (FF). FF is a dense metal made of high-Z materials (stainless steel, copper or tungsten), in the shape of a cone, which is placed in the path of beam to attenuate more of the high energy photons through the central axis resulting in a uniform planar fluence at a reference depth. The FF is designed to produce uniform dose distribution across the field in a homogeneous medium. The major disadvantages of FF are it acts as an attenuator, beam hardener and the scatterer. It decreases the dose rate, increases electron contamination, increases leakage radiation from the treatment head etc. Recently, there has been an increasing interest in operating medical Linac without FF. A flattening filter-free (FFF) Linac is basically a standard Linac with the FF removed from the beam line. The main advantages of removing the FF are increased dose rate in addition to reduced scatter and leakage radiation inside and outside the target volume. These benefits result from removal of attenuation of the primary beam and decrease in beam energy due to the presence of low energy components. Reduction of the head scatter improves dosimetry of the FFF beams due to reduction of output variation with field size and field size dependent parameters. However, reduced beam energy and physical absence of FF added several challenges in establishing acceptance criteria for dosimetric parameters for FFF beam.

Due to the above facts, there are differences in the beam characteristics of Linac operated in FFF mode to that of the Linac operated with the FF mode. FFF beams are not standard in terms of the parameters describing its field characteristics such as beam profiles, flatness, symmetry, penumbra, field size, off axis ratio, percentage depth dose, surface

dose, beam quality index etc. and shielding parameters, such as the tenth-value layers and scatter fractions etc. as calculated for flattened beams. Hence, it is not possible to use the above parameters in the same way as they are commonly used for the flattened beams.

The objective of the present study, undertaken for the thesis were

- Study of structural shielding design of Linac vault housing operated in FF and FFF mode.

- Analysis of beam characteristics and quality assurance parameters from commercially available FFF Linacs.

- Monte Carlo-based study of the indigenously developed Linac (Siddharth) in FFF mode.

  ➢ To calculate the dosimetric characteristics and benchmark the results with measured data.

  ➢ To calculate the optimum thickness & material of enhancer plate which is required to be kept in the place of flattening filter for the indigenous Linac.

- Measurement and comparison of surface doses for FFF and FF photon beams using various dosimeters for different commercially available Linac.

This thesis comprises of seven chapters arranged as follows:

Chapter 1: Introduction

This chapter introduces the basics of cancer biology, the causes of cancer and its subsequent treatment, focusing specifically on radiotherapy treatments. The concepts of medical linear accelerator, its operation and its major components are introduced. The role of flattening filter various characteristics of FFF photon beam such as dose rate,

output, depth dose profiles, lateral beam profiles, spectrum, scatter, leakage radiation and the consequences of removing it were briefly described. It also briefly compares the technical differences between the various commercially available Linacs operated in FFF mode. This chapter ends with literature review and aim of the thesis.

Radiotherapy can be delivered by external beam therapy and/or brachytherapy. External beam radiotherapy is used for most cancer patients requiring radiotherapy. The linear accelerator (Linac) which produces megavoltage X-rays and electrons are the most preferred device for external beam radiotherapy. Commercially available Linacs produce multi energy photon (about 4-18 MV) and electron (4 - 20 MeV) beams. Flattening filter (FF) is one of the components of Linac head that produces uniform dose distribution in the patient. For certain advanced beam therapy techniques, such as stereotactic radiosurgery/radiotherapy (SRS/SRT), intensity-modulated radiotherapy (IMRT) inhomogeneous dose distributions with varying fluence pattern across the beam are delivered. For this purpose a Linac with FF removed from its beamline is preferred due to increased dose rate capability. The removal of the FF results not only in an increase in dose rate but also softening of the X-ray spectra, reduction in head scattered radiation and generates the non-uniform beam profile. The reported dose rate of FFF beams is about 2 - 4 times higher than that of the flattened beams,

Chapter 2: Monte Carlo method and EGSnrc code system

In this chapter, an overview of fundamental principles of the Monte Carlo technique and its application to radiotherapy is briefly discussed. A short description about the transport of electron and photon using Monte Carlo method and various Monte Carlo codes available are outlined. Overview of the codes used in this study i.e. EGSnrc code system

4

and its user-codes such as BEAMnrc, DOSXYZnrc, DOSRZnrc and BEAMDP are described.

Chapter 3: Monte Carlo study of indigenously developed Linac in FFF mode

SAMEER (Society for Applied Microwave Electronics Engineering and Research), Mumbai, India has developed an indigenous Linac unit named as Siddharth which is capable of delivering cost effective radiotherapy treatment in India. Presently, the Linac unit is being used clinically at various hospitals in India in FF mode with photons of energies 4 and 6 MV. Due to the increase interest of operating the Linac in FFF mode, we have carried out the feasibility study of this Linac for its clinical use in FFF mode.

Dosimetric characteristics study of the indigenously developed Linac in FFF mode

The dosimetric characteristic such as percentage depth dose (PDD), $TPR_{20,10}$, beam profiles, surface dose, build-up dose, mean energy, photon fluence and contaminant electron fluence spectra of this Linac were investigated in FFF mode using Monte Carlo method and the results were verified with the measured data. The measured data were generated in service the mode of the Linac. A Monte Carlo model of the indigenous FFF Linac (6 MV) was developed using the Monte Carlo-based BEAMnrc user-code of the EGSnrc Monte Carlo code system. The dosimetric parameters such as PDD and beam profiles were calculated using DOSXYZnrc user-code and the phase space files were analyzed using BEAMDP user-code of EGSnrc code system.

The results of this study indicate that, the differences between calculated and measured PDD values were less than 1 % in the tail region and less than 0.5 % in the superficial depth region for all the investigated field sizes. The d_{max} was occurred at 1.5 cm and mostly remained constant with field size. Surface dose and build-up region doses vary

with field size. Surface doses increases with increase in field size. Good agreement was found between Monte Carlo-calculated and measured lateral beam profiles (X and Y) obtained at SSD of 100 cm for all the investigated field sizes at depths of d_{max}, 5 cm and 10 cm. The difference between calculated and measured dose values were less than 1 %, except for the penumbra region where the maximum deviation between calculated and measured dose values were found to be around 3% (at d_{max}).

Calculation of optimum thickness and material of enhancer plate for indigenous FFF Linac

Practically, flattening filter cannot simply be removed but needs to be replaced by a thin metal 'enhancer' plate in the same position of the FF. The role of enhancer plate material is to generate electrons which provide build-up dose to the ionisation chamber to give sufficient signal and position-dependant information to the servo plates. They, in turn, can then operate correctly to control the beam quality and steering. It also removes the contamination electrons generated from the primary collimator and target, which do not provide useful position information but do increase surface dose to the patient. It is also necessary to prevent direct incident of the electron beam on the patient in the unlikely event of a target failure. The appropriate thickness and material of the enhancer plate depends on the particular make and model of a Linac. In the present study, optimized thickness and material of enhancer plate was calculated for the indigenously developed FFF Linac. Materials copper (Cu), aluminum (Al) and combination of both (Cu and Al) of varying thicknesses were considered as enhancer plate material since these two materials are commonly used in other FFF Linacs and also the effect of atomic number (Z) of enhancer plate material could be investigated. The results obtained from the study indicate that higher thicknesses approximately 6 mm of Cu or 14 mm of Al is needed to

absorb the electrons in the case of target failure if the CSDA range of Cu and Al is considered. However, 2 mm Cu or 7 mm Al is sufficient to create electron fluence useful for steering of the beam and reducing the surface dose. Using Cu as an enhancer plate also increases the surface dose as compared to the equivalent thickness of Al due to production of more low energy bremsstrahlung photons that reaches the patient plane as compared to Al. The results imply that combination of 3 mm Al and 1 mm Cu would be the appropriate enhancer plate material for the indigenously developed FFF Linac.

Chapter 4: Structural shielding design of FFF Linear accelerator: Indian Scenario

The beam characteristics of the Linac operated in FFF mode are different from the Linac operated with FF mode. FFF Linac beam is softer, for example, the central axis percent depth dose in water for a 6 MV FFF beam resembles with a 4 MV FF beam in some Linac models. Additionally, the lateral dose profile is peaked on the central axis, and less integral target current is required to generate the same dose to the tumor. As a result, the shielding parameters, such as the tenth-value layers and scatter fractions, calculated for flattened beams, may not be appropriate for shielding evaluations for unflattened beams. Since FFF beam is used for advanced modalities requiring higher Monitor Units (MUs) to be delivered, it must be determined whether shielding need to be enhanced or reduced to use an FFF machine in comparison to vault of FF machine. The present study was carried out to assess the structural shielding requirements of a 6 MV Linac operated in both FF and FFF modes as compared to a standard 6 MV Linac operated in FF mode only. This study includes the detailed calculations of thicknesses required for the shielding of primary and secondary barriers of 6 MV Linac bunker operated for FF and FFF photon beams. The calculations have been carried out by two methods, one by using the

approach given in NCRP Report No. 151and the other one is based on the MUs delivered in clinical practice.

The removal of FF significantly decreases local dose rates outside the treatment vault. The results based on NCRP approach suggest that the primary and secondary barrier thicknesses are higher by 24 % and 26 % respectively, for a Linac operated in FF mode to that of a Linac operated in both FF and FFF modes with an assumption that only 20 % of the workload is shared in FFF mode. Primary and secondary barrier thicknesses calculated from the delivered MU (dose) data on clinical practice also show the same trend and are higher by 20 % and 19 % respectively, for a Linac operated in FF mode to that of a Linac operated in both FF and FFF modes. Hence, it is found that overall the barrier thickness for a Linac operated in FF mode is higher about 20 % to that of a Linac operated in both FF and FFF. As a result, the wall thickness can be saved by about 20 % for a Linac operated in both FF and FFF modes in comparison to the Linac operated in FF modes only. Hence, the lower consumption of shielding material and space for new treatment vaults housing the Linacs with FFF and FF modes may reduce the building cost, whereas for existing facilities, one might take the benefits in terms of increased weekly workload. Further, this approach of calculations of shielding thickness for 6 MV bunker can also be extended for higher energies such as 10 MV, 15 MV and 18 MV as well.

Chapter 5: Study of quality assurance parameters for commercially available FFF beams

The removal of FF results in change in beam characteristics from that of the characteristics of flattened beam. The dosimetric parameters such as field size definition, beam quality, surface dose, off axis ratio, beam flatness, symmetry and penumbra as well

as depth dose profiles of FFF beam differs from the flattened beam.FFF beams are not standard in terms of the parameters describing the field characteristics. Hence, it is not possible to use the parameters in the same way as they are commonly used for the flattened beams. The present study was carried out to study the different quality assurance parameters of the FFF beams generated by the commercially available Linacs from different manufacturers. Varian Medical System make Edge and Elekta Ltd. make Versa HD were investigated as per the AERB Task Group recommendations and the method suggested by Fogliata et al and the results obtained were compared. The dosimetric parameters were studied over a period of time after duly verifying the consistency of beam parameters in three months and six months interval, after verifying their compliance to baseline data. Considering the data analysis requirement as stipulated in both the protocols, several lateral beam profiles for 6MV, 10MV, 6FFF and 10FFF beam were generated to study the beam characteristics. This study highlights the range of variation in the determined values of dosimetric parameters and suggests additional requirements to establish the FFF beam acceptance criteria.

Chapter 6: Measurement and comparison of surface dose and leakage radiation for flattening filter free and flattened photon beams

Surface dose plays a significant role in radiotherapy. Doses received by the basal skin layer can result in complications such as skin erythema, epilation, dry desquamation, wet desquamation, necrosis etc depending on the magnitude of doses received. Accurate measurement of dose at the surface is essential for proper treatment of patients. However, accurate measurement of surface dose is difficult since it is machine dependent and can be affected by many parameters such as field size, SSD, beam energy, materials present in the beam line, type of dosimeter used for its measurement etc. Energy spectrum and

electron contamination are the two factors which can change the surface dose in FFF beam. Since the FF is responsible for the majority of contamination electrons reaching the patient surface its removal is likely to reduce the surface dose. However, FF also acts as a beam hardener by removing low-energy photons from the spectrum. With the FF removed, this low-energy component is allowed to pass through to the patient and will act to increase the surface dose. The present study was carried out to measure relative surface dose using different detectors such as plane parallel plate ionization chamber, Al_2O_3 optically luminescent dosimeter and EBT3 GafChromic film for different field sizes with Varian make True Beam and Elekta make Versa HD Linacs generated FF and FFF photon beams (6 MV and 10MV). Absorbed dose due to leakage radiation for FF and FFF beam were also studied.

The results of the present study indicate that, Versa HD unit present very similar relative surface doses for small and medium field sizes, with lower doses for FFF beams as compared to FF beam. However, for True Beam FFF, relative surface doses are higher than the corresponding FF beams for small and medium size fields. Comparing the two unit types, the variation of the relative surface dose with respect to the field size is smaller for FFF than FF modes, for both True Beam and Versa HD. For larger fields, Versa HD FFF beams deliver lower relative surface dose than the corresponding FF beams. Further leakage radiation due to FFF beam is found to be lower in comparison to FF beam.

Chapter 7: Summary, conclusion and future work

This chapter summarizes the major findings of the thesis and outlines the scope for future work. Success of radiotherapy treatment depends on the accuracy of dose delivery. Over

the decades, the standard high energy radiotherapy beam acceptance criteria have been well established. Following those established criteria the dose delivery accuracy can be maintained within ± 5%. Owing to the removal of FF from the beam path in a Linac, difficulties have been raised by user institutes for acceptance of the beam parameters. This study elaborated the beam characteristic and QA parameters analysis from different commercially available FFF Linacs. Accordingly, it has been suggested to incorporate more dosimetric parameters in FFF beam acceptance regime which will enhance accuracy in FFF beam acceptance and the user's confidence in using the technology. Study on structural shielding design of FFF Linac bunker indicates that the wall thickness can be saved about 20 % for a Linac operated in both FF and FFF modes in comparison to the Linac operated in FF modes only. Hence, the lower consumption of shielding material and space for new treatment vaults housing the Linacs with FFF and FF modes may reduce the building cost, whereas for existing facilities, one might take the benefits in terms of increased weekly workload. Feasibility of indigenous Linac to operate in FFF mode was carried out using Monte Carlo method. Monte Carlo model of indigenous Linac was benchmarked with measured data and good agreement was found between Monte Carlo-calculated and measured data. Additionally appropriate enhancer plate material and thickness was studied which is optimized to be the combination of 3 mm Al and 1 mm Cu.

The scope for future work includes: 1) use of FFF beam is increasing and new technologies are being introduced from different manufacturers. Recently a new model Halcyon from Varian Medical System has been introduced which is producing only 6FFF beam. Although FFF accelerators have been released there is still some ambiguity surrounding the specification of beam parameters and the quality control tests necessary.

2) It is expected that the reduced scatter in FFF beams will increase the dosimetric accuracy of patient dose distributions, but so far this has not been elaborately demonstrated. Treatment planning systems may need optimization for FFF beam delivery.

3) Bunker design studies can be extended for the facilities for Linacs having multiple FFF beam are installed sharing common primary/secondary walls.

CHAPTER 1

Introduction

1.1 Cancer and Radiotherapy

1.1.1 Background

Cell multiplication is a normal physiological process that occurs in almost all tissues. Normally the balance between proliferation and cell death is tightly regulated to ensure the integrity of organs and tissues, but mutations in DNA (deoxyribonucleic acid) can disrupt these processes leading to cancer. Cancer refers to uncontrolled cell divisions which lead to growth of abnormal tissues. It is further classified in two general categories namely benign and malignant tumour. Benign tumours are generally well differentiated and slow growing. They do not invade surrounding normal tissue and majority of benign tumours do little harm to the host. However, malignant tumours are almost opposite in character to benign tumours. Malignant tumours, on the other hand, can invade other organs, spreading to distant locations in the body via the lymphatic system or the bloodstream and becomes life threatening.

Cancer treatment modalities comprise of radiotherapy, surgery and chemotherapy. Radiotherapy is the use of ionizing radiation to treat cancer. Radiation is a physical agent, which is used to destroy the cancer cells. The radiation used is called ionizing radiation because it forms ions and deposits energy in the cells of the tissues it passes through. This deposited energy can kill cancer cells. It damages the DNA of cells, thus blocking their ability to divide and proliferate further (Jackson and Bartek 2009). Radiation remains an important modality for cancer treatment with ongoing efforts towards designing new radiation treatment modalities and techniques which continue to improve the survival and quality of life of cancer patients (Baskar et al 2012). Radiotherapy is one of the most effective ways of treating cancer (Eatmon 1996). Although radiation damages both normal cells as well as cancer cells, the goal of radiation therapy is to maximize the

23

radiation dose to abnormal cancer cells while minimizing exposure to normal cells. Normal cells usually can repair themselves at a faster rate and retain its normal function than the cancer cells. Cancer cells in general are not as efficient as normal cells in repairing the damage caused by radiation which results in differential cancer cell killing (Begg et al 2011). Radiotherapy remains an important component of cancer treatment with approximately 50% of all cancer patients undergo radiotherapy during their course of treatment. It contributes towards 40% of curative treatment for cancer and also a cost effective treatment modality (Ringborg et al 2003, Delaney et al 2005, Begg et al 2011, Barnett et al 2009, Bernier et al 2004, Rath 2002). Radiotherapy can be delivered either by Teletherapy or by brachytherapy. Teletherapy is used for most of the cancer patients requiring radiotherapy and briefly discussed below:

1.1.2 Teletherapy

External beam therapy, also known as Teletherapy, is a method of delivering a beam or several beams of high-energy X-rays or electrons to the tumor of the patient. It directs the radiation to the tumor from outside the body i.e, radiation is delivered from an external source which is present outside the patient body. These high energy X-rays or electrons deposit dose to the tumor and destroy the cancer cells. With careful treatment planning, normal tissues surrounding the tumor volume can be spared to a great extent.

In external beam radiotherapy, several energies of photons and electrons are being used (Attix 1986, Gerig et al 1994, Khan 2010) for example, orthovoltage (superficial) X-rays and electrons are used for treating skin cancer and superficial structures. Whereas megavoltage X-rays are used to treat deep-seated tumors. Cobalt units which produce stable, dichromatic beams of 1.17 and 1.33 MeV from radioactive isotope ^{60}Co are used

in radiotherapy. Due to technology advancement and limitations in the use of cobalt beam because of lower radiation output, frequent source replacement and also security issues the use of cobalt unit are getting reduced. Medical Linear Accelerator (Linac), which produces mega voltage X-rays and electrons have shown significant rise. Typically in India, during last 10 years Linac growth is around 40% and Cobalt units shows a decreased tend of around 30% (AERB annual report 2007 and 2017). High-energy Linac, having multi energy photon and electron beam capabilities, are the most commonly used device for external beam radiotherapy. There are several techniques available for external beam therapy (Webb 2003, Teh et al 1999, Reco and Clifton 2008, Gupta and Anand 2012) such as conventional radiotherapy, three-dimensional conformal radiotherapy (3D-CRT), intensity modulated radiotherapy (IMRT), Image guided radiotherapy (IGRT), Stereotactic radiotherapy (SRT), Stereotactic radio surgery (SRS) etc. These techniques allow the dose distribution to be more conformal around the tumor volume and a lesser dose to the volume of normal tissues around the target. Recently, a small number of centers started to operate employing beams of heavier particles, particularly protons.

1.2 Medical Linear Accelerator

Linac produces megavoltage photon and electron beams which are used for the treatment of cancer (Livingston and Blewett 1962). By heating a tungsten filament (the electron gun), electrons are liberated and then accelerated through a linear tube (waveguide). The high energy electron beam itself can be used for treating superficial tumours (Jackson 1970, Karzmark 1987). Photons are produced by the rapid deceleration of electrons in a target material, typically a tungsten alloy via bremsstrahlung radiation. These photons are then collimated and modified by using beam modifiers. Various types of Linac are available for clinical use. Some provide X-rays only in the low megavoltage range (4 or 6

MV), while others provide X-rays with an energy range about 4-20 MV and electrons about 4 to 25 MeV. The photograph of a standard Linac unit is shown below in Fig. 1.1.

Fig. 1.1 Photograph of a Linac at a gantry angle of 90° (Source: Varian Medical System).

1.2.1 Operation of Medical Linear Accelerator

Linac is mounted in a gantry, which can rotate about a horizontal axis. The radiation beam emerging from collimator is always directed through and centered on the gantry axis. The beam central axis intersects the gantry rotation axis and couch rotation axis at a point in space called the isocentre. The couch is positioned in such a way that the patient's tumor is centred at the isocentre. Usually, the patient lies supine or prone on the treatment couch. The couch basically incorporates three linear motions and a rotation motion about the isocentre to facilitate positioning the patient for treatment (Podgorsak et al 1999). However, to achieve maximum dose delivery to tumor cells and sparing normal tissues, various other movements of the couch are also available in the modern Linacs.

Laser lights are installed at side walls and ceiling in the treatment room which produces narrow beam lines that intersect at isocenter. These facilitate positioning the patient in conjunction with reference marks, often tattoos, placed on the patient's skin. The mechanical or digital position indicators display the treatment field size together with collimator and gantry rotation angles. The isocentric system facilitates to achieve precision for reproducible treatment using multiple fields directed at the tumour from different gantry angles. A constant radiation Source to Axis Distance (SAD), usually 100 cm is employed in Linac. Alternatively, some treatment techniques also use a constant radiation Source to Skin Distance (SSD) of 100 cm.

1.2.2 Major components of Linear Accelerator

A schematic diagram of Linac components is shown in Fig 1.2. The main beam forming Linac components can be grouped into six categories (Podgorsak 2005) as below:

   a.   Injection system

   b.   RF power generation

   c.   Accelerating waveguide

   d.   Beam transport

   e.   Beam collimation and monitoring

   f.   Auxiliary systems (e.g. cooling, vacuum)
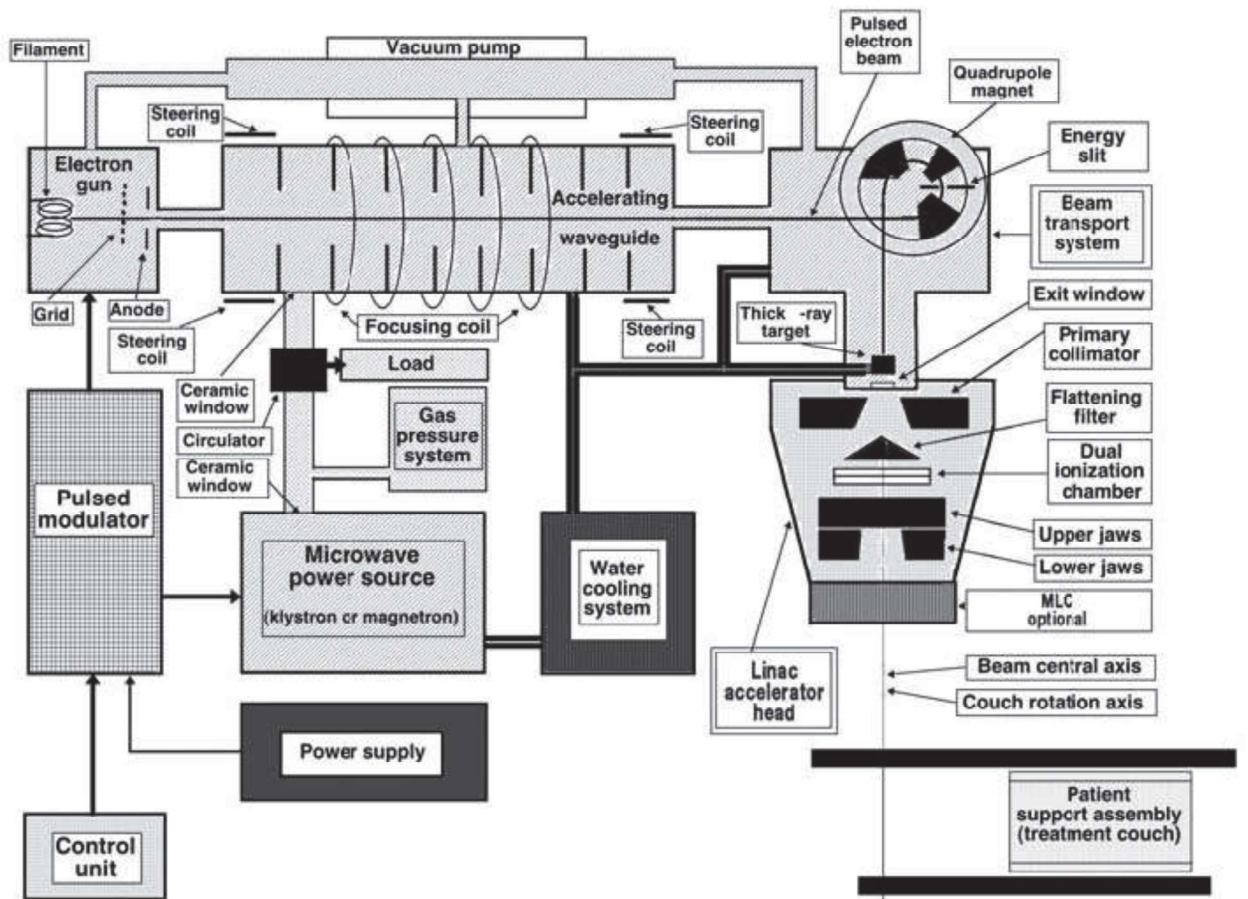
Fig. 1.2 Schematic diagram of a typical Linac (Source: IAEA Hand book reference Podgorsak 2005).

a. **Injection system:** The injection system is the source of electrons called an electron gun. Two types of electron gun are in use as sources of electrons in Linac namely Diode type and Triode type. Both electron gun types contain a heated filament cathode and a perforated grounded anode. In addition, the triode electron gun also incorporates a grid.

b. **RF power generation:** Electrons are thermionically emitted from the heated cathode, focused into a pencil beam by a curved focusing electrode and accelerated towards the perforated anode through which they drift to enter the accelerating waveguide.

28

The injection of electrons into the accelerating waveguide is then controlled by voltage pulses, which are applied to the grid and must be synchronized with the pulses applied to the microwave generator.

c. **Accelerating waveguide:** Two types of accelerating waveguides have been developed for the acceleration of electrons 1) traveling wave structure and 2) standing wave structure. In the travelling wave structure the microwaves enter the accelerating waveguide on the gun side and propagate towards the high energy end of the waveguide, where they either are absorbed without any reflection or exit the waveguide to be absorbed in a resistive load or to be fed back to the input end of the accelerating waveguide. In this configuration only one in four cavities is at any given moment suitable for electron acceleration, providing an electric field in the direction of propagation. In the standing wave structure each end of the accelerating waveguide is terminated with a conducting disc to reflect the microwave power, resulting in a buildup of standing waves in the waveguide. In this configuration, at all times, every second cavity carries no electric field and thus produces no energy gain for the electrons.

d. **Beam transport:** In low energy Linacs the target is embedded in the accelerating waveguide and no beam transport between the accelerating waveguide and target is required. Bending magnets are used in Linacs operating at energies above 6 MeV, where the accelerating waveguides are too long for straight-through mounting. The accelerating waveguide is usually mounted parallel to the gantry rotation axis and the electron beam must be bent to make it strike the X-ray target or be able to exit through the beam exit window. For a usable clinical beam it is necessary for the electron beam to enter the treatment head at the correct angle and energy. Since it is

difficult to control the energy spread, an achromatic bending system is generally used, which will ensure that electrons of different energies exit the bending system at the same point and in the same direction regardless of their initial energy.

e. **Beam collimation and monitoring:** The automatic frequency control (AFC) system constantly monitors the frequency within the accelerator and tunes the magnetron for optimum output.

f. **Auxiliary systems:** The vacuum system provides the low pressures needed for the electron gun, accelerator waveguide and bending system. Without this the gun would quickly burn out, and the electrons would quickly disperse due to collisions with air molecules. A water cooling system is used for cooling the accelerating guide, target and RF generator. An optional air pressure system is also used for pneumatic movement of the target and other beam shaping components.

1.2.3 Linear Accelerator treatment head

Linac head contains several components that influence the production, shaping, localizing and monitoring of the clinical photon and electron beams as shown in Fig.1.3.Clinical electron beams are produced by retracting the target and flattening filter (FF) from the electron pencil beam. Either scattering the pencil beam with a single or dual scattering foil or deflecting and scanning the pencil beam magnetically to cover the field size is done for electron treatment. Special cones (applicators) are used to collimate the electron beams. Clinical photon beams are produced with a target and FF combination. Bremsstrahlung X-rays are produced when the accelerated electrons in the accelerating structure incident on a target of a high atomic material such as tungsten. The target is water cooled and is thick enough to absorb most of the incident electrons. The electron

energy is converted into a spectrum of X-ray energies with maximum energy equal to the

incident electron energy as a result of bremsstrahlung interaction.
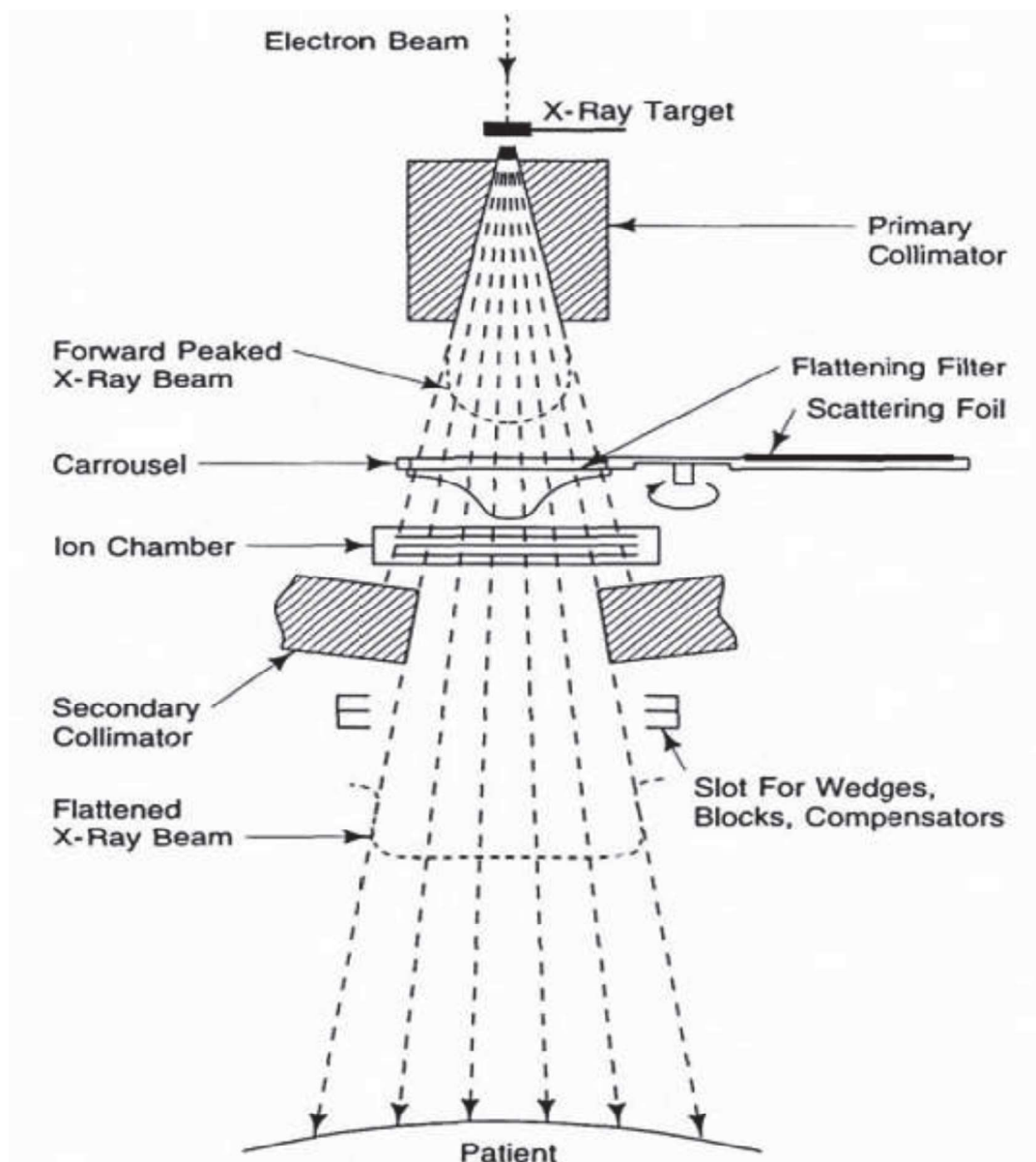
Fig. 1.3 Simplified view of Linac treatment head

The high-energy X-ray emerging from the target is forward-peaked in intensity, i.e higher

intensity is along the beam central axis and less intensity is away from it. The forward-

peaked X-ray is flattened to provide uniform treatment fields. This is accomplished by FF,

a conical metal absorber, placed on the central axis of radiation beam. The primary

collimator defines a maximum circular field, which is then further truncated with an adjustable rectangular collimator consisting of two upper and two lower independent jaws and producing rectangular and square fields at the Linac isocenter. The dual ionization chamber system samples the radiation beam (X-ray or electrons) passing through the treatment head and produces electrical signals that terminate the treatment when the prescribed dose is delivered. Two independent ionization chamber channels ensure that the prescribed dose is delivered accurately and safely wherein one serving as a check on the other. The field defining light simulates the X-ray field and facilitates positioning of the patient. It provides an intense field, duplicating in size and shape of the X-ray field incident on the patients defined by the secondary collimator consisting of four thick metal blocks, often made of tungsten. The secondary collimator rotates about the beam axis, allowing angulations of the fields. Accessories to modify the emergent X-ray field externally, such as wedges, tissue compensators, individually shaped apertures and shadow blocks, may be mounted on the trays that slide into slots of an accessory mount attached to the treatment head. The Optical Distance Indicator (ODI) light projects a numerical scale on the patient's skin to define SSD.

1.3 Flattening filter (FF)

FF is a dense metal in the shape of a cone that is placed in the path of beam to attenuate more of the high energy photons through the central axis resulting in a uniform planar fluence at a reference depth (typically 10 cm) within the allowed variation. FF consists of conical shaped pieces of metal, typically made of high-Z materials such as iron, copper or tungsten, and are specific for particular beam energy. The central part of these filters can be several cm thick (Izewska 1993). The filters are usually mounted on a rotating

carousel so that the appropriate filter can be positioned in the photon beam. The image of FF and effect of FF on lateral dose profile is shown in Fig 1.4 as below:
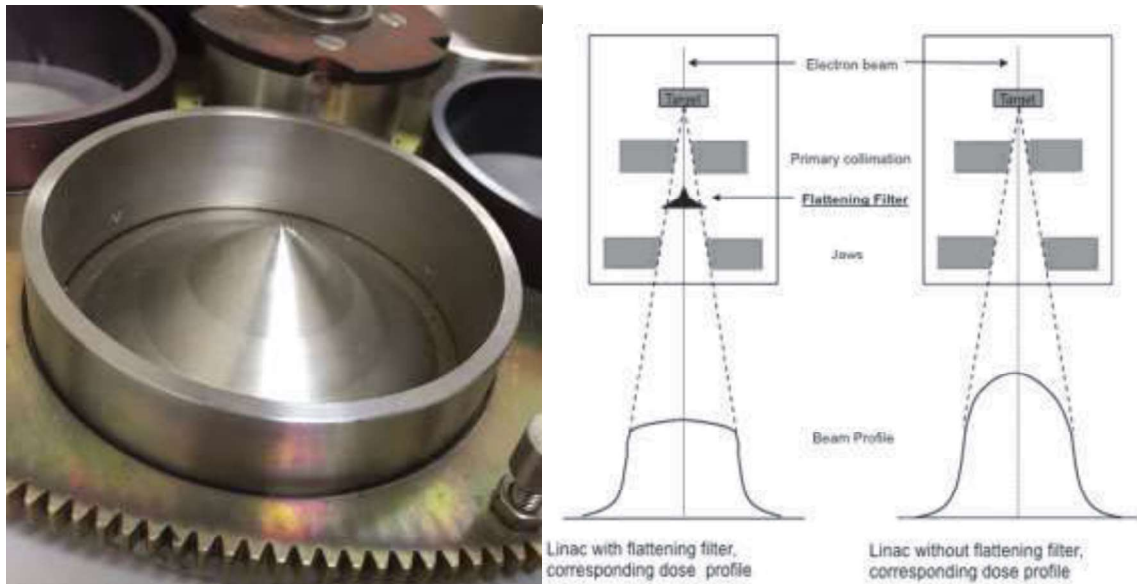
Fig. 1.4 (a) Image of FF (b) Lateral dose profile with and without FF (Source: Varian Medical System).

1.3.1 Removal of Flattening filter and rationale of flattening filter free Linac

FF has been standard in Linac design since the 1950's but there are certain disadvantages of using FF. It acts as an attenuator, beam hardener and the scatterer. Monte Carlo studies have shown that FF is responsible for the majority of scatter radiation produced in the treatment head (Petti et al 1983, Zhu and Bjarngard 1995). Further, it acts as the main source of electron contamination which is also very difficult to model in the treatment planning system (Nilsson and Brahme 1986, Hounsell and Wilkinson 1999, Klein et al 2003). Monte Carlo studies for an 18 MV photon beam from Varian accelerators has shown that FF is responsible for roughly 10 % of the neutron production in the treatment

head (Kry et al 2007, Zanini et al 2004) which is dependent on the material of the FF. The major disadvantages of FF are:

- Decreased primary beam intensity leading to reduced dose rate

- Creation of a significant source of extra-focal scattered radiation within the beam

- Electron contamination in the primary beam

- Increased leakage radiation from the treatment head

- Amplification of beam steering errors necessitating active beam monitoring and servo control

The advanced beam therapy techniques, such as SRS/SRT where inhomogeneous dose distributions are applied and IMRT where varying fluence pattern across the beam are delivered, have stimulated the increasing interest in operating the Linac in a flattening filter free (FFF) mode (Georg et al 2011). The removal of the FF results in an increase in dose rate, softening of the X-ray spectra, reduction in head scattered radiation, and the non-uniform beam profile. The reported dose rate of FFF beams is about $2-4$ times higher than that of the FF beams, i.e., FFF Linac can typically be operated at a dose rate higher than 1000 MU/min under the normal operating conditions. The increased dose rate decreases the dose delivery time, especially for hypo-fractionated SRT, and is thought to be useful in managing the intra-fractional target motion. The softening of the x-ray spectra affects the depth as well as lateral dose distribution at all depths and results in increased surface dose and slight shifting of the d_{max} towards the surface. The lateral transport is reduced, which may result in greater control over gradients with the field and at target boundaries. The magnitude of contaminating electrons of FFF beam is relatively low and the photo-neutron fluence per monitor unit (MU) produced by the high-energy FFF beam is also relatively less in comparison to that produced by the FF beam.

1.3.2 Characteristics of Flattening Filter Free (FFF) photons beams

Dose rate and Output: The first most obvious consequence of running a Linac without FF is the huge increase in dose rate. A range of dose rates for FFF beams have been reported in the literature (Vassiliev et al 2006, Kragl et al 2009, Cashmore 2008, Fu et al 2004, O'Brien et al 1991). FFF beams can be run at higher MU/min than FF beams. Elekta 6 MV and 10 MV FFF beams have maximum dose rates of 1400 MU/min and 2200 MU/min respectively. The Varian 6 MV FFF beam runs at a maximum of 1400 MU/min and the 10 MV FFF beam at a maximum of 2400 MU/min (Fu et al 2004, Pönisch et al 2006, Titt et al 2006, Vassiliev et al 2006a, 2006b, Cashmore 2008). Output of the Linac is defined as the absorbed dose per MU delivered under reference condition (TRS 398, TG 51). The two most pronounced effects of removing the FF are the increased output in terms of dose per pulse and dose rate.

Depth Dose profiles: The attenuating properties of FFF photon beams are different from conventional beams due to the difference in beam filtration. Depending on the Linac design the FFF beams with the same accelerating potential as a conventional 6 MV beam, will generally have a depth dose distribution corresponding to a 4–5 MV conventional photon beam (Cashmore 2008, Vassiliev et al 2006b). The depth of dose maximum (d_{max}) will be affected by the energy reduction and the reduction of scattered radiation when the FF is removed. Production of contaminant electrons also affects depth doses beyond d_{max} but the differences due to this are mainly observed in the surface region. In a conventional beam the filter attenuates the low energy component of the spectrum

increasing the apparent energy of the beam. With FFF beams these soft X-rays pass through and the addition of these to the beam spectrum lowers the observed energy.

Surface dose: Changes in beam spectrum and scatter affects the dose in the build-up region, in particular, surface doses. The target, primary collimator and FF all act as both producers and absorbers of electrons. Contamination electrons arising from the primary collimator act to increase surface doses in the patient. FF removes the majority of these electrons but generates its own electrons. If the FF is removed the contamination electrons from the primary collimator reaches the patient directly. To avoid this some kind plate material is used in the place of FF. Surface dose changes with field size.

Lateral Dose profiles: When comparing conventional and FFF beams the most notable differences are the increase in dose rate and the shape of the lateral dose profiles. FF is designed to give a flat beam over the maximum field size (usually 40 x 40 cm^2) in many Linac models. Beam profiles of small field sizes (5x5 cm^2 and below) exhibits little or no change in profile. Larger field sizes show enhanced central axis dose with a rounding of the profiles (Vassiliev et al 2006b). Outside the treatment field the doses are lower for FFF beams due to the reduction in out-of-field scatter. This would effectively act to reduce the dose to surrounding normal tissues.

1.3.3 Enhancer plate

Practically, FF cannot be simply removed, but needs to be replaced by a thin metal enhancer plate also called replacement filter in the same position of FF. The role of replacement filter material is to generate electrons which provide build-up dose to the ionisation chamber to give sufficient signal and position-dependant information to the servo plates. They, in turn, can then operate correctly to control the beam quality and steering (Cashmore 2008, Cashmore et al 2006). Furthermore, Titt et al (2006) reported

about primary electrons penetrating the target when the accelerator was operated in 6 MV mode. This poses a potential risk to produce high surface doses which can be eliminated by using a replacement filter. It also removes the contamination electrons generated from the primary collimator and target, which do not provide useful position information but do increase surface dose to the patient. Replacement filter is also necessary, so that the electron beam is never directly incident on the patient in the unlikely event of a target failure.

1.3.4 Other Flattening Filter Free treatment devices

Some treatment devices specifically designed for delivery of IMRT are not equipped with FF. In Cyber Knife, Linac (Accuray Incorporated, USA) is mounted on a robotic arm and delivers small circular fields with a diameter ranging from 5 mm to 60 mm at a SSD of 80 cm. The treatment is delivered though hundreds of individual fields by repositioning the unit using the robotic arm (Adler et al 1997). In this unit, FF has been replaced with what is called an electron filter, i.e. a flat metal plate made of lead. In intensity modulated arc therapy (IMAT), a form of IMRT, the radiation source (Linac) continuously delivers radiation while rotating around the patient. The Tomotherapy unit (Accuray Incorporated, USA) is dedicated for IMAT delivery and it has a delivery technique similar to how Computer Tomography (CT) imaging is performed (Mackie et al 1993). In Tomotherapy machines the Linac is mounted on a rotating disc. The radiation field is collimated by a binary MLC combined with motorised jaws with three different field width positions (maximum field size is 5 cm x 40 cm). A fan beam is continuously delivered in a helical arc by rotating the Linac and the treatment couch is moved through the radiation field, with the modulation achieved by switching individual MLC leaves in and out. With this modality the FF is not necessary and has been replaced by a flat beam hardener (Jerajet al

2004).The MM50 racetrack microtron proposed in the 1980s is a radiotherapy unit lacking a FF, but still producing a flat photon beam. This is achieved by scanning the incident electron beam on a thinner target plate (Brahmeet al1980, Karlsson et al 1988). In principle this technique could also be used for scanned photon beam IMRT, where the intensity modulation is performed by the scanning pattern of the incident electron beam rather than the collimating structures. Recently Varian Medical System introduced Halcyon Linac which is producing 6 MV FFF photon beam and the structure is similar to Tomotherapy unit.

1.4 Literature review

Monte Carlo methods serve as a powerful tool for simulating and benchmarking the photon beams generated from radiotherapy equipment such as Linac (Andreo 1991, Rogers et al 1995, DeMarco 1995, Keall 2001, Sheikh-Bagheri 2000). Department of Science and Technology, Govt. of India has entrusted the responsibility of development of indigenous Linac to one of its constituent unit SAMEER (Society for Applied Microwave Electronics Engineering and Research) under Jai Vigyan National Science and Technology Mission. Due to its development under indigenous technology, the machine has the potential of delivering cost effective radiotherapy treatments in India. The Linac unit is named as Siddharth and is capable of producing photon beam energy of 6 MV. Presently, the Linac unit is being used clinically at various hospitals in India in FF mode with photons of energies 4 and 6 MV. Recently, Subhalaxmi et al (2018) have reported the dosimetric characteristics of this Linac unit for 6 MV photon beam using Monte Carlo method as well as by measurement. However, due to the increase interest of operating the Linac in FFF mode, the feasibility study has been carried out for the same

unit in FFF mode. The present study was carried out to evaluate the dosimetric characteristics of indigenously developed Linac in FFF mode using Monte Carlo method and verify the results with the measured data. It may be noted that the measured data were generated in the service mode of Linac to find the feasibility for clinical use of this Linac in FFF mode.

FFF Linac is basically a standard Linac with the FF removed from the beam line. Practically, the FF cannot simply be removed but needs to be replaced by a thin metal 'enhancer' plate in the same position of the FF. The role of enhancer plate material was already discussed under section 1.3.3. Several studies have been undertaken to determine the most appropriate material and thickness of enhancer plate which will satisfy these functions. Cashmore (2008) performed tests on an Elekta Precise Linac and compared 1.1 mm Al vs 1.9 mm Cu. Both plates enabled the operation of the Linac with negligible differences on the patient surface dose. Titt et al (2006) studied the characteristics of unflattened 6 MV beams for a Varian 2100 Linac by Monte Carlo methods. They simulated the effect of 11 mm nylon and 2 mm Cu filters to prevent the monitor chamber from saturation. Stathakis et al (2009) tested a 1 mm steel plate in a Varian 23EX Linac. While several millimeters of copper or steel seem to be sufficient for an almost normal operation of the monitor chamber, thicker ones are also in use. For example, Kragl et al (2009) and Tyner et al (2009) reported a 6 mm copper plate that was used in recent studies for Elekta precise Linacs. O'Brian et al (1991) described the modification of a Therac-6 Linac in FFF mode, where a 13 mm Al plug was inserted beneath the target. Thicker plates provide a security advantage in case the target breaks. Lind et al (2009) performed Monte Carlo simulations of Elekta Linac to study the optimal thickness of the enhancer plate. Although, 1 or 2 mm Cu plates were found to be sufficient for 6 MV

photon beams in order to create an energy fluence to steer the beam with the unmodified monitor chamber, thicker plates were recommended for safety reasons, i.e., to absorb electrons in case of target failure. All these studies performed by several investigators are not consistent because of the engineering need and consideration towards radiation safety and electronic operation. It is also obvious that the appropriate thickness and material of the enhancer plate depends on the particular make and model a Linac. In the present study optimised thickness and material of enhancer plate was investigated for the indigenously developed Linac. Accordingly, different materials and thicknesses were investigated and their influences on the photon and electron fluence were studied at the entrance window of the monitor chamber as well as at the surface of the water phantom using Monte Carlo methods.

As expected, there are differences in the beam characteristics of Linac operated in FFF mode to that of Linac with the FF mode (Vassiliev et al 2006a, 2006b, Huang et al 2012). As a result, the shielding parameters, such as the tenth-value layers and scatter fractions, calculated for flattened beams may not be appropriate for shielding evaluations for unflattened beams (Dalaryd et al 2010, Stephen et al 2009, Julia et al 2014). In the recent time several technical changes have been augmented in the treatment delivery modality which enables higher dose escalation to tumor and rapid dose fall off outside the tumor. The technologies involved for such delivery enhances the MUs generated from the Linac due to presence of different beam modifying techniques. Since FFF beam is used for advanced modalities requiring higher Monitor Units (MUs) to be delivered, it must be determined whether shielding need to be enhanced or reduced to use an FFF machine in comparison to vault of FF machine. Considering the Linacs with FFF beam available and their growth in India, the present study was carried out to find the impact of FFF beam on

bunker design of Linac facility in Indian scenario. In this study the structural shielding requirements of a 6 MV Linac operated in both FF and FFF modes in comparison to a standard 6 MV Linac were assessed. This study includes the detailed calculations of thicknesses required for the shielding of primary and secondary barriers of 6 MV Linac bunker operated for FF and FFF photon beams. The calculations have been carried out by two methods, one by using the approach given in NCRP Report No. 151(2005) and the other one is based on the MUs delivered in clinical practice. This study also includes the radiation survey of the installation.

The dosimetric parameters such as field size definition, beam quality, surface dose, off axis ratio, beam flatness, symmetry and penumbra as well as depth dose profiles of FFF beam differs from the flattened beam. FFF beams are not standard in terms of the parameters describing the field characteristics. Hence, it is not possible to use the parameters in the same way as they are commonly used for the flattened beams. Several investigators had proposed new parameters for FFF beam description. Ponisch et al (2006) suggested normalizing the FFF beam profiles to the 50 % dose level at the inflection point of the fall-off at the field edge, with the objective to have the same description of the field edge region as normally used for the flattened beam profiles. Fogliata et al (2012, 2015) suggested a different procedure to normalize the FFF beam profiles through a renormalization factor in a way to superimpose the FFF dose fall-off at the field edge with the corresponding flattened profile (normalized by default at the beam central axis to 100%). However, evaluating the dosimetry characteristics of FFF photon beam applying their definitions are complex in nature which requires the use of dedicated software and understanding. Further, the Atomic Energy Regulatory Board (AERB) of India constituted a Task Group (TG) and recommended an evaluation criterion for FFF photon

beam from standard Linac (Sahani et al 2014). It may be noted that the differences between FFF and FF in terms of quality assurance is mainly related to beam dosimetry and not to mechanical characteristics of the Linac, for which the standard quality assurance procedures still hold. In this study the different quality assurance parameters of the FFF beams generated from the commercially available Linacs of different manufacturers were investigated. Varian Medical System make Edge and Elekta Medical System make Versa HD were investigated as per the AERB TG recommendations (Sahani et al 2014) and the results obtained were compared with the published similar parameters as suggested by Fogliata et al (2012, 2015).

Surface dose plays a significant role in radiotherapy. Doses received by the basal skin layer can result in complications such as skin erythema, epilation, dry desquamation, wet desquamation, necrosis etc depending on the magnitude of doses received (Carl and Vestergaard 2000, Kim et al 1998, Ishmael Parsai et al 2008). At the same time it is also important that doses to targets which are lying close to the surface are accurately known so that under dosage does not occur. Since the FF is responsible for the majority of contamination electrons reaching the patient surface its removal is therefore likely to reduce this contribution. However, FF also acts as a beam hardener by removing low-energy photons from the spectrum. With FF removed, this low-energy component is allowed to pass through the patient and increase the surface dose. Energy spectrum and electron contaminations are the two factors, which can change the surface dose in FFF. Whether these results in higher or lower surface doses is therefore the point of interest. Although surface doses have been studied under a range of conditions for conventional flattened beams (Lamb and Blake 1998, Nilsson and Sorcini 1989, Butson et al 2000, Kim et al 1998, Klein et al 2003, Tatsiana et al 2015, Ugur et al 2016) and different

correction factors were suggested by investigators (Velkley et al 1975, Gerbi and Khan 1990, Mellenberg 1990), there is limited data available for FFF beams (Cashmore 2016, Sigamani et al 2016, Wang et al 2012, Javedan et al 2014, Sigamani et al 2017). Further, due to the steep dose gradient near the surface as well as in the buildup region, careful considerations are required in the selection of detectors for measurement of surface dose. It is worth noting that surface dose in FFF radiotherapy beam investigated in previous studies (Cashmore 2016, Sigamani et al 2016, Wang et al 2012, Javedan et al 2014, Sigamani et al 2017) involving one or multiple different detectors such as parallel plate chamber, small volume ion chamber, GafChromic films were limited to only single variant of commercially available Linac. The present study evaluates and compares the trends of the relative surface dose delivered by a FF and FFF beam photon beam of energy 6 MV and 10 MV generated from Varian make True Beam and Elekta make Versa HD Linacs for different square field sizes (5x5, 10x10, 15x15, 20x20, 25x25 cm^2) with a plane parallel plate ionization chamber, Al_2O_3 optically luminescent dosimeter, GafChromic films EBT3.

1.5 Aim of the thesis

The objectives of the present study are the following:

- Monte Carlo-based study of the indigenously developed Linac (Siddharth) in FFF mode.

  ➢ To calculate the dosimetric characteristics and benchmark the results with measured data.

  ➢ To calculate the optimum thickness and material of enhancer plate which is required to be kept in the place of flattening filter for the indigenous Linac.

- Study of structural shielding design of Linac vault housing operated in both FF and FFF mode.

- Analysis of beam characteristics and quality assurance parameters from commercially available FFF Linacs.

- Measurement and comparison of surface doses for FFF and FF photon beams using various dosimeters for different commercially available Linacs.

CHAPTER 2

Monte Carlo method and EGSnrc code system

2.1 Basics of Monte Carlo Technique

Monte Carlo techniques have become important in medical physics over the last 50 years (Rogers 2006). The interest in Monte Carlo techniques has grown from the need for accurate numerical methods for solving a variety of radiation transport problems that arise in radiotherapy, medical imaging, and nuclear medicine. Regarding the radiotherapy problems, the issue of large computing times has traditionally led to the Monte Carlo method being viewed as a clinically unfeasible approach. However, due to the most recent improvement in computer technology and development of faster codes optimized for radiotherapy calculations, the method has become now an excellent alternative to the analytical solving of complex transport equations (Mohan 1997). In fact, radiotherapy treatment planning systems (TPS) based on the Monte Carlo method are being implemented for the dose calculations (Emiliano and Geraint 2008, Li et al 2001).

The general idea of Monte Carlo analysis is to create a model, which is similar as possible to the real physical system of interest, and to create interactions within that system based on known probabilities of occurrence, with random sampling of the probability density functions. All physics processes involving the transport and interaction of radiation with matter have a random nature, where the probability distribution governing the event is known. Because of this stochastic behavior of the radiation, the Monte Carlo method represents an excellent tool for modeling these processes. As the number of individual events (called histories) is increased, the statistical uncertainty decreases. Assuming that the behavior of physical system can be described by probability density functions, the Monte Carlo simulation can be proceeded by sampling from these probability density functions, which necessitates a fast and

46

effective way to generate random numbers. A random number is a particular value of a continuous variable uniformly distributed on the unit interval [0, 1]. Particles are generated within the source region and are transported by sampling from probability density functions through the scattering media until they are absorbed or escaped the volume of interest. The outcomes of these random samplings or trials, must be accumulated or tallied in an appropriate manner to produce the desired result, but the essential characteristic of Monte Carlo is the use of random sampling techniques to arrive at a solution of the physical problem (Papoulis 1965, Metropolis 1987, Mackie 1990, Bielajew 2001, Rogers 2002).

The major components of Monte Carlo methods for random sampling of a given event are as follows (Kushwaha and Srinivasan 2009):

Probability density function: Statistical estimation is a process through which we deduce parameters that characterize the behavior of a random experiment based on a sample or a set of typically large but in any event finite number of outcomes of repeated random experiments. In most cases, we postulate a probability distribution which is based on some plausible assumptions or based on some descriptive observations with several parameters which is then estimated. A probability distribution function may be effectively used to characterize the outcome of experiments whose deterministic characterization is impractical due to a large number of variables governing its state and/or complicated functional dependencies of the outcome on the state.

In Monte Carlo simulations, the physical system is described by a set of probability density functions which is similar to the real physical system to be simulated and to create interactions within that system based on known probabilities of occurrence i.e. the

cross section values. Hence, Monte Carlo codes must include cross section libraries for calculating the probability of a particle interacting with the medium through which it is transported. The cross section for each interaction is dependent on the incident particle, its energy and through the material it travels.

Random number generator: A high quality random number sequence is a long stream of numbers with the characteristic that the occurrence of each number in the sequence is unpredictable. Generally, there are three different approaches to get random numbers in a program. One can use pre-generated sequences of random numbers stored in tables (an old but very easy to implement method), one can use a (true) random number generator (generally produced by physical devices such as noise generator which are coupled with a computer) or a pseudorandom number generator. True random number generators suffer from the disadvantages that the maintenance of the system is difficult and it is very difficult to check the quality of the numbers generated. Thus, mathematical algorithms for the generation of 'pseudorandom numbers' are the most popular choice as random number generator (RNG). The outputs of the RNG cannot be considered exactly random; they only approximate some of the properties of random numbers. Hence, a careful mathematical analysis is required to ensure that the generated numbers are sufficiently random for the particular simulation. The length of the period of a RNG must be long enough to avoid repetitions in the sequence of numbers used during the simulation process, as otherwise correlations can be produced.

Sampling technique: The selection of a random value of a specific quantity is realized in Monte Carlo simulation through sampling techniques. These techniques help us to convert a sequence of random numbers (R_i), uniformly distributed in the interval [0,1] to

a sequence (x_i) having the desired density, say f(x). There are several techniques available to do this conversion such as inversion technique, rejection technique etc.

- **Inversion Technique:** This is the simplest technique based on the direct inversion of cumulative distribution function of random variable. Let X be a random variable whose distribution can be defined by cumulative distribution function is F_X. Using this inverse sampling technique values of X can be generated. For this, generate a random number R from the standard uniform distribution in the interval [0,1]. Find the inverse of the described cumulative distribution function i.e $F_X^{-1}(x)$. Now compute $X = F_X^{-1}(R)$, the computed random variable X has the distribution of F_X.

- **Rejection Technique:** This technique is frequently used to increase the efficiency of the Monte Carlo computation in cases where the previous method is difficult and time consuming. Let f(x) be the probability distribution function defined in the interval a and b from which the sampling is needed and let M be the upper limit of f(x). Now select two independent random numbers R_1 and R_2. Compute x=a+(b-a)R_1 which is a point uniformly distributed over [a, b]. Accept this value as the sampled value of x if $R_2 \leq [f(x)/M]$. Otherwise select two fresh random numbers and repeat the steps.

Scoring: In the Monte Carlo approach, the transport of an incident particle and all of its secondary particles subsequently are set in motion and is referred as particle history. Simulated particles are followed as they lose energy, generate other particles, and ultimately 'killed' as they either escapes from the geometry of interest or their energy

falls below a given threshold. By simulating a large number of histories N, reliable average values of different macroscopic quantities of interest (absorbed dose, kerma, fluence, energy deposition etc) can be obtained. The scored quantities are estimates or tallies or scores, which lie within confidence intervals corresponding to certain probabilities.

Error estimation: An estimation of statistical error (variance) must be determined. Since large number of histories are modeled, the result approaches the average photon and electron distribution, calculated to within a statistical uncertainty which decreases inversely with the square root of the computation time. For example, the uncertainty associated with the result is a function of the number of particle histories simulated (N). By running more histories, the uncertainty gets smaller, following a $1/\sqrt{N}$ relation.

Variance reduction techniques: These techniques have been developed to increase the efficiency of Monte Carlo simulation by reducing not only the variance but also by decreasing the computational time to achieve it.

2.2 General purpose Monte Carlo codes

Several general-purpose Monte Carlo codes are in use for simulation of radiation transport as mentioned below:

- MCNP "Monte Carlo N-particle system" (Los Alamos National Laboratory) (Briesmeister 1988 and 1997)

- GEANT4 "Generation of Events ANd Tracks" (Cern, Switzerland / France) (Agostinelli et al 2003)

- Penelope "PENetration and Energy LOss of Positrons and Electrons" (Barcelona, Spain) (Baro et al 1995)

- ETRAN "Electron TRANsport" (Seltzer 1988)

- ITS "Integrated TIGER Series of Coupled Electron/Photon Monte Carlo Transport Codes System" (Halbleib 1988)

- FLUKA developed by the Italian National Institute for Nuclear Physics (INFN) and European Organisation for Nuclear Research (CERN) (Ferrari et al 2005),

- EGS4 (Nelson et al 1985)

- EGS "Electron-Gamma Shower" (Nelson et al 1985,Kawrakow et al 2010)

- EGSnrc (developed by National Research Council of Canada) (Kawrakow et al 2010).

2.3 EGSnrc Code System

2.3.1 General Description

The general purpose Monte Carlo code used in this study is EGSnrc code system (Kawrakow et al 2010). The EGSnrc, an acronym of Electron-Gamma Shower, is a general-purpose package of Monte Carlo codes used for the simulation of the coupled transport of electrons and photons through an arbitrary geometry and for particle energies ranging from a few tens of keV up to a few hundred GeV (Kawrakow et al 2010). As indicated by the names they simulate particle transport of electrons (and positrons) and photons, but disregards other particles such as neutrons and protons. This code is the most recent in the family of the EGS Monte Carlo codes and it is substantially improved

from its predecessor, the EGS4 version originally developed at Stanford University Linear Accelerator Center (SLAC) (Nelson et al 1985).The first code (EGS3) was developed in 1978 for the simulation of electromagnetic cascades for high energy physics. Later, the algorithms of transport were extended to lower energies. The EGSnrc system has been benchmarked against EGS4 for a range of situations relevant to radiotherapy. Although the results are generally in agreement, the small differences found are attributed to the improvements made to EGSnrc in general and the multiple scattering theory (Kawrakow and Rogers 2003). It is one of the most widely used Monte Carlo codes for simulating coupled electron-photon transport in medical physics applications. The EGSnrc code is written in the MORTRAN programming language, which is a string preprocessor for the FORTRAN language. This code has been well benchmarked in the energy region of dosimetric interest. EGSnrc consists of several user-codes dedicated to address specific situations. These user-codes allow to model specific geometry, set-up various particle sources (e.g. parallel beam of photons with certain spectral distribution, seed sources), and the scoring of quantities sufficient for most of the problems. In the present study user-codes BEAMnrc (Rogers et al 2016), DOSXYZnrc (Walters et al 2016) and BEAMdp (Ma and Rogers 2004) were used which are briefly described in the next section.

2.3.2 User-codes used

BEAMnrc

The BEAMnrc code (Rogers et al 2016) is a Monte Carlo simulation tool for the modeling of radiation beams from any radiotherapy units, including ^{60}Co units and medical linear accelerators. BEAMnrc was developed as a user-code of EGSnrc code system intended to simulate mostly medical linear accelerator. It is able to accurately

model all aspects of a Linac including the details of target, FF, primary collimator, secondary collimator monitor chamber etc. The code comprises of various Component Modules (CMs) perpendicular to the incident beam, each of these CMs can be fully specified by the user and intended to model a specific component of a Linac. A model of the Linac is constructed by stacking CMs along the beam direction in a non overlapping manner. Currently, there are 24 CMs available in BEAMnrc code. Typical component modules used in Linac modeling are: SLABS for X-ray target, CONESTAK for primary collimator, FLATFILT for FFs, CHAMBER for ionization chambers, JAWS for secondary collimator etc. The user can interact with the software through the Graphical User Interface (GUI). The code allows the placement of scoring planes which can be located at the bottom of any CM in the Linac model and the phase space files are generated accordingly. A phase space file consists of the particles crossing the scoring plane and their characteristics. The characteristics recorded in the phase space file are particle charge, position (X and Y) in the scoring plane, direction and the particle weight. The transport history of the particle is also recorded, which allows the code to calculate the dose contribution from user defined region. One of the major advantages of the Monte Carlo technique is that it gives detailed information about each particle's history. For this purpose, BEAMnrc includes a general technique built upon the LATCH feature. LATCH is a variable which indicates the positions where the particles have interacted or have been created. With LATCH it is possible to keep track of each particle history and it is used in the analysis of the relative dose distributions from various accelerator components. Along with the phase space file another file (.egslst) listing a summary of the simulation parameters, warning messages if any, dose and fluence results of the

simulation is also produced as the output file. Furthermore the dose and deposited energy in all user defined dose scoring zones are listed.

DOSXYZnrc

The DOSXYZnrc (Walter et al 2016) is a user-code of general-purpose EGSnrc code system for 3-dimensional absorbed dose calculations. It simulates the transport of photons and electrons in a rectilinear geometry and scores the energy deposition in the designated volume elements (voxels). The geometry is a Cartesian coordinate with the x-y plane on the page, x to the right, y down the page and the z-axis into the page. Dimensions are completely variable in all three directions where every voxel can have different materials and varying densities. The code allows different sources including phase-space data generated by BEAMnrc simulation as a source. DOSXYZnrc was run using the ".egsinp" file extension while the results can be found in the ".egslst" file extension with the same given file name. The main output of a DOSXYZnrc simulation is a 3ddose file, which lists the dose and the relative statistical uncertainty for each voxel defined in the simulation geometry. The dose is given in Gy per incident particle. The statistical uncertainty is estimated using a history by history method (Walters et al 2002) in which the uncertainty of the dose is estimated by grouping all energy depositions originating from the same primary particle rather than using the variance of individual events. The method takes the latent variance of a phase space file into account, which means that the uncertainty introduced by statistical variations in the phase space file itself is accounted for. More information about the GUI can be found from the EGSnrc manual (Walter et al 2016).

BEAMdp

Full phase-space files can be analyzed using beam data processing software BEAMDP (BEAM Data Processor) (Ma and Rogers 2004). This can be used to analyze the phase-space parameters of a clinical electron beam generated using BEAMnrc and to derive the data required by a multiple-source model for representation and reconstruction of the electron beam for use in Monte Carlo radiotherapy treatment planning. The idea behind the model-based beam characterization is that particles from different parts of a Linac may be treated as they are from different sub-sources. This is supported by the fact that particles from different components of a Linac have different energy, angular and spatial distributions. The particles from the same component, however, have very similar characteristics, in terms of energy range and incident directions, which are almost independent of their positions on the scoring plane. Each sub-source has its own spectral and planar fluence distributions derived from the simulated phase-space data. By sampling the particle position on the sub-source and on the phantom surface, the correlation between the particle position and incident angle is naturally retained. For charged particles, a small perturbation of the incident direction is sampled to correct for the effect of charged particles scattering in the air.

PEGS4

PEGS4 (Preprocessor for EGS) is a set of FORTRAN sub-programs which generate the material data set for subsequent use by EGSnrc code system and also provide utilities for researchers studying electro-magnetic interactions. The active operations of PEGS are functionals; that is, they are operations whose arguments are functions (the functions related to physics interactions). All the user-codes of EGSnrc code system run using the cross-section data of the material in the pegs4 folder in the directory on area

55

EGSnrc/pegs4/data. This default cross-section data that is stored in the folder uses Storm and Israel compilation set. The files 700icru.pegs4dat and 521icru.pegs4dat contain a large number of commonly used materials. The numbers in the file identifiers correspond to electron energy of 521 and 700 keV, relating to thresholds for secondary electron production of 10 and 189 keV kinetic energy, respectively. These data sets go up to 55 MeV in both cases. Both files contain data for the photon energy from 0.01 MeV to the upper energy of 55 MeV.

CHAPTER 3

Monte Carlo study of Flattening Filter Free Linear accelerator

3.1 Introduction

Department of Science and Technology, Govt. of India, has entrusted the responsibility of development of indigenous medical linear accelerator (Linac) to one of its constituent units SAMEER (Society for Applied Microwave Electronics Engineering and Research) under Jai Vigyan National Science and Technology Mission. The Linac unit is named as Siddharth which is capable of delivering cost effective radiotherapy treatment in India. Presently, the Linac unit with photons of energies 4 and 6 MV is being used clinically at various hospitals in India in conventional mode i.e with FF. Due to the increase interest of operating the Linac in FFF mode, the feasibility study has been carry out for the same unit in FFF mode with 6 MV FF photon beam. Monte Carlo method has become a powerful tool in radiotherapy dose calculations and many studies have been performed using this method for studying beam characteristics of Linacs. In this thesis, the dosimetric characteristics of the indigenously developed Linac were calculated in FFF mode using Monte Carlo method and the results obtained were verified with the measurement. It may be noted that the measured data were generated in service the mode of Linac to find the feasibility for clinical use of this Linac in FFF mode.

As discussed in Section 1.3.3 of Chapter 1, FF needs to be replaced by a thin metal 'enhancer plate' in the same position of the FF. The appropriate thickness and material of the enhancer plate depends on the particular make and model a Linac. In this thesis, the optimised thickness and material of the enhancer plate i.e. FF replacement in a FFF beam for the indigenously developed Linac was investigated using Monte Carlo method. Different materials and thicknesses were investigated and their influences on the photon and electron fluences were studied at the entrance window of the monitor chamber as well as at the surface of the water phantom.

For these above studies, the user-codes BEAMnrc (Rogers et al 2016) and DOSXYZnrc (Walter et al 2016) of the EGSnrc code system (Kawrakow et al 2010) were used. The BEAMDP (BEAM Data Processor) user-code (Ma and Rogers 2004) of the EGSnrc code system was used to analyze the phase-space files and to extract the spectra of particles such as photons and electrons reaching the monitor chamber as well as at the surface of the water phantom at a SSD of 100 cm.

3.2 Simulation of Medical Linear Accelerator (Siddharth)

The geometry of indigenously developed Linac was simulated using the BEAMnrc (Rogers et al 2016) user-code of EGSnrc (Kawrakow et al 2010) code system based on the detailed design specification provided by the vendor. Different components of the Linac head such as target, primary collimator, enhancer plate, monitor chamber, and secondary collimator are accurately modeled. Figure 3.1 shows the Linac modeled in the present study. In this simulation, Z-axis is taken along the beam axis and the origin is taken at the front face of the target.
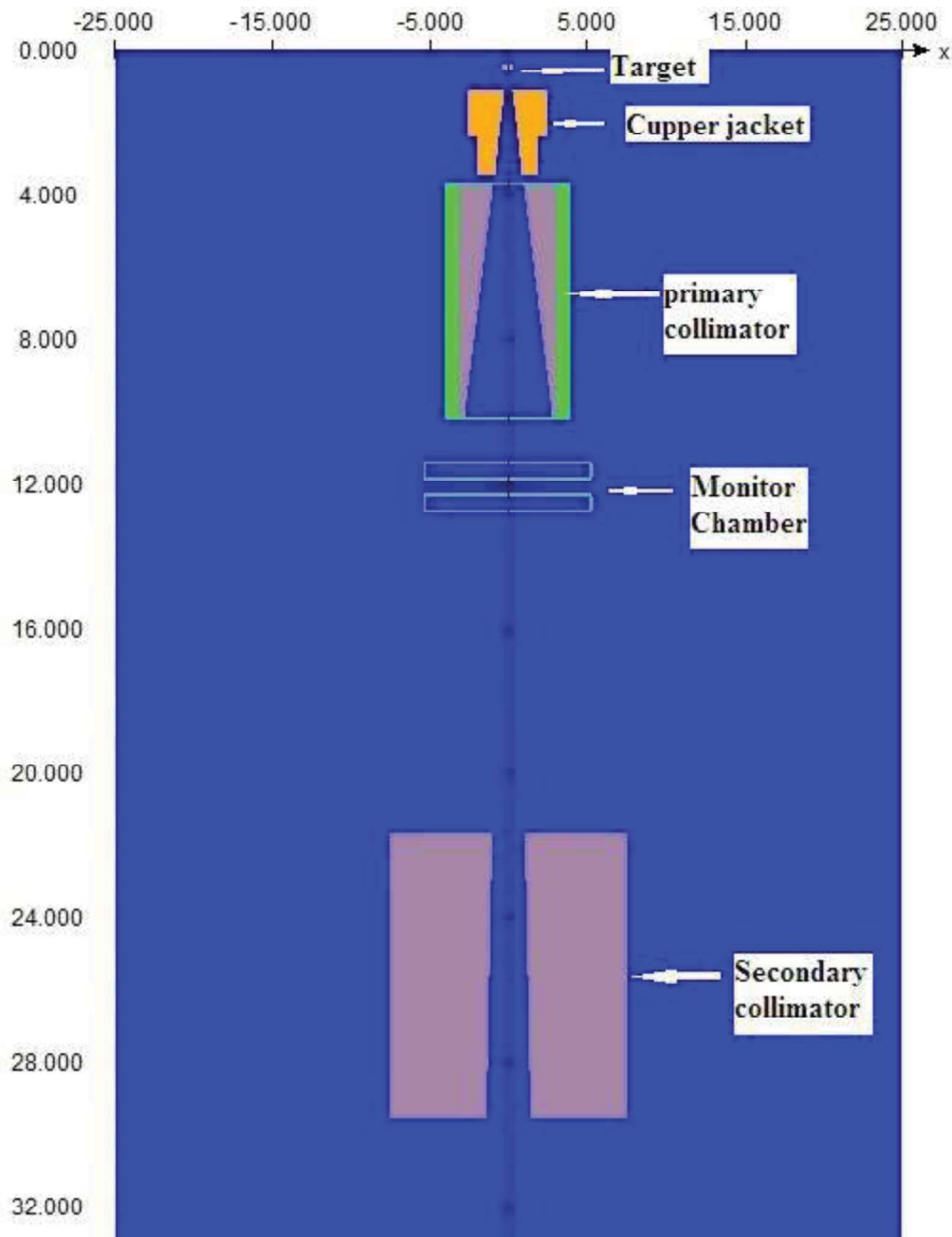
Fig 3.1 Structure of the indigenous FFF medical linear accelerator considered in the Monte Carlo-calculation. The dashed line is the Z-axis, with the positive X direction to the right and the Y direction coming out of the page. The origin is on the target surface at position 0.

Incident electron parameters play an important role on the dose distributions. In order to identify appropriate electron parameters, following three cases were studied. For each case, the kinetic energy of the incident electron was varied from 6 to 6.5 MeV (0.1 MeV increment).

Case 1 As per the manufacturer's specification, the electron beam is a point and divergent with a half-angle of 14^0. The source is positioned on Z-axis and 4 mm above the target (see Fig. 3.2). The radius of the beam at the target is 1 mm.
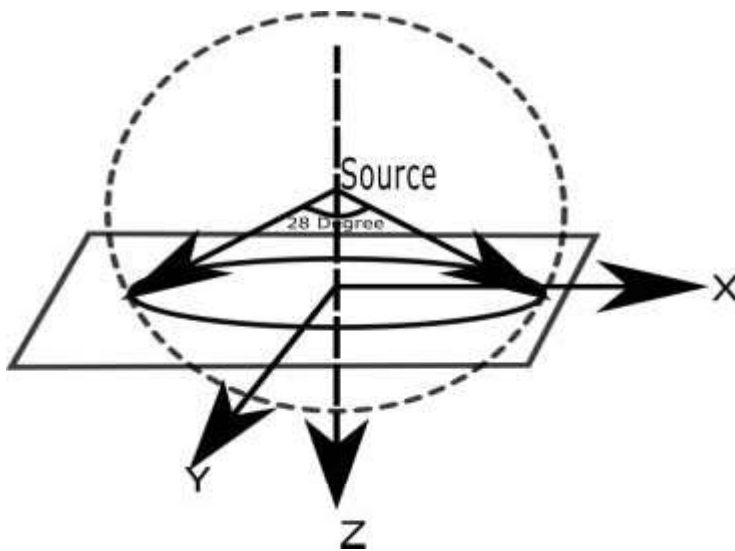
Fig.3.2 Isotropic Point Source on Z-axis (Case 1) showing the electron beam divergence angle which is the half angle of the circular field at the point of incident (14°) and the directions of X,Y and Z axes. The beam is centered on the Z axis.

Case 2 In this case, the incident electron beam is a circular parallel beam with diameter of 2 mm (see Fig. 3.3). The electron beam is incident in the XY plane.
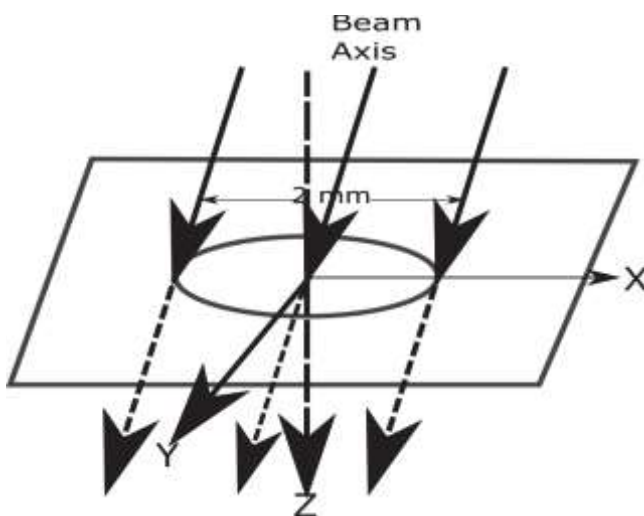
Fig.3.3 Parallel Circular Beam (Case 2) showing the beam diameter (2 mm) measured perpendicular to the beam central axis and the directions of X, Y and Z axes. The beam is along the Z-axis

Case 3 In this case, the beam is circular and the spatial distribution of electrons is defined by a Gaussian intensity distribution (see Fig. 3.4). The Full Width Half Maximum (FWHM) of the incident beam is considered to be 1 mm in both X and Y directions.
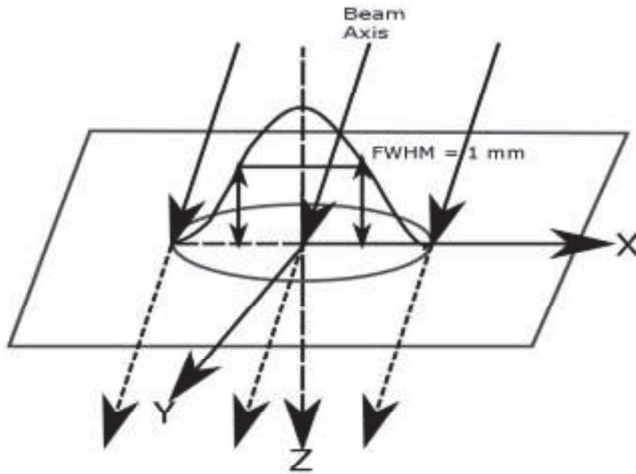
Fig.3.4 Circular Beam with Gaussian Distributions in X and Y (Case 3). The shape of the circle is defined by FWHM (1 mm) of the Gaussian intensity distributions in the X- and Y-directions respectively.

In order to identity the incident electron beam parameters initial simulations were carried out for 10 x 10 cm^2 field size and at a depth of 10 cm. Analysis of central axis percentage depth dose (PDD) data for 10 x 10 cm^2 field size and profiles (both X and Y) for 10 x 10 cm^2 field size at a depth of 10 cm, suggest that the incident electron beam energy of 6.2 MeV with Gaussian distribution of FWHM = 1 mm (Case 3) provides optimum agreement with the measurements.

3.3 BEAMnrc and DOSXYZnrc simulations

The Monte Carlo simulations were done in two steps. In the first step, a mono-energetic electron beam of kinetic energy 6.2 MeV with a Gaussian distribution of FWHM 0.1 cm was incident on the target. Phase space data was scored at a distance of 100 cm SSD for all the treatment field sizes ranging from 5x5 cm^2 to 25x25 cm^2 in an increment of 5 cm^2 using the BEAMnrc user-code of EGSnrc code system. The phase space is a set of information about the particles state (energy, position, direction etc). The electron

transport cutoff (ECUT) and photon transport cutoff (PCUT) energy was set to 0.7 and 0.01 MeV, respectively. No photon interaction forcing was used. Range rejection was turned on with ESAVE value of 0.7 MeV in the target and 2 MeV in the other part of the Linac geometries as they do not contribute significantly and helps in optimizing the computational time. The PEGS4 data set needed for the simulations was based on the state-of-art XCOM compilation (Berger and Hubbell 1987). The number of particles histories simulated in the Monte Carlo calculation was 6×10^9.

In the second step of Monte Carlo simulations, the phase space data from afore-mentioned simulations served as the source for the simulations using the DOSXYZnrc user-code of EGSnrc code system. This user-code is capable of performing 3D absorbed dose calculations in cartesian coordinates in the water phantom. In DOSXYZnrc, the water phantom size was 50 x 50 x 50 cm^3 and the phase space source was positioned on the water surface i.e at Z=100 cm. Fig. 3.5 represents the voxel phantom set up in the DOSXYZnrc simulations.
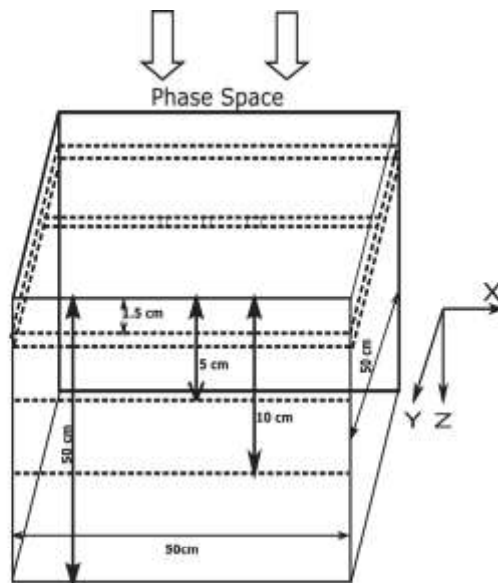
Fig. 3.5 The voxel water phantom of dimension 50x50x50 cm^3 used for DOSXYZnrc simulation. The size of voxels set for PDD and beam profile calculations (for 10 x10 cm^2 field size) were also shown.

63

The water phantom was divided into number of voxels. For high dose gradients regions, small voxel sizes were adapted. For central axis PDD simulation, up to a depth of 2 cm absorbed dose was scored in voxel dimension of 1.0 x 1.0 x 0.05 cm^3 and for depths from 2 to 25 cm voxel dimension of 1.0 x 1.0 x 0.1 cm^3 were considered. The beam profiles (both X and Y directions) were calculated at three different depths such as d_{max} (1.5 cm), 5 cm and 10 cm. For beam profile simulations, different voxel dimensions were chosen for the shoulder, penumbra and flattened regions. For example, for dose profile simulation in X-direction for a field size of 10x10 cm^2 voxel dimensions of 0.1x1.0x0.1 cm^3 (from -4.0 to +4.0) for unflattened region and 0.05x1.0x0.1 cm^3 for shoulder and penumbra regions (from -7.5 to -4.0 and +7.5 to +4.0) were used. The EGSnrc parameters set for DOSXYZnrc simulation were ECUT = AE = 0.521 MeV, PCUT = AP = 0.01 MeV. All the simulations utilized PRESTA-II electron step length algorithm. Up to $2x10^8$ particle histories were followed in the simulation. The statistical uncertainties associated with the absorbed dose values were less than 0.5 %.

3.4 Measurement of photon beam dosimetric parameters

PDD and beam profiles measurements were carried out in service mode (as FFF beam is under investigation before its clinical implementation) using PTW, Germany make RFA dosimetric system (water tank MP3-M and 0.125 cm^3 ion chamber). The measurements were performed with 1 mm resolution for PDD curves, beam profiles and $TPR_{20/10}$. Field sizes considered were from 5x5 to 30x30 cm^2 at SSD of 100 cm. Beam profiles were measured at three different depths i.e d_{max}, 5 cm and 10 cm for both X and Y directions.

3.5 Analysis of spectra

The BEAMDP user-code (Ma and Rogers 2004) of the EGSnrc code system (Kawrakow et al 2010) was used to analyze the phase-space files, extract the various types of spectra of all particles reaching the plane at SSD 100 cm and to determine the photon fluence spectra, mean energy distribution and electron contamination fluence spectra.

3.5.1 Photon fluence spectra

Photon emerging from the target passes through the primary collimator and other components of the collimating system on its way to the scoring plane at SSD 100 cm. Fig. 3.6 shows on-axis photon fluence spectra calculated at the scoring plane for different field sizes. Scoring plane is an annular region of 2.5 cm radius around the central axis.

(a)   (b)

Field size 15x15 cm² (c)

Field size 20x20 cm² (d)
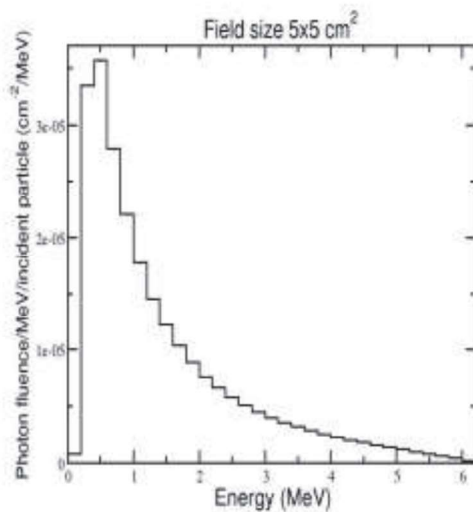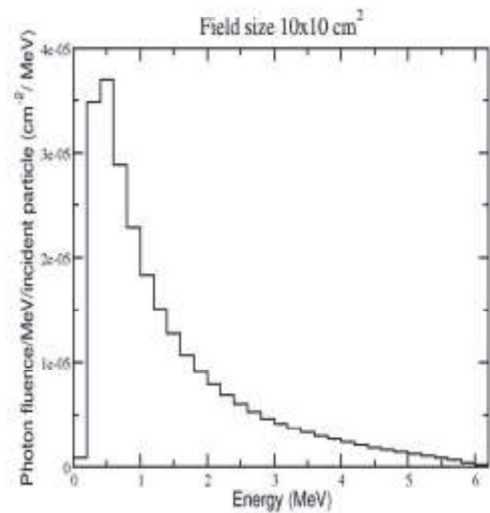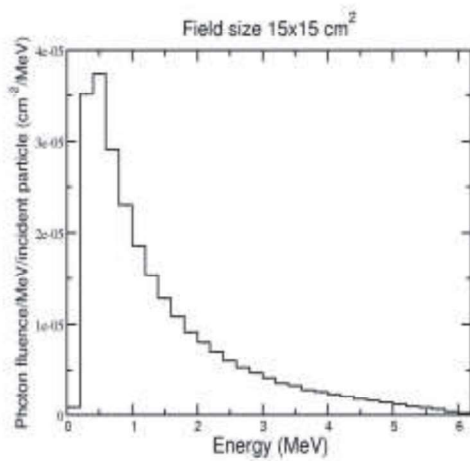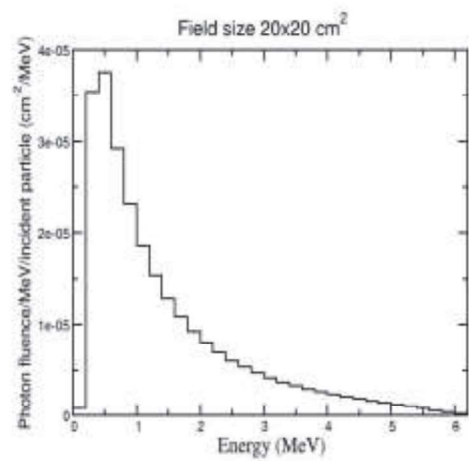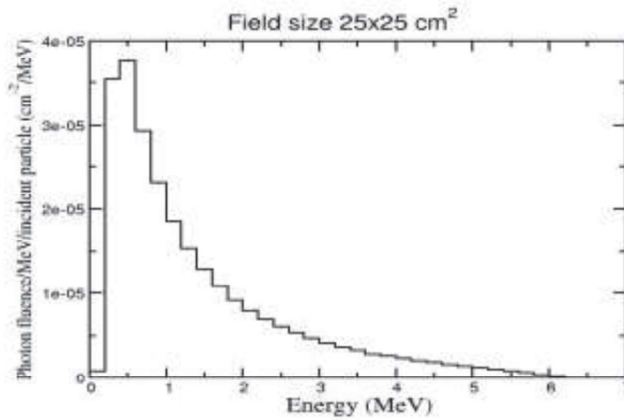
Field size 25x25 cm² (e)

Fig. 3.6Monte Carlo-calculated photon fluence spectrum for field sizes (a) 5x5 cm²
(b) 10x10 cm² (c) 15x15 cm² (d) 20x20 cm² (e) 25x25 cm².

3.5.2 Contaminant Electron fluence spectra

Secondary electrons generated from different components of the Linac head and also by the primary photons inside the phantom are the sources of contaminant electrons. Fig. 3.7 shows the calculated contaminant electrons fluence spectra along the central axis for all the investigated field sizes. The contaminant electrons fluence spectra were scored in an

annular region of radius 2.5 cm around the central axis. It is observed that the number of electrons reaching the phantom surface strongly depends upon the field size and increases with increase in field size. The mean electron fluence for field size 20x20 cm^2 was found to be 1.8 times higher than that for 10x10 cm^2 and 3.6 times for 5x5 cm^2 field size.
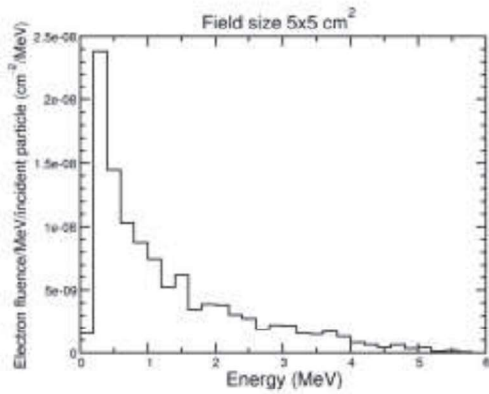
(a)
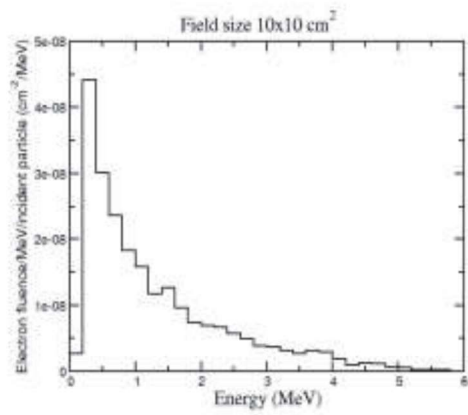
(b)
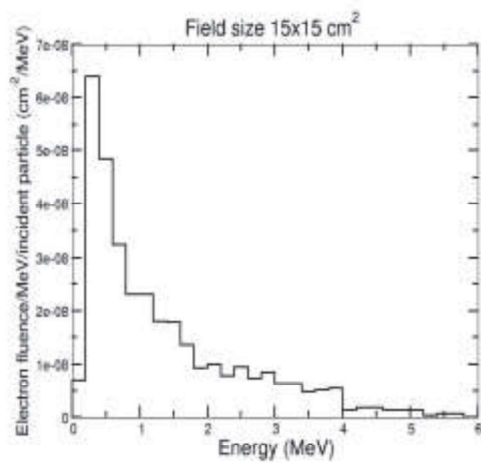
(c)
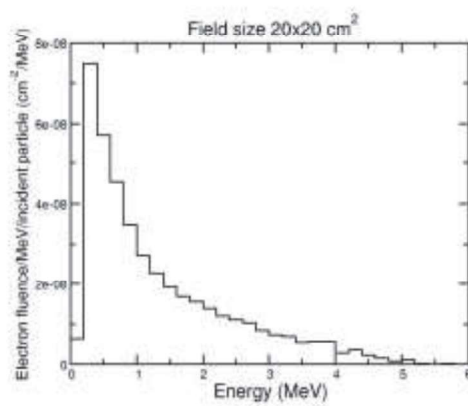
(d)
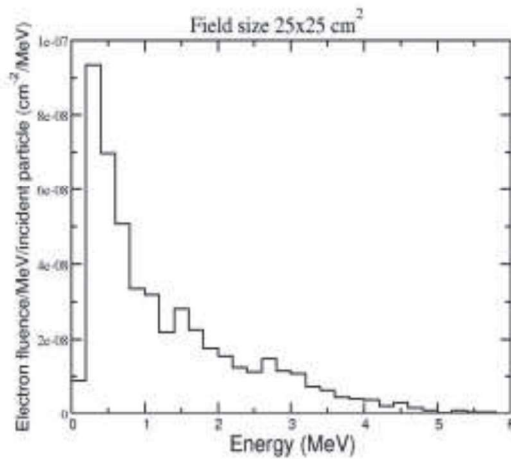
(e)

Fig. 3.7 Monte Carlo-calculated contaminant electron fluence spectrum for field sizes (a) 5x5 cm^2 (b) 10x10 cm^2 (c) 15x15 cm^2 (d) 20x20 cm^2 (e) 25x25 cm^2.

3.5.3 Mean energy

The fluence-weighted mean energies of photons were calculated for field sizes of 5x5, 10x10, 15x15, 20x20, 25x25 cm^2 and summarized in Table 3.1. The mean energy of photon decreases with the increasing field size due to the increased contribution of more low-energy scattered photons from the Linac head.

Table 3.1. Variation of mean energy and surface dose with field size for FFF indigenous Linac of photon energy 6 MV.

Field Size (cm^2)	Mean Energy (MeV)	Surface dose (%)
5x5	1.29	55.7
10x10	1.27	59
15x15	1.21	61.5
20x20	1.17	62.9
25x25	1.14	64.2

3.6 Dosimetric characteristics

3.6.1 Percentage depth dose

PDDs were calculated for depths from 0 to 25 cm for the field sizes from 5x5 cm^2, 10x10 cm^2, 15x15 cm^2, 20x20 cm^2 and 25x25 cm^2. Both the calculated and measured central axis depth-dose curves were normalized to the value of maximum dose for the respective field size on the central axis and then compared. Fig. 3.8 shows the comparison between the calculated and measured PDDs for all the field sizes studied in this work.
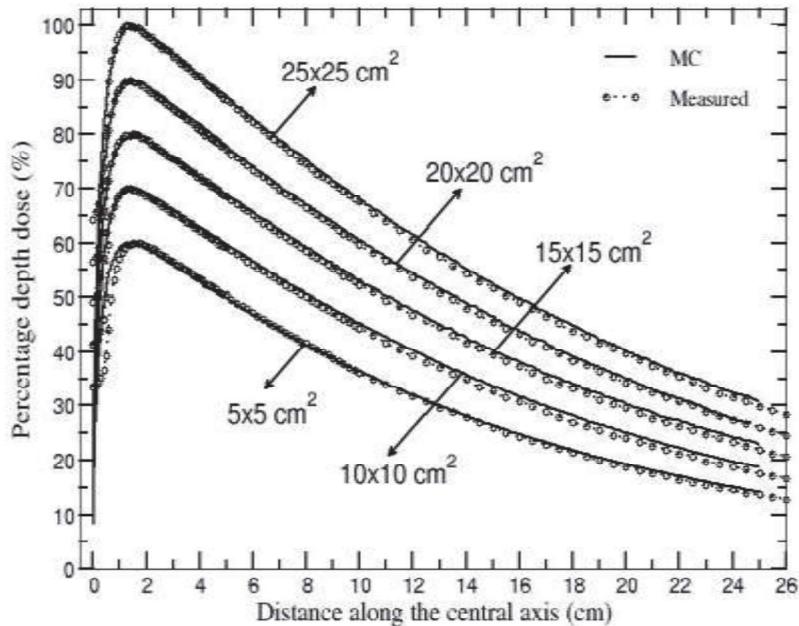
Fig. 3.8 Comparison of Monte Carlo-calculated and measured percentage depth dose curves of 6 MV FFF photon beam (at SSD=100 cm) for 25x25, 20x20, 15x15, 10x10, and 5x5 cm^2 field sizes. Depth dose profiles for 20x20, 15x15, 10x10 and 5x5 cm^2 field sizes are scaled by 0.9, 0.8, 0.7 and 0.6, respectively, for inclusion on the same graph, and all profiles are normalized at their respective value of d_{max} and multiplied by 100.

69

The dose difference between the calculated and measured PDD values were under 1 % for all the investigated field sizes. The differences between calculated and measured values were less than 1 % in the tail region and less than 0.5 % in the superficial depth region for all the investigated field sizes.

The measured d_{max} occurred at 1.4 cm for all the investigated sizes except 5x5 cm^2 for which it occurred at 1.6 cm. The Monte Carlo-calculated d_{max} occurred at about 1.5 cm for all the investigated field sizes. Depth of maximum dose was mostly constant with increase in field size for FFF beams. The measured and calculated PDD value at a depth of 10 cm for a field size of 10x10 cm^2 is about 64 % which is comparable to the literature quoted value of 63.4 % by Vassiliev et al (2006a) and Ankit et al (2017) for a FFF 6 MV Varian Clinac 21EX.

3.6.2 TPR$_{20/10}$

An energy parameter value for comparison purposes was obtained by using a TPR$_{20/10}$ ratio. The TPR$_{20/10}$ value was determined from the calculated PDD values at20cm and 10cm using an empirical approximation relation(TPR 20/10 = 1.2661 PDD 20/10 - 0.0595), where PDD 20/10 is the ratio of PDD at 20 cm to the PDD at 10 cm depth (Followill et al 1998). The calculated TPR$_{20/10}$ value was found to be 0.6385 which is in close agreement with the measured TPR$_{20/10}$ value of 0.6342.

3.6.3 Surface dose and build up dose

Surface dose or skin dose is the dose calculated at the entrance of the phantom. The surface dose for any field size is defined as the dose measured at the surface for that field size divided by the dose at d_{max} for a 10x10 cm^2 field size. The region between the surface and the point of maximum dose is called the build-up dose region. Both surface dose and

build-up region doses are affected by variation in field size. Surface dose increases with increase in field size. Table 3.1shows the variation of Monte Carlo-calculated surface dose with field size. For the first 10 mm build-up depths the dose increased from 55.7 % to 95.1%, 59 % to 98.3%, 61.5 % to 98.4%, 62.9 % to 98 % and 64.2 % to 98 % for the field sizes 5x5, 10x10, 15x15, 20x20 and 25x25 cm^2, respectively. The maximum difference was observed for smaller field size and the difference reduces with increase in field size. Surface dose for a field size of 10x10 cm^2 is 59 % which is comparable to the literature quoted value of 56.2 % by Ankit et al (2017).

3.6.4 Beam Profiles

The beam profiles (both X and Y directions) were calculated at three different depths of d_{max} (1.5 cm), 5 cm and 10 cm for the above field sizes. All the beam profiles were normalized to their central axis value. As there is symmetry between X and Y profiles, only X profile is presented. Fig. 3.9 shows the comparison of Monte Carlo-calculated and measured beam profiles obtained at 100 cm SSD for the investigated field sizes at depths of d_{max} and 10 cm inside the water phantom in X direction. The agreement between calculated and measured dose values was within 1 %, except for the penumbra region where the maximum deviation was about 2.6 %. At the d_{max}, the agreement between the calculations and measurements is about 2 % in the flat region and about 3 % in the penumbra region.
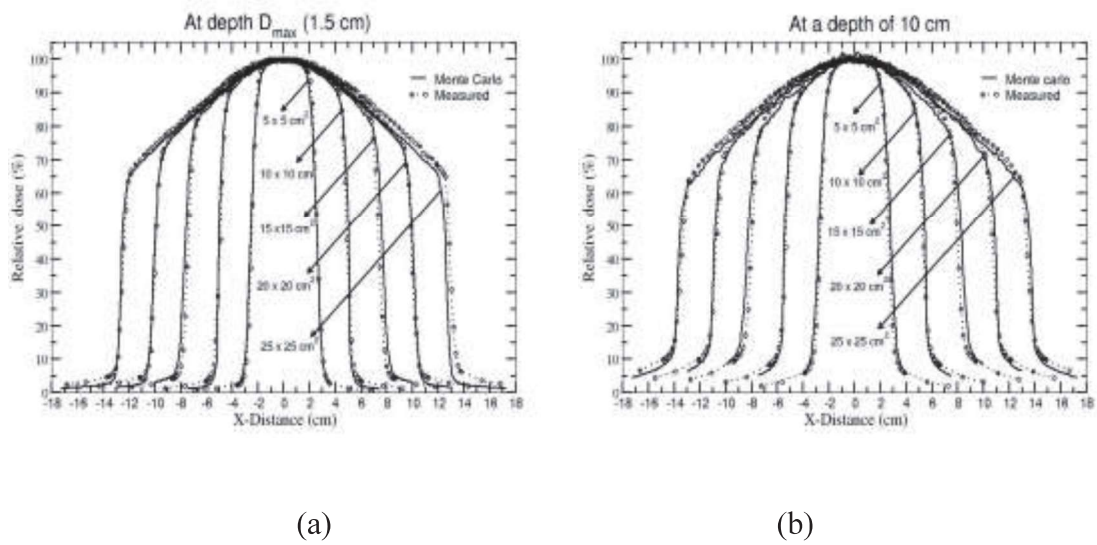
Fig. 3.9 Comparison of Monte Carlo-calculated and measured X-profiles of all the investigated field sizes. All profiles are normalized to the central axis dose and multiplied by 100 (a) at d_{max} (1.5 cm) depth (b) at 10 cm depth.

3.7 Optimum thickness and material of enhancer plate

The main roles of enhancer plate material are:

1. To generate electrons which provide build-up dose to the ionisation chamber to give sufficient signal and position-dependant information to the servo plates. They, in turn, can then operate correctly to control the beam quality and steering.

2. To remove the contaminant electrons generated from the primary collimator and target, which do not provide useful position information but do increase surface dose to the patient.

3. To prevent the direct incident of the electron beam on the patient in the unlikely event of a target failure.

In the present study, optimized thickness and material of enhancer plate was calculated for the indigenously developed FFF Linac. Materials Copper (Cu), Aluminum (Al) and

combination of both (Cu and Al) of varying thicknesses were considered as enhancer plate material since these two materials are commonly used in other commercially available FFF Linacs. Further, the effect of atomic number (Z) of enhancer plate material could also be investigated. The thicknesses considered were chosen keeping in view of the above three roles of enhancer plate. For satisfying the role 1 criteria, the thickness of the enhancer plate material should be such that, the electron fluence generated at the plane of Monitor Chamber should be equal to or more than the electron fluence generated with the same model of Linac with FF at the place of enhancer plate at the plane of Monitor Chamber. For satisfying the role 2 and 3 criteria, the thickness of the enhancer plate material should be such that, the thickness should be equal to or greater than the CSDA range (13 mm for Al and 5 mm for Cu) of the incident electron beam.

For the above purposes, thickness and materials considered were 14 mm Al, 6 mm Cu, 7 mm Al + 1 mm Cu, 7 mm Al + 2 mm Cu, 5 mm Al + 1 mm Cu, 5 mm Al + 2 mm Cu, 3 mm Al + 1 mm Cu and 3 mm Al +2 mm Cu. In the Monte Carlo calculations, phase space files were generated at the plane of Monitor Chamber as well at the surface of the phantom (at 100 cm) for a field size of 10x10 cm^2. The electron fluence spectra obtained at the plane of Monitor Chamber for the above thicknesses were shown in Fig. 3.10.
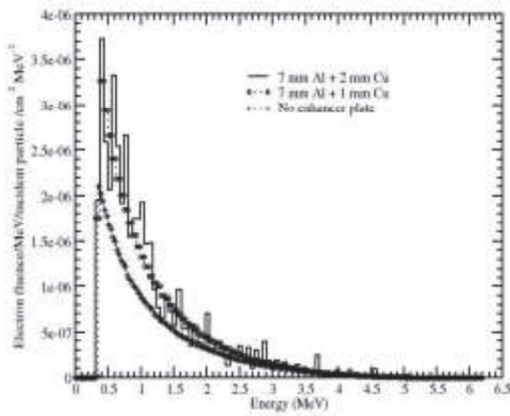
(a)
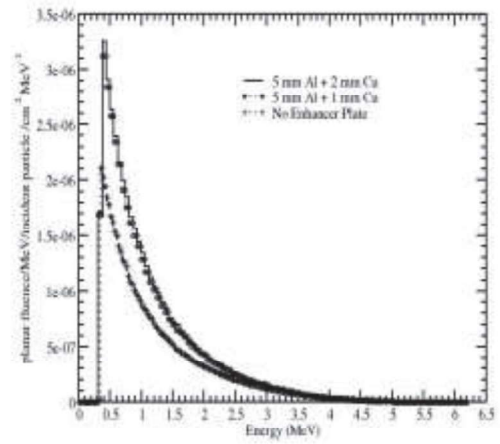
(b)
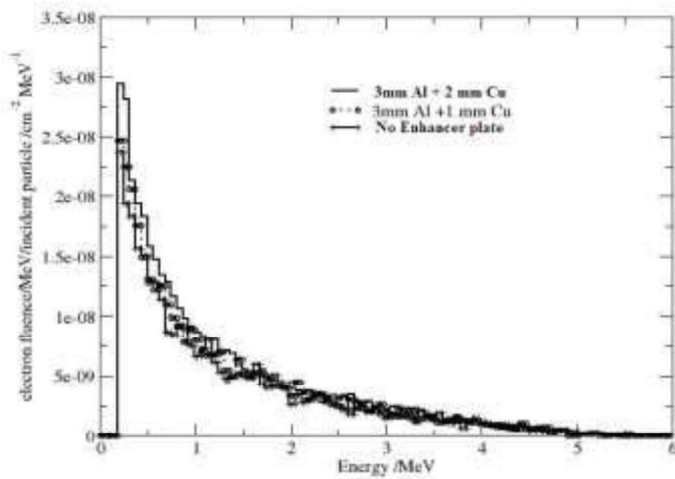
(c)

Fig. 3.10 The electron fluence spectra obtained at the plane of Monitor Chamber for the various thicknesses (a) 7 mm Al + 1 mm Cu, 7 mm Al + 2 mm Cu, and no enhancer plate(b) 5 mm Al + 1 mm Cu, 5 mm Al + 2 mm Cu and no enhancer plate, (c) 3 mm Al + 1 mm Cu, 3 mm Al + 2 mm Cu and no enhancer plate.

The results obtained from the study indicate that higher thicknesses approximately 6 mm of Cu or 14 mm of Al is needed to absorb the electrons in the case of target failure if the

CSDA range of Cu and Al is considered. However, 2 mm Cu or 7 mm Al is sufficient to create electron fluence useful for steering of the beam and reducing the surface dose (to satisfy role 1).

Using Cu as an enhancer plate also increases the surface dose about 6 % more as compared to the equivalent CSDA thickness of Al due to the production of more low energy bremsstrahlung photons that reaches the patient plane as compared to Al. The enhancer plate was optimized with layer of low Z material such as Al at the top facing the incident beam (so that less bremsstrahlung is produced) and then a layer of high Z material such as Cu which will attenuate the bremsstrahlung. Therefore, it was predicted that, the combination of 3 mm Al and 1 mm Cu would be the appropriate enhancer plate material and thickness for the indigenously developed FFF Linac. With this combination the electron fluence was found to be comparable with the aforesaid results. In this combination the surface dose was found to be 57 %, whereas the measured surface dose was obtained as 59 % for the indigenously developed Linac with no enhancer plate.

3.8 Summary and Conclusions

In this study, a Monte Carlo model of indigenous FFF Linac (6 MV) has been developed using the Monte Carlo-based BEAMnrc user-code of the EGSnrc Monte Carlo code system. The dosimetric parameters such as PDD and beam profile were calculated using DOSXYZnrc user-code. Phase space files were analyzed using BEAMDP user-code of EGSnrc code system. This Monte Carlo model was benchmarked against the measured data. The differences between calculated and measured PDD values were less than 1% in the tail region and less than 0.5 % in the superficial depth region for all the investigated field sizes. The d_{max} was occurred at 1.5 cm and mostly remained constant with field size.

Surface dose and build-up region doses vary with field size. Surface doses increases with increase in field size. Results indicate good agreement between Monte Carlo-calculated and measured lateral beam profiles (X and Y) obtained at SSD = 100 cm for all the investigated field sizes at depths of d_{max}, 5 cm and 10 cm. The difference between calculated and measured dose values are less than 1 %, except for the penumbra region where the maximum deviation between calculated and measured dose values are found to be around 3 % (at depth d_{max}).

In addition, the optimized enhancer plate material and thickness were also investigated in this study. Copper and Aluminum were considered as enhancer plate material since these two materials are commonly used in other FFF Linacs. Different thicknesses of Al, Cu and combination of both Cu and Al were investigated. It was found that, higher thicknesses approximately 6 mm of Cu or 14 mm of Al is needed to absorb the electrons in the case of target failure if the CSDA range of Cu and Al is considered. However, 2 mm Cu or 7 mm Al is sufficient to create electron fluence useful for steering of the beam and reducing the surface dose. Using Cu as an enhancer plate also increases the surface dose about 6 % more as compared to the equivalent CSDA thickness of Al. The combination of 3 mm Al and 1 mm Cu was found to be the appropriate enhancer plate material for the indigenously developed FFF Linac.

CHAPTER 4

Structural shielding design of Flattening Filter Free Linear accelerator bunker: Indian Scenario

4.1 Introduction

The beam characteristics of a Linac operated in FFF mode is different from the Linac with FF mode. As a result, the shielding parameters such as the tenth-value layers and scatter fractions, calculated for flattened beams may not be appropriate for shielding evaluations of FFF beams (Stephen et al 2009, Dalaryd et al 2010, Julia et al 2014). FFF beam is mostly used for advanced modalities which require higher MUs to be delivered. Hence, it must be determined whether vault shielding need to be enhanced or reduced for a Linac operated in FFF mode in comparison to FF mode.

Considering the Linac with FFF beam available in India and their growth, this study was carried out to find the impact of FFF beam on bunker design of a Linac facility in Indian scenario. The structural shielding requirements of 6 MV Linac operated in both FF and FFF modes in comparison to a standard 6 MV Linac operated only in FF mode was assessed . The Linac bunker is comprised of primary and secondary barriers. This study includes the detailed calculations of thicknesses required for shielding of primary and secondary barriers of Linac bunker for 6 MV FF and FFF photon beams. For the Linac bunker design several points must be considered such as location, Workload, use, permissible limit to be achieved, occupancy all around the installation, shielding materials etc. In general, a conservative approach should be followed to ensure the maximum radiation safety for radiation worker and general public. Protection is required against three types of radiation: (i) primary radiation, (ii) scattered radiation and (iii) leakage radiation through the source housing. A barrier is sufficient to attenuate the direct useful beam to the required degree is called the primary barrier. A primary barrier is required where the main radiation beam can strike i.e. two sides of the four walls, ceiling and floor. The barrier to provide protection against stray radiation (leakage and scatter) is

78

called the secondary barrier. Primary barriers are much thicker than the secondary barriers. Similarly few additional factors are also considered such as controlled areas and uncontrolled areas. A control area is a limited access area in which the occupational exposure of personnel to radiation or radioactive material is under supervision of an individual in change of radiation protection such as Radiological Safety Officer. That is the access, occupancy & working condition are controlled for radiation protection e.g. control consoles, treatment rooms etc. Uncontrolled areas for the purpose of radiation protection are all other areas (other than controlled areas) in the hospital & the surrounding environments e.g. office rooms, examination room, rest room etc.

Considering the shielding design goals and effective dose, it is not possible to base shielding design directly on Effective dose (E), set by the National Regulatory Authority, as it is complex to determine. Therefore, design goal (to achieve the radiation levels within the permissible limit, P) is used in the design calculations and evaluation of barriers constructed for the protection of workers or members of the public. In India, Atomic Energy Regulatory Board (AERB) is the National Regulatory Authority empowered to prescribe the dose limits. Permissible dose limit for the area occupied by:

(i)   Radiation worker = 20mSv/y = 40mR/wk

(ii)   Member of the public = 1mSv/y = 2mR/wk

The above values were considered in this study.

There are recommended guidelines for calculating these barrier thicknesses such as NCRP Report No. 151 (2005), IAEA Safety Report Series No. 47 (2006), IPEM Report No. 75 (1997) and they can also be based on different assumptions. In this study, calculations were carried out by two methods, one by using the approach stipulated in

NCRP Report No. 151 and the other one is based on the MUs delivered in clinical practice considering the workload as a most significant factor. In the recent time several technical changes have been augmented in the treatment delivery modality which enables higher dose escalation to tumor and rapid dose fall off outside the tumor. The technologies involved for such delivery enhances the MUs generated from the Linac due to presence of different beam modifying techniques. This study also includes the radiation protection survey all around the installation.

4.2 Shielding materials and bunker design features

Selection of shielding materials is very important while designing a radiation bunker. It may vary depending upon the space available for setting-up the facility. Building to house radiation treatment facilities, concrete is usually the material of choice since it is the least expensive. However, if space is at a premium (or constrained) it may be necessary to use a higher density building material. Density in concrete is usually taken as 2.35 gm/cm^3. However, density will depend upon aggregate used. At radioherapy energies, Compton scattering dominates and the shielding material will absorb the radiation according to density of the material. Some of the materials and their density are listed as below:

Building material	density (gm/cm^3)
Concrete	2.35gm/ cm^3
Heavy concrete	> 2.35gm/ cm^3
Lead (Pb)	11.35gm/ cm^3
Steel	7.9gm/ cm^3
Earth	1.6 gm/ cm^3

For therapy installation operating above 10 MV, shielding against neutrons must be considered because of production of Photo neutrons (γ, n) in both the accelerator head and the room shielding. Photo neutrons produced when the primary photons have energies above the neutron binding energy of roughly 8 MeV for most nuclides. Photo neutron yields from most of the accelerator do not become significant until the incident energy exceeds 10 MeV.

Concrete contains relatively high hydrogen content and is therefore efficient at shielding against fast neutrons. Boron and Cadmium have large cross section for the capture of slow neutrons. Boron is incorporated into polyethylene which has high hydrogen content to form an efficient neutron shield. Slow neutron capture in the boron results in the production of a low energy gamma ray of 0.473 MeV. A 5 % composition by weight of boron (B10) in polyethylene is commonly used in neutron shielding door in treatment rooms. Similarly, Polyethylene and Paraffin both materials are used for neutron shielding. Paraffin, sometimes called paraffin wax has the same percentage of hydrogen (14.3 %) as polyethylene and is less expensive. However, it has lower density and is flammable so it is voided in any permanent barriers. Polyethylene, is perhaps the best neutron shielding material available, and it is relatively expensive. It is available both pure and added with varying percentage of boron to increase the thermal upon capture.

Concrete is most commonly used material because it is readily available as well provide good X-ray shielding, structural strength and neutron shielding, its density is 2.35 g/cm^3. This density may vary depending on aggregate used. A concrete with a density of more than 2.35 g/cm^3 can be considered heavy concrete. Heavy concrete usually used where space is at a premium. The increased density is achieved by adding various higher density

aggregates to concrete to increase photon attenuation, among those are iron ores and minerals such as limonite, barium minerals such as barites etc. The density can range up to 5.2 g/cm^3 for ores, 4.4 g/cm^3 for barium minerals and more than 7 g/cm^3 for ferrous materials. Lead has a very high density of 11.3 g/cm^3 and is an excellent shielding material for X-rays and gamma rays. However, it has several drawbacks such as lack of structural integrity as it is malleable. It needs to be sandwiched between either concrete or steel. It is transparent to fast neutrons and it has high neutrons production cross section for high energy photons and low absorption cross section for neutrons. This restricts the use of lead as a shielding material for accelerator operated above 10 MV. Also lead is toxic in nature. Steel is relatively expensive in comparison to concrete but not toxic like lead. The density of steel is 7.9 g/cm^3. It is also nearly transparent to neutrons but does reduce neutron energy. Steel is a good structural material.

Earth is also commonly used as a shielding material at radiotherapy facilities partially or entirely underground. Earth is not a well-defined material and its density can vary considerably. However, it is sufficient to consider it as equivalent to concrete with a density of 1.5 g/cm^3.

4.2.1 Design features of a radiotherapy installation

Radiotherapy departments are usually located on the periphery of the hospital complex to avoid radiation protection problems arising from therapy rooms being adjacent to high occupancy areas. It should preferably be located in the basement to reduce the shielding costs. However, cost should be weighed against the expense of excavation, watertight sealing and providing access, provision for future expansion, increased workload and operational efficiency when locating a therapy installation.

Access to the treatment room for delivery, movement of patient and replacement of the treatment unit or major components must be considered. There should be conduit in one of wall of the treatment room for dosimetry equipment cable. This dosimetry duct (conduit) should always be through secondary barrier so that primary beam can never strike it and should be at an angle of nearly 45º.

In the context of room size, the machine manufacture's pre-installation manual provides the minimum dimensions (length, width and height). The room should be large enough to allow full extension of the couch (table top) in any direction with space margin for the operator to wall around it and safe movement of gantry along with gantry mounted components. The desirable size also depends upon the type of treatments e.g. for a Total Body Irradiation (TBI) procedure it will require a larger treatment distance to one wall.

In order to reduce the radiation dose near the entrance to the room, restricted access passage way leading to the room should be incorporated in design. This passage way is termed as maze. The minimum width may be determined by the dimensions of the treatment unit to be delivered by this route or for taking bed ridden patient into treatment room. Since, the treatment room containing the radiotherapy equipment will be controlled area and therefore it is highly recommended that a barrier should be installed at the entrance to maze or treatment room to restrict the access during exposure. All the doors must be interlocked to the treatment unit to prevent an exposure if a door is open. The interlock must also ensure that when the door is opened the irradiation will be terminated. The radiation output of the device should not be resumed automatically after the door is closed again.

Another area need to be identified where the control console of the equipment will be installed and operator control the machine using various features available at the control panel. This area should be close to the entrance to the treatment entrance room so that the operators can view the entrance area. The control area should be sufficiently large to accommodate the treatment unit control console and associated equipment.

4.3 Calculation based on NCRP 151

A standard layout of 6 MV accelerator bunker with room layout and cross sectional layout used in this study is presented in Fig. 4.1.
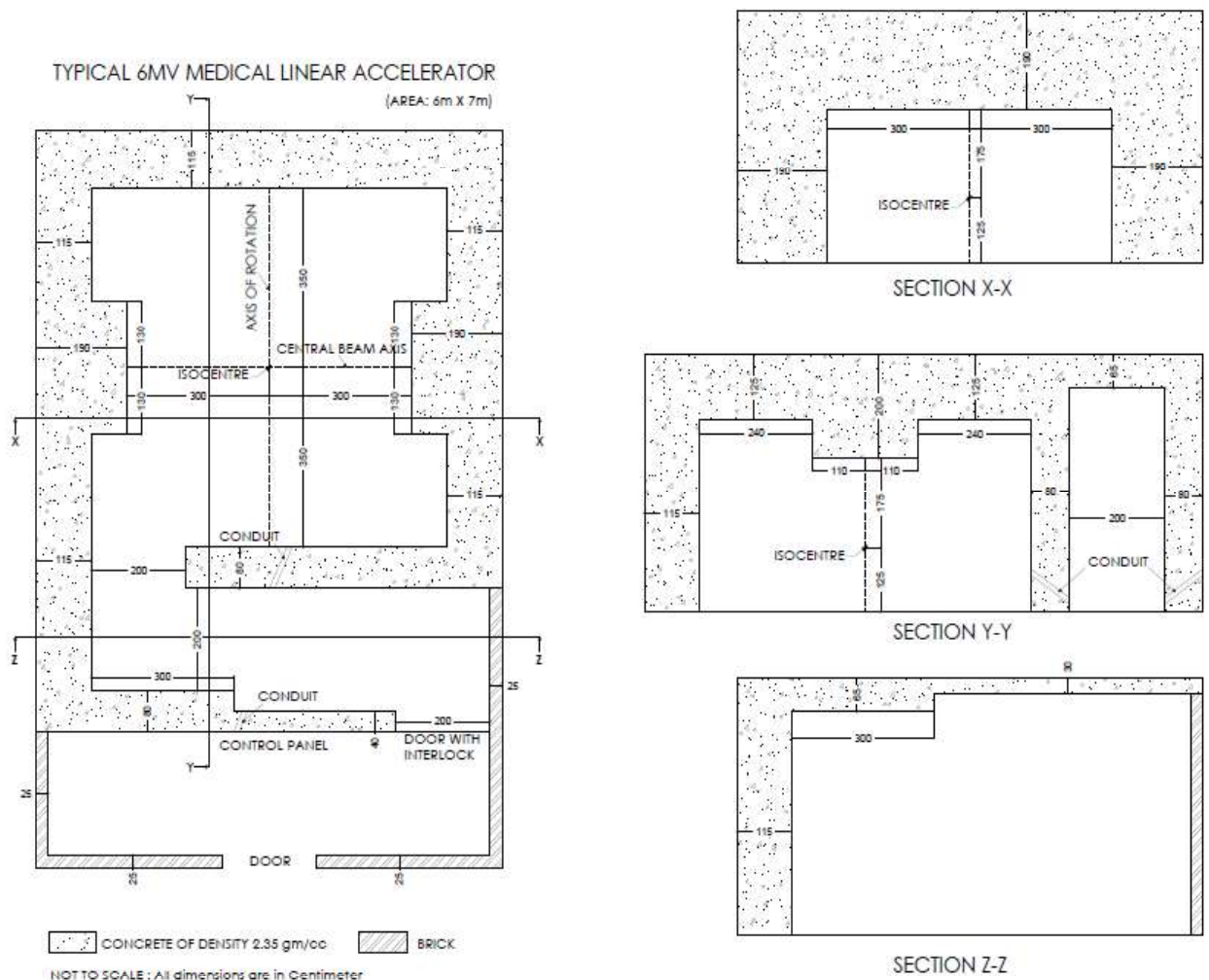
Fig.4.1. Standard layout of a 6 MV Linac bunker.

Radiation generated by Linac can be divided into primary and secondary components, the latter can further be divided into scatter and leakage radiation. The calculations for basic shielding parameters includes Workload (W), Use Factor (U) , Occupancy factor (T), distance from the radiation source (d) and permissible dose limit (P) as prescribed by the regulatory authority of the country and are briefly described as below.

4.3.1 Workload (W): Workload of a Linac is usually stated in terms of weekly dose delivered at 1 m from the source. This is estimated by multiplying the number of patients treated per week with the dose delivered per patient at 1m distance. It is the time integral of the absorbed dose rate at the depth of the maximum absorbed dose at 1 m from the source considering maximum possible number of the patient treated and physics work. The most common period of time over which W is specified is one week and is expressed in cGy/wk at 1m. Here we have considered only the delivered radiation dose for clinical use. Physics workload is not included since it is significantly less except during commissioning measurements and during measurements after major repair work. W is calculated as below by considering an average of 200 cGy dose given per patient at 10 cm as the average depth of dose delivery in clinical cases:

$$W = D_P \times N_P \times N_d \times \frac{1}{DD_{10}} \tag{4.1}$$

Where D_P is dose (in cGy) delivered per patient, N_P is number of patients treated per day, N_d is number of days per week, DD_{10} is central axis dose at 10 cm depth normalized to dose value where dose maximum occurs.

In conventional FF Linacs the workload has been calculated considering 70 number of patients treated in a day and 5 days in a week. However, based on the clinical data it is observed that number of patients treated in a Linac capable of delivering FF and FFF beam is maximum 50 instead of 70. Using equation 4.1, W is found to be around 33 %

less for FFF beam than the W calculated for FF beam (i.e W is about 1.04×10^5 for FF and 0.78×10^5 for FFF). Further, it is also noted that in clinical practice around 80 % of the patients are treated in FF mode and 20 % in FFF mode, W is calculated by using the weighted W for FF and FFF beams i.e.

Total workload, $W = 0.8 \ast W_{FF} + 0.2 \ast W_{FFF}$ (4.2)

Percentage depth dose (PDD) at a depth of 10 cm for FF beam reported by Vassiliev et al (2006) is 66.1 % whereas for FFF beam it is 63.4 %. Using $D_P = 200$ cGy/patient, $N_d = 5$ for FF and FFF and using $N_P = 40$ and $DD_{10} = 0.661$ for FF and $N_P = 10$ and $DD_{10} = 0.634$ for FFF, total workload, W is:

$W = 0.76 \times 10^5$ cGy/wk @1m (4.3)

4.3.2 Use factor (U): U is the fraction of the operating time during which the radiation under consideration is directed toward a particular barrier. Although the use factors vary depending on the techniques used in a given treatment facility, if conventional treatment techniques are to be used, beam that rotates about an isocentre will usually have symmetric distribution of gantry treatment angles and these will be predominantly in the four primary angles 0^0, 90^0, 180^0 and 270^0 facing floor, left side primary barrier, ceiling and right side primary barrier respectively. Thereby, U is assumed to be 0.25 for each primary barrier and 1 for secondary wall.

4.3.3 Occupancy factor (T): T is the fraction of the operating time during which the area of interest is occupied by any individual. Areas that are intermittently occupied, such as corridors, would have a slightly greater occupancy and an area such as an office even greater. All things being equal, an adjacent area that is occupied more often will require more shielding. The occupancy factor for an area should be considered as the fraction of

time spent by a single person who is there the longest. Based on occupancy, the occupancy factor is assumed to be full (T = 1), partial (T = 1/4) or occasional (T = 1/16). In this study T is considered as 1 for all the locations.

4.3.4 Distance (d): The distance in meters from the radiation source to the area to be protected becomes a parameter to calculate the barrier thickness. Because of the Inverse square law, which is assumed for both the primary and stray radiation, the barrier thickness reduces as the distance of the area to be protected increases.

4.3.5 Permissible dose limit (P): The design philosophy for the radiation barriers will depend on the dose limits in force. For protection calculations, the dose equivalent limit is assumed to be 400 µSv/wk for occupational worker and 20 µSv/wk for public, which correspond to AERB directives of annual dose limits of 20 mSv in one year and 1mSv in one year, respectively. The desired radiation levels or the design goal are expressed most often as weekly values since the workload for a radiotherapy source has traditionally utilized a weekly format.

4.3.6 Primary barrier:

Expression for the reduction factor (RF) to achieve the radiation level 'P' is given by,

$$RF = \frac{WUT}{Pd^2} \qquad (4.4)$$

Where, W, U, T, P and d are having their usual meaning. Then the primary barrier thickness (t_{pri}) can be determined by using number of tenth value layers (TVLs), n, based on energy of the treatment unit and the type of shielding material being used.

$$t_{pri} = n \times TVL = \log(RF) \times TVL = \log\left\{\frac{WUT}{Pd^2}\right\} \times TVL \qquad (4.5)$$

It may be noted that wall thicknesses determined for primary barriers will be more than the thickness required to shield leakage and scattered radiation, which are comparatively insignificant and hence no further calculations are required. The values of TVL reported for corresponding energy of FF and FFF beams are different (Stephen et al 2009) and accordingly they have been used in our calculation.

For primary barriers, the values of U and T are 0.25 and 1 respectively. Thickness for primary wall was calculated using equation 4.2 and published value of TVL for FF and FFF beam for concrete of density 2.35 g/cm^3 (Stephen et al 2009). Since, the initial considerations are 1m from source to isocenter distance and a clearance of 3m from isocenter to the point of interest where the P value is desired, calculations have been carried out for multiple iterations till the thickness becomes constant. It is found that primary barrier thickness for a Linac operated in FF mode is higher by 24 % to that a Linac operated in both FF and FFF modes with an assumption that only 20 % of the workload is shared in FFF mode.

4.3.7 Secondary barrier: These barriers are not in the direct line of the radiation beam but necessary to shield from leakage radiation from the treatment head and scatter from the patient and the treatment room walls.

4.3.7.1 Leakage Radiation: IEC standards state that the leakage from the treatment head of a Linac shall not exceed 0.5% of the primary beam and a maximum of 0.2% over 2m radius measured from the central axis at isocentre (IEC 60601-2-1 1998). In general, manufacturers provide adequate shielding on head of the Linac resulting in leakage of less than 0.1% of primary. Therefore, it is reasonable to take leakage as 0.1% in the

shielding calculations. RF required to achieve design goal (P) against head leakage radiation is as follows:

$$RF = \frac{\alpha_0 WUT}{P(d_s)^2} = \frac{0.001 \times WUT}{P(d_s)^2} \tag{4.6}$$

Where, α_0 is the leakage from the head (0.1%), d_s is the distance from the isocentre to the point of interest in meters. U is unity for secondary barriers. Then the secondary barrier thickness $(t_{sec})_L$ can be determined as,

$$(t_{sec})_L = n \times TVL = \log(RF) \times TVL = \log \left\{ \frac{0.001 \times WUT}{P(d_s)^2} \right\} \times TVL \tag{4.7}$$

For secondary barrier thickness calculations, the total radiation level is contributing with respect to head leakage as well as scatter from patient. The thickness required was calculated using equation 4.4 and found that the secondary barrier thickness for a Linac operated in FF mode only is higher by 26 % to that a Linac operated in both FF and FF mode with an assumption that only 20 % of the workload is shared in FFF mode.

4.3.7.2 Scattered Radiation

Patient scatter: RF of radiation scattered by the patient to achieve design dose limit (P) is given by:

$$RF = \frac{\alpha_s WUT \left(\frac{F}{400} \right)}{P(d_{sca} \times d_s)^2} \tag{4.8}$$

Where, P, W and T have their usual meaning. The scatter to primary ratio (α_s) depends on the energy of the photon and the scattering angle. Values of α_s are available per 400 cm^2 irradiated field area for all clinical beams, F is the field area incident on the patient in cm^2, d_{sca} is the distance from the radiation source to the patient in meters, d_s is the distance from the patient to the point of interest in meters. Radiation scattered by a patient is

usually less than 0.1 % of the incident radiation per 1000 cm^2 (= 0.1 m^2) area irradiated. For large scatter angles, the energy of the scattered radiation will be degraded and the protection designed against leakage radiation should provide adequate protection against scattered radiation from the patient.

Wall scatter: RF against scattered radiation when the primary beam strikes a wall is given by the following expression:

$$RF = \frac{\alpha_{w,s}AWUT}{Pd_w^2 d_r^2}$$
(4.9)

Where, $\alpha_{w,s}$ is the wall reflection coefficient, which depends on the wall material, scattering angle and beam energy. A is the field area projected on the scattering surface (wall) in m^2, d_w is the distance from the radiation source to the scattering surface (wall) in m, d_r is the distance from the scattering surface (wall) to the point of interest, in m. The photons scattered by the wall and by the patient are of about the same energy. If the thickness required to shield from patient scatter is different from that needed to shield from wall scatter by one TVT or more, the larger thickness is used, otherwise, one HVT is added to the larger thickness. Similarly, one HVT is added to higher thickness, if the thickness required to protect from leakage differs from that required to protect from scatter by less than one TVT.

Roofs: The roof section that can be struck directly by the primary radiation is also a primary barrier and the formula used to determine the required thicknesses are the same as that for primary.

Mazes: Since for X-ray units (accelerator) operating below 10 MV there is no production of neutron, the scatter and transmission of primary, leakage and scattered radiation need to be considered while estimating dose at maze entrance.

When the gantry rotation axis is perpendicular to the maze axis, the total dose at the entrance door i.e. D_d (Photon dose) will be given by:

$$D_d = \sum_G D_P + \sum_G f \times D_W + \sum_G D_L + \sum_G D_T \tag{4.10}$$

Where, $\sum_G$ integrates through all gantry angles, D_P is the dose arising from patient scatter, f is the primary radiation transmitted through the patient, D_W is the primary radiation scattered by the wall into the maze, D_L is the leakage radiation scattered down the maze (see Fig. 4.2), D_T is the leakage radiation transmitted through the maze wall. When gantry rotation axis is parallel to the maze axis (i.e. maze is a primary barrier), the above expression can be written as:

$$D_d = \sum_G D_P + \sum_G f \times D_{W,T} + \sum_G D_L + \sum_G D_T \tag{4.11}$$

All the symbols have the same meaning except $D_{W,T}$, which will be primary radiation transmitted through the maze wall and further scattered to the maze entrance.
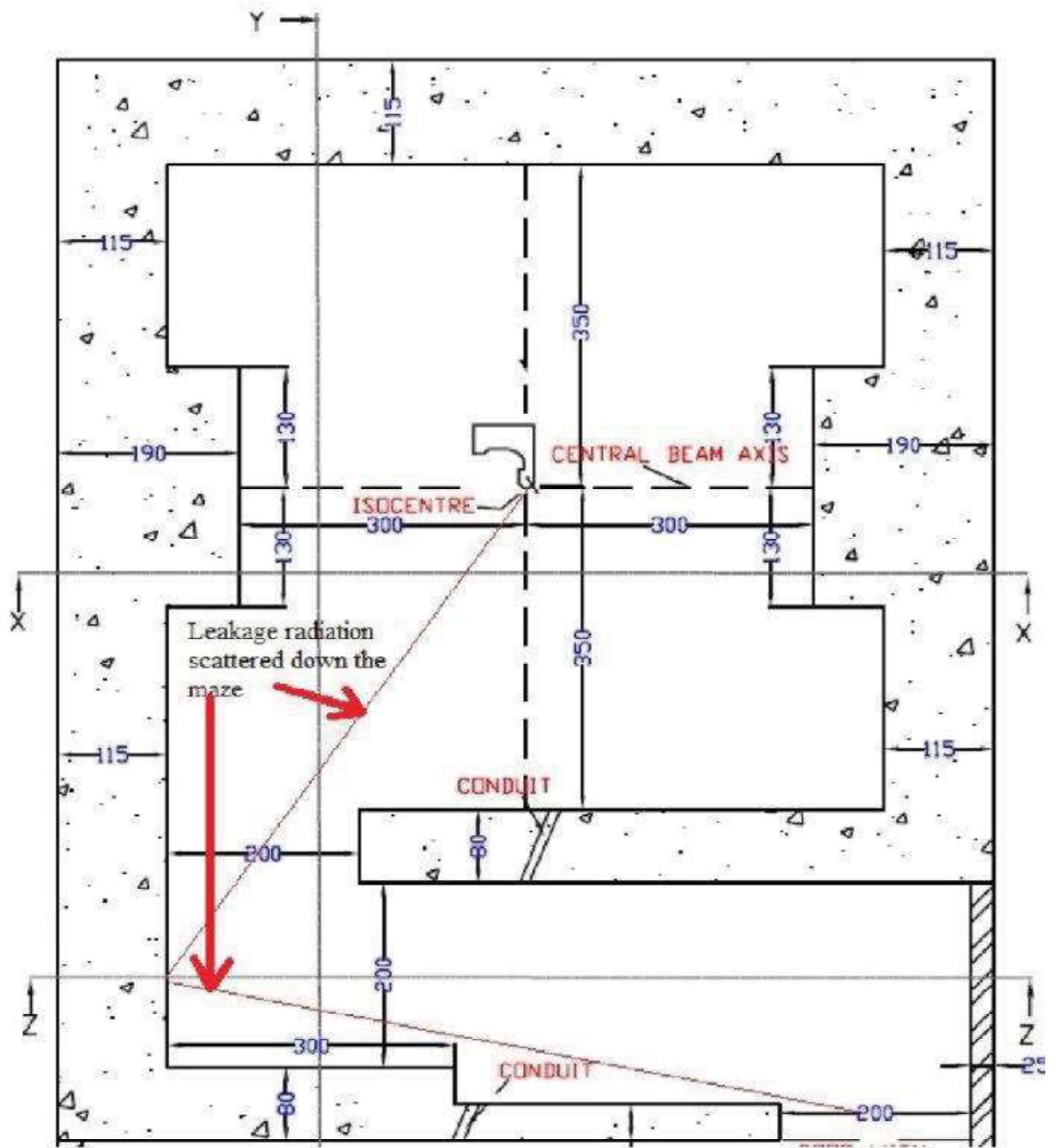
Fig. 4.2 Layout of a 6 MV Linac bunker indicating leakage radiation scattered down the maze.

Using equations 4.4, 4.5 and 4.6 patient scatter, wall scatter and maze scatter are calculated. It is found that secondary barrier thickness calculated for leakage radiation is adequate to shield the scattered radiation as well.

4.4 Calculation based on Monitor Units delivered

Around one thousand patients data were taken from geographically different regions (considering the variation in patient physique) and from Linacs of different manufacturers (Varian Medical System, USA and Elekta Medical System, UK) capable of delivering FF and FFF beam. Patients data were grouped for five different major clinical sites such as brain, head and neck, thoracic, abdomen and pelvic region. Actual MUs delivered have been obtained from the planning systems for these different cases using 6 MV photon beam in both FF and FFF modes. The data generated are presented in Table 4.1.

Table 4.1 *Details of MUs delivered for major clinical cases using 6 MV photon beam with FF and FFF modes. MUs are considered for intensity modulated beam delivery. MUs presented here are the average of 1000 clinical cases divided in 20 such groups, 5 major clinical sites in each group and 10 number of patients for each site (rounded to nearest value of multiple of 10).*

Sr. No	Major clinical treatment sites	Total MUs delivered for 10 no. of patients treated in 6 MV using FF mode	Total MUs delivered for 10 no. of patients treated in 6 MV using FFF mode
1	Brain	500	900
2	Head and Neck	550	1400
3	Thorax	450	1300
4	Abdomen	1200	1650
5	Pelvic	1200	2200

Practical workload, W is arrived by analysing these data of MUs delivered. The workload for FF mode is the cumulative MU delivered for five days, which is estimated from the daily average dose for stated clinical sites observed over a period of six months. Over this period we have noted that 80 % of the patients are treated in FF mode and only 20 % of

patients are treated in FFF mode. Therefore, in this study the workload for a facility using both FF and FFF mode is assumed to be the combination of workloads for 80 % of beam in FF mode and 20 % of beam in FFF mode. Based on the W barrier thicknesses are evaluated using the values of TVL reported for corresponding energy of FF and FFF beams (Stephen et al 2009).

4.4.1 Workload: The data of delivered MUs in FF and FFF mode for different clinical sites have been analysed to arrive at a practical workload (see Table 4.1), which is the major factor in shielding calculation. MUs delivered per patient for both FF and FFF modes are presented in Table 4.1. Hence W is the total MUs delivered in 5 days (in one week period). It is found that W is about 1.95×10^5 cGy/wk at 1 m for FF beam and 2.3×10^5 cGy/wk at 1 m for FFF beam.

4.4.2 Primary Barrier: The same modality of calculation is adopted for evaluating shielding adequacy of accelerator bunker i.e. the contribution of FF beam is 80 % and to that of FFF beam is only 20 %. For barrier calculations, workload $W = 1.95 \times 10^5$ cGy/wk in case of 6 MV beam in FF mode and 2.3×10^5 cGy/wk in case of FFF mode has been considered. It is found that primary barrier thickness for a Linac operated in FF mode only is higher by 20 % to that of a Linac operated in both FF and FFF modes.

4.4.3 Secondary barrier: Similarly, secondary barrier thickness were calculated and found that the secondary barrier thickness for a Linac operated in FF mode is higher only by 19 % to that a Linac operated in both FF and FFF modes.

94

4.5 Radiation survey measurements

The radiation survey measurements were carried out in these installations, from where the patient data were used. In this study, we have measured the instantaneous dose rate for both FF and FFF modes all around the installation at different locations. For radiation level measurement a calibrated pressurized ion chamber based Fluke Biomedical, USA make 450R survey meter was used. The Linac was operated in maximum available dose rate for both FF and FFF modes. All measurements were performed with the maximum achievable field size (40×40 cm^2) for both FF and FFF modes. For primary beam the radiation level measurement was carried out without a phantom in the beam path considering the worst possible scenario. For secondary beam the radiation levels were measured with a water phantom of dimension $40 \times 40 \times 40$ cm^3 phantom to simulate full scattering condition. The phantom was positioned on the treatment couch with the center of the phantom at the isocenter. On each wall, a matrix of dimension 20×20 cm^2 had been created. For each location measurements were taken at the point where the survey meter reading was the maximum. Radiation levels were measured at seven locations i.e. primary wall 1, primary wall 2, ceiling, secondary wall (gantry side), secondary wall (couch side), door location and the control console. At each point measurements were taken at four gantry angles 0^0, 90^0, 180^0 and 270^0. The measured data are presented in Table 4.2.

Table 4.2 *Presents the measured radiation survey data in μSv/hr, with maximum achievable field size (40 x 40 cm²) and dose rate of 1400 MU/min at normal treatment distance for seven different locations for different gantry positions.*

Gantry Angle (in deg)	Primary Wall1 (without phantom)	Primary Wall2 (without phantom)	Ceiling (without phantom)	Secondary Wall (Gantry Side) (with phantom)	Secondary Wall (Couch Side) (with phantom)	Door location (with phantom)	Console (with phantom)
0	0.13	0.08	0.06	0.72	0.87	2.80	0.18
90	0.15	0.09	0.07	0.48	0.30	2.40	1.10
180	0.05	0.07	2.30	0.52	0.41	2.90	0.30
270	0.10	5.70	0.04	1.45	1.30	6.20	0.13

Weekly radiation level (R_w) expressed in μSv/wk was estimated for 6 MV beam in both FF and FFF modes as per the IAEA SRS 47 (2006) using the following equation:

$$R_w = IDR \times \frac{WU}{\dot{D}}$$

(4.12)

Where, IDR is the instantaneous dose rate and is the dose rate of the photon beam. W and U are having their usual meaning.

R_w is estimated using equation 4.12 for both FF and FFF modes of Linac. In this calculation, W is the clinical workload, IDR is measured for both FF and FFF modes using the maximum dose rate available and the suitable value for U is considered depending on the location. The radiation survey was carried out in all installations from where the clinical data was taken for this study. However, representative data of the radiation survey of only one installation has been presented in Table 4.2. As bunkers were constructed for FF mode of use, the measured radiation level is further scaled for FFF mode with a factor of $\left\{ \frac{e^{-\mu t_{FFF}}}{e^{-\mu t_{FF}}} \right\}$, where t_{FFF} and t_{FF} are the thicknesses estimated for FFF and FF mode, respectively. It is found that, the radiation level all around the installations are within the acceptable limit.

4.6 Summary and Conclusion

Earlier investigations by Kry et al (2009) and Julia et al (2014) on the vault shielding of Linac operated in FF and FFF mode estimated an overall reduction of 20 % in the primary and secondary wall thickness of the Linac bunker for FFF mode of operation in comparison to FF mode of operation. In our study also it is observed that the reduction in primary and secondary wall thickness of the Linac bunker for practical situations is 20 % for primary and 21 % for secondary, which is consistent with those reported in the literature.

The removal of FF significantly decreases local dose rates outside the treatment vault. In the present study shielding requirements of a 6 MV medical linear accelerator operated in both with and without the FF are assessed using the NCRP Report No.151 and also by MUs delivered for clinical practice in Indian scenario. The results based on NCRP approach suggest that the primary and secondary barrier thicknesses are higher by 24 % and 26 % respectively, for a Linac operated in FF mode to that of a Linac operated in both FF and FFF modes with an assumption that only 20 % of the workload is shared in FFF mode. Primary and secondary barrier thicknesses calculated from the data on clinical practice also show the same trend and are higher by 20 % and 19 % respectively, for a Linac operated in FF mode to that of a Linac operated in both FF and FFF modes. Hence, it is found that overall the barrier thickness for a Linac operated in FF mode is higher about 20 % to that of a Linac operated in both FF and FFF. As a result, the wall thickness can be saved by about 20 % for a Linac operated in both FF and FFF modes in comparison to the Linac operated in FF modes only. Hence, the lower consumption of shielding material and space for new treatment vaults housing the Linacs with FFF and FF modes may reduce the building cost, whereas for existing facilities, one might take the

benefits in terms of increased weekly workload. Further, it is also suggested to use similar workload while estimating the weekly radiation level around the Linac bunker.

CHAPTER 5

Investigation of quality assurance parameters for commercially available FFF beams

5.1Introduction

Conventional Linac produces flat beam because of the presence of a thick conical filter called as FF in the beam path inside the Linac head. Photon beams produced from the Linac in the presence of FF deliver homogeneous dose distribution which is much important in conventional radiotherapy where mostly single field, parallel opposed, four field box techniques are used. However, for advance treatment techniques such as SRT, SRS and IMRT, the homogeneous dose delivery is insignificant which in turn attracts the researchers to apply the technology to remove the FF. Further, an increased dose rate (high dose delivered in less time) is particularly beneficial for the above mentioned advanced radiotherapy. FFF beams in radiotherapy thus have the advantage of shorter treatment delivery time and lower out-of field dose compared to conventional flattened beams (Titt et al 2006, Georg et al 2011). These properties can be achieved by removal of the FF. The photon beams produced in the absence of FF are identified as FFF beams. FFF beams have been extensively investigated and characterized before their introduction in the clinical practice (Brien et al 1991, Cashmore 2008, Kragl et al 2009, Vassiliev et al 2006a). The removal of FF from a conventional Linac results in change of beam characteristics from that of the flattened beam. Because of FF location on a rotating carousel within the treatment head its removal from the beam-line of a Linac is a straight forward process. In practice though, FF cannot simply be removed but needs to be replaced by a thin metal 'enhancer' plate in the same position as the FF. This plate generates electrons which provide build-up dose to the ionisation chamber to give sufficient signal (and position-dependant information) to the servo plates. They, in turn, can then operate correctly to control the beam quality and steering (Vassiliev et al 2006a, Cashmore 2008).Without this material most of the low-energy photons pass through,

resulting in lower average beam energy and altering the penetration of the beam. Removal of FF and positioning the enhancer plate has significant contribution in surface dose (Cashmore 2016, Mukesh et al 2016, Ravindra et al 2016).

Due to all the above-mentioned modifications Linac can produce FFF beams. The characteristics of FFF beam are different from that of the flattened beam. The dosimetric parameters which were established for a flattened beam, over the decades, such as field Size definition, beam quality, surface dose, Off Axis Ratio, beam flatness, symmetry and penumbra as well as depth dose profiles are no longer remain same for FFF beam. Hence, it is not possible to use the parameters in the same way as they are commonly used for the flattened beams.

Several investigators had proposed various parameters for FFF beam description. Ponisch et al (2006) recommended to normalize the FFF beam profiles to the 50 % dose level at the inflection point of the fall-off at the field edge, with the objective to have the same description of the field edge region as normally used for the flattened beam profiles. Fogliata et al (2012, 2015) recommended a different procedure to normalize the FFF beam profiles through a renormalization factor in a way to superimpose the FFF dose fall-off at the field edge with the corresponding flattened profile (normalized by default at the beam central axis to 100%). Budgell et al (2016) published a topical report which provides practical implementation advice and references for centres implementing FFF beams clinically emphasizing mainly on output measurement. However, evaluating the dosimetry characteristics of FFF photon beam applying the definitions proposed by the above investigators, are complex in nature which requires the use of dedicated software (in some cases) and understanding. In order to adopt this FFF technology in India, the

Atomic Energy Regulatory Board (AERB) of India constituted a Task Group (TG) and recommended an evaluation criteria for FFF photon beam (Sahani et al 2014).In the present study the different quality assurance parameters of the FFF beams generated by the commercially available Linacs from different manufacturers were investigated. The characteristics of FFF photon beams from Varian Medical System make Edge and Elekta Ltd. make Versa HD were investigated as per the AERB TG recommendations and the results were compared with the published similar parameters recommended by Fogliata et al (2012, 2015). Since Siemens left the Linac market in 2012, only the Varian and Elekta make Linacs were investigated in this study.

5.2 Materials and methods

5.2.1 Linear accelerators and Flattening Filter Free beams

FFF beams are now commercially available on a range of conventional Linac from Varian, Elekta and Siemens. Considering the fact that FFF beam contains more low-energy component which alters the beam quality, some of the manufacturers have tried to enhance the incident electron beam energy on the target in order to achieve beam matching with respect to FF beam. A FFF beam can never be completely matched to a conventional beam as there are irreconcilable differences in the beam spectrum and in the relative contributions of low-energy photons and electrons to make this possible. The conical shape of the FF also leads to differential beam hardening, most prominent at the central axis and gradually reducing with distance towards the field edge. Therefore any 'matching' can only exist in one position in the beam; the central axis. Some of the details on beam characteristics of Varian and Elekta Linac are mentioned in Table 5.1.

Table 5.1 Beam characteristics of Varian and Elekta Linac (Adopted from: IPEM topical report Ref: Budgell et al (2016)).

		Nominal energy (MV)	Filtration	Effective energy (MV)[a]	d_{max} (cm)	D_{10}(%)	$TPR_{20/10}$	Max dose rate (MU min^{-1})	Dose(mGy) Per pulse[b]
Varian	FFF	6	0.8 mm Brass plate	4	1.3	64.2	0.63	1400	0.8
		10		8	2.2	71.7	0.705	2400	1.3
	cFF	6	6/10 MV flattening filter	6	1.4	66.4	0.666	600	0.3
		10		10	2.3	73.6	0.738	600	0.3
Elekta	FFF	6	2.0 mm stainless steel plate	6	1.7	67.5	0.684	1400	0.6
		10		10	2.4	73	0.734	2200	0.9
	cFF	6	6/10 MV flattening filter	6	1.5	67.5	0.678	600	0.2
		10		10	2.1	73	0.721	600	0.4

[a]Clinical effective energy, based on $TPR_{20/10}$ and percentage depth dose fall off.
[b]Measured at d_{max} on beam central axis for standard reference conditions.
Note: d_{max} refers to depth of maximum dose. MU are monitor units.

Varian Medical System offers 6 and 10 MV FFF beams in addition to the conventional flattened beams available in their various models of Linac. In their implementation, the same electron beam is used to create both FF and FFF beams of the same nominal energy. Therefore, electron energy at the target is the same and removal of the FF increases output, but also reduces the penetrative quality of the photon beam due to the reduced beam hardening. In the other hand the same electron beam is not used to create the FFF and corresponding flattened beam in Elekta make Linacs. Each of the beams on the Elekta Linacs is defined by its own independent set of parameter values, referred to as its 'Energy Set'. Each Energy Set includes the radio frequency and gun settings that define the electron beam energy and also the dosimetry calibration settings. This allows the penetrative quality of the FFF beams to be restored to the nominal value for that energy. Though, Siemens is no more in the market, it is worth noting that the FFF beams produced in their Linac were using the higher incident electron energy at the target.

Details on beam characteristic for Siemens Linac can be found from the report (Flattening filter-free accelerators: a report from the AAPM Therapy Emerging Technology Assessment Work Group) published by Xiao et al (2015).

5.2.2 Measurement of dosimetric parameters

Percentage depth dose (PDD) curves were measured from surface to 30 cm depth for 5x5, 10x10, 15x15, 20x20 and 25x25 cm^2 field sizes at a SSD of 100 cm with a resolution of 2 mm. Collimator settings of 5x5, 10x10, 15x15, 20x20 and 25x25 cm^2 were referred as set field size. Corresponding to this collimator setting of field sizes, all dosimetric parameters for 6 FFF and 10 FFF for both the Linacs were generated.

Beam profiles were measured at a depth of 10 cm along the cross plane (CR) and in plane (IN) with SSD 90 cm for 10x10, 15x15, 20x20 and 25x25 cm^2 field sizes. All the measurements were carried out by PTW MP3 Radiation Field Analyser (RFA) and 0.125 cm³ ionization chamber (PTW make Semiflex). The measurements were performed with 2 mm resolution for both PDD and beam profiles. PTW software MEPHYSTO mcc (Version 3.3) was used to calculate the dosimetric parameters.

5.2.3 Analysis of beam dosimetric parameters

All measured profiles were analyzed as per the AERB TG recommendations and methods outlined by Fogliata et al (2012, 2015). Lateral beam profiles were normalized to 100% dose level on central axis as recommended by the AERB TG and alternately this has been renormalized with respect to FF beam profile which was generated in the same experimental setup as recommended by Fogliata et al (2012, 2015). The parameters which were common with respect to both the modalities were compared. However, the

individual parameters in each protocol, has been analyzed and inference drawn from these values were discussed.

5.2.3.1 Beam energy and Quality Index (QI)

As per IAEA TRS-398 (Andreo et al 2000) the beam quality index 'TPR$_{20,10}$' which is defined as the tissue phantom ratio at depths of 20 cm and 10 cm in water for a 10x10 cm^2 square field at a constant source-to-detector distance of 100 cm. TPR$_{20,10}$ was measured as per the reference conditions of IAEA TRS 398 (Andreo et al 2000) code of practice. In this study the measured values of beam quality index (QI) were reported for 6FFF and 10FFF of the investigated Linacs.

5.2.3.2 Percentage Depth Dose (PDD)

PDD for 5x5, 10x10, 15x15, 20x20 and 25x25 cm^2 collimator setting were measured and analysed. As per AERB TG suggestion, the d$_{max}$ and percentage depth dose value at 10 cm depth should be indicated for all the available unflattened photon beam energies. The PDD values were normalized to 100% at d$_{max}$ and analysed for 10x10 cm^2 field size.

5.2.3.3 Relative Surface dose

As recommended by AERB TG, relative surface dose should be measured for the collimator settings of 10x10 cm^2 and 20x20 cm^2 and compared with the corresponding nominal flattened photon beam energy. The relative surface dose (D_s) is defined as the ratio of dose at depth of 0.5 mm depth to the dose at d_{max} (International Electrotechnical Commission (IEC) 1998: CEI / IEC 60601-2-1). Both AERB TG and Fogliata et al (2012, 2015) recommended the same method of surface dose determination. The surface dose for FF and FFF beam were measured using a plane parallel plate ionization chamber (NACP-02 IBA-Scanditronix, Germany) in a solid water phantom with SSD of 100 cm.

5.2.3.4 Beam Profile analysis

As per the AERB TG recommendations, beam profile for 20x20 cm^2 collimator setting at 10 cm depth in isocentric setup of SAD for all the available unflattened photon beam energies need to be measured and the profiles shall be analyzed to evaluate different parameters. However, Fogliata et al (2012, 2015) recommended, to renormalize the beam profile with respect to the corresponding conventional FF beam profile generated from the same Linac and then to evaluate the required parameters. In the present study, IN and CR beam profiles for 10x10 cm^2, 15x15 cm^2, 20x20 cm^2 and 25x25 cm^2 field sizes at 10 cm depth were investigated.

5.2.3.5 Renormalization factor

Calculation of renormalization factor is recommended by Fogliata et al (2012, 2015). Once the FF beam is normalized to the 100% dose level at the beam central axis, the renormalization factor for the corresponding FFF beam can be calculated. It is defined as the percentage dose level at the beam central axis when the FFF profile is normalized to the same dose level as the FF beam at the position of the second maximum of the third derivative of same profile. The renormalization factor can also be calculated using the following equation:

$$\mathrm{Re}\,normalisation = \frac{a + b * FS + c * depth}{1 + d * FS + e * depth} \qquad (5.1)$$

where FS = field size in centimeter, depth = measuring depth in centimeter, a toe = fit parameters (can be referred from the published values of Fogliata et al (2012, 2015)). In the present study renormalization factors of square fields for both Varian and Elekta Linacs generated FFF beams were determined.

5.2.3.6 OAR (Off Axis Ratio)

As per the AERB TG recommendations, the off-axis ratio at $\pm$ 3 cm lateral distance from central axis at 10 cm depth for 10x10 cm^2 collimator setting should be measured and indicated for all the available unflattened photon beam energies. Protocol recommended by Fogliata et al (2012, 2015) does not incorporate the OAR measurement. OAR values were recorded from the measured profiles.

5.2.3.7 Symmetry

Symmetry is a parameter for checking the equality level between left and right sides of a profile. AERB TG recommended that the symmetry shall be evaluated following the methods recommended for flattened photon beams by International Electrotechnical Commission (IEC 60976 2008)whereas Fogliata et al (2012, 2015) recommended to use the method same as FF beam with due consideration for identifying the field region (as described under Degree of Unflatness) for evaluation. In the present study, we have calculated the maximum dose ratio (D_x/D_{-x}) considering the field region as 80% of the field size for reporting symmetry. Here D_x and D_{-x} are the doses at x and $-x$ positions (Symmetric to central axis).

5.2.3.8 Unflatness and degree of Unflatness

In the context of beam flatness, which is defined for FF beam energies is no longer remain in FFF beam dosimetry. Alternately, AERB TG recommended the flatness for FFF beam limited to 10x10 cm^2 field size can be measured using the established method for FF beam, if the value exceeds $\pm$ 3% (i.e., beyond the acceptable tolerance for flattened photon beam) the following method need to be applied in the form of Degree of Unflatness. Similarly, a new terminology was introduced by Fogliata et al (2012, 2015)

i.e. Unflatness. To quantify the degree of unflatness, the lateral distance from the central axis at 90%, 75% and 60% (represented as $X_{90\%}$, $X_{75\%}$, $X_{60\%}$) dose points on either side of the beam profile should be recorded along major axes for all the available unflattened photon beam energies as shown in Fig.5.1.
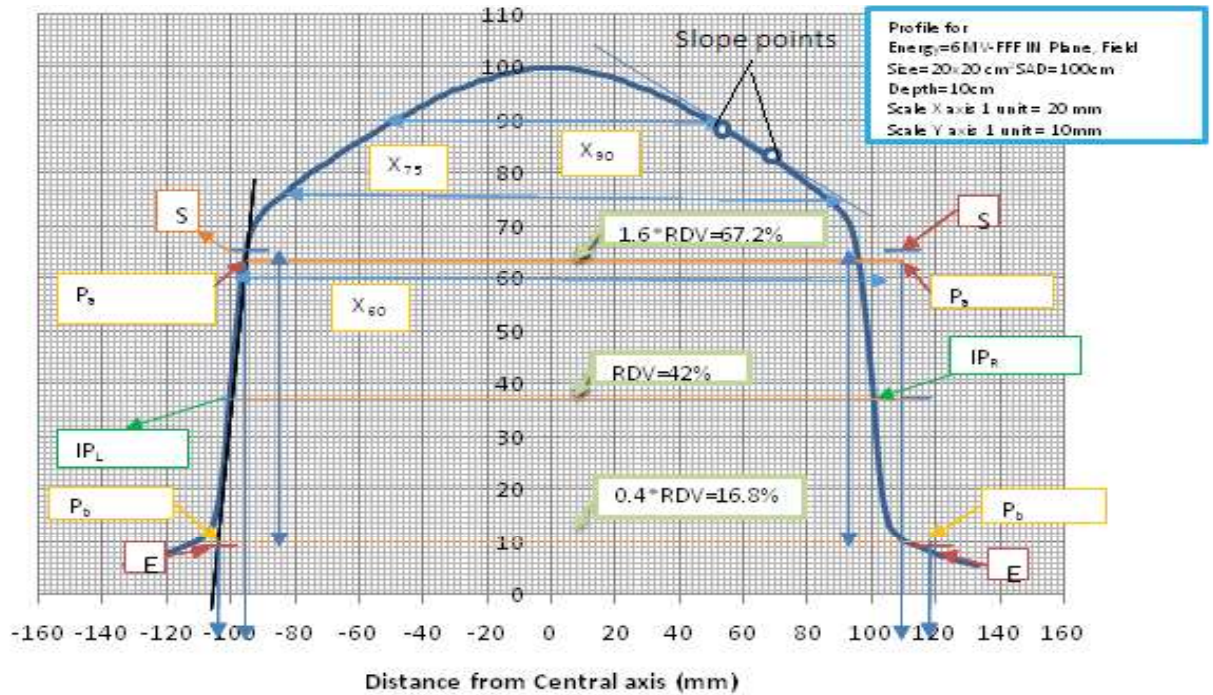
Fig. 5.1 Schematic diagram of the beam profile describing $X_{90\%}$, $X_{75\%}$, $X_{60\%}$.

As per the method recommended by Fogliata et al (2012, 2015), Unflatness is a parameter related to the FFF beams as flatness is related to FF beams. Unflatness can be defined as the ratio between the dose level at the beam central axis and the dose level at a predefined distance from the central axis as a function of field size, or at the edge of the field region. In this study, Unflatness values for different field sizes are considered, X off axis = 80% of field size (field side ⩾10) and 60% (field side <10). Profiles are calculated at SSD = 90 cm and at a depth of 10 cm.

5.2.3.9 Field Size

Methodology recommended by Fogliata et al (2012, 2015) for determining the field size is to normalize the beam profile with respect to the FF beam generated from the same model of the Linac for the same beam energy and following the established standards for estimating the field size which is the distance between 50 % dose levels. However, AERB TG recommended to derive field size from the separation between inflection point (IP) of the measured beam profile defined by collimator settings only. For verifying the consistency of the beam profiles along major axes (cross-plane and in-plane), the separation between IPs were recorded. IP shall be identified as per its mathematical definition. However, as recommended for practical purposes, it is approximated as the mid-point on either side of the high gradient region (sharply descending part) of the beam profile. It can be identified as follows [see Fig.5.1]:

- Locate the starting point (S) and end point (E) of high gradient region of the beam profile

- The vertical separation between S and E is the height (h) of the high gradient region

- Inflection point is located at h/2 on the beam profile from either location (S or E).

In the present study, the field size for different set field sizes (by collimator) apart from 20x20 cm^2 field (for in plane profile) as recommended by AERB TG were calculated.

5.2.3.10 Penumbra

For determining radiation beam penumbra, dose value at IP is taken as reference dose value (RDV). RDV, P_a (dose point at the field edge where RDV is 1.6 time than its base value) and P_b (dose point at the field edge where RDV is 0.4 time than its base value) are

shown in Fig.5.1. Lateral separation between P_a and P_b on either side of the profile were measured which is the radiation beam penumbra as recommended by AERB TG. Considering the approach recommended by Fogliata et al (2012, 2015) penumbra can be defined as per the existing protocols i.e the distance between 20% and 80% dose levels in the field edge provided the profiles are mutually renormalized. In this study, penumbra was analyzed by both the methods for the field sizes and beam energies of different models of Linac.

5.2.3.11 Slope and Peak Value

Fogliata et al (2012, 2015) recommended to measure the slope and peak value from the beam profile. The main interest of slope measurement lies with the fact that it assures that the beam is symmetric around the collimator axis (together with the symmetry parameter) by checking its value along the main axes and on the other side its value assures the correctness of the beam energy (not directly). The peak shape of the FFF profile can be defined by the "slope" parameter describing the left and right inclinations of the profiles. This slope parameter can be the slope of the line passing through two fixed points on the profiles located at 1/3 and 2/3 of the half beam (defined by the field size) and can be written as:

$$Slope = \frac{\{(x_1 - x_2) * (y_1 - y_2)\}}{(x_1 - x_2)^2} \quad (5.2)$$

where x_1, y_1 and x_2, y_2 are the coordinates at 1/3rd and 2/3rd points as indicated in Fig. 5.1. As the small field profiles are relatively flat, accordingly the slope values are determined above 10x10 cm^2 field sizes. The peak position parameter is the off axis position of the interception point of the left and right slopes and can be written as:

$$PeakPosition = \frac{\left(I_L - I_R\right)}{\left(S_R - S_L\right)} \tag{5.3}$$

where I_L and I_R are the left and right intercepts, respectively. S_L and S_R are the left and right slopes, respectively. Intercepts were calculated as per the mathematical definitions.

5.3 Results

5.3.1 Beam energy and Quality Index (QI)

Table 5.2 presents the nominal beam energies and their measured quality index values for 6 and 10 MV FFF beams for the Linacs used in this study. The measured QI values of the present study are compared with published data (Followill et al 1998, Castrillón et al 2009). Castrillón SV et al (2009) reported QI values for conventional beam energy of 4 MV, 6 MV, 8 MV,10 MV and 18 MV (presented in Table 5.3). It is observed that the measured QI values are within the specified limit for 4 MV to 8 MV in case of Varian Edge and 6 MV to 10 MV in case of Elekta Versa HD. This may be due to enhanced beam current used in Elekta Versa HD in FFF mode to match the beam energy and Varian Edge left with the same beam current which is used for FF beam mode. Further, the measured QI values are in close agreement with the reported values of IAEA, TRS 398. For example, for Elekta Versa HD the values differ by 1.02%, 0.76% and for Varian Edge the values differ by 1.07% and 0.28% for 6 FFF and 10 FFF photon beams, respectively.

Table 5.2 Beam quality index values for 6 and 10 MV FFF beams for the Elekta Versa HD and Varian Edge Linacs.

Linac Make & Model	Energy	TPR $_{20,10}$	d_{max}	PDD at 10 cm depth
Elekta Versa HD	6FFF	0.6803	1.61	64.7
Elekta Versa HD	10FFF	0.7207	2.4	74.1
Varian Edge	6FFF	0.6302	1.42	63.2
Varian Edge	10FFF	0.7052	2.32	70.9

Table 5.3 Values of TPR$_{20,10}$ measured by Castrillón et al (2009) and other investigators. Our measured values are compared with IAEA (4th column) values.

Energy	TPR$_{20/10}$ (measured)	TPR$_{20/10}$ (Followill)	TPR$_{20/10}$ (IAEA)	TPR$_{20/10}$ (Rogers)	TPR$_{20/10}$ (Kalach)
4 MV	0.6381 ± 0.0019	0.6355 ± 0.0068	0.6347 ± 0.0042	0.6443 ± 0.0032	0.6394 ± 0.0073
6 MV	0.6690 ± 0.0018	0.6710 ± 0.0065	0.6694 ± 0.0040	0.6765 ± 0.0030	0.6745 ± 0.0072
8 MV	0.7082 ± 0.0018	0.7102 ± 0.0078	0.7000 ± 0.0046	0.7050 ± 0.0036	0.7048 ± 0.0074
10 MV	0.7303 ± 0.0019	0.7314 ± 0.0077	0.7221 ± 0.0044	0.7278 ± 0.0033	0.7280 ± 0.0072
18 MV	0.7782 ± 0.0017	0.7812 ± 0.0075	0.7714 ± 0.0038	0.7845 ± 0.0025	0.7798 ± 0.0068

5.3.2 PDD

The PDD curves for the investigated Linacs of photon beams 6FFF and 10FFF for 10x10 cm^2 field size are presented in Fig. 5.2 (a-d). The measured values of d_{max} and PDD at 10 cm depth are presented in Table 1(a). It is observed that, d_{max} for Elekta Versa HD is at a higher depth as compared to Varian Edge (1.61 cm for 6 FFF beam Elekta Versa HD, 1.42 cm for 6FFF of Varian Edge). However, the relative variation is less in case of 10 FFF.
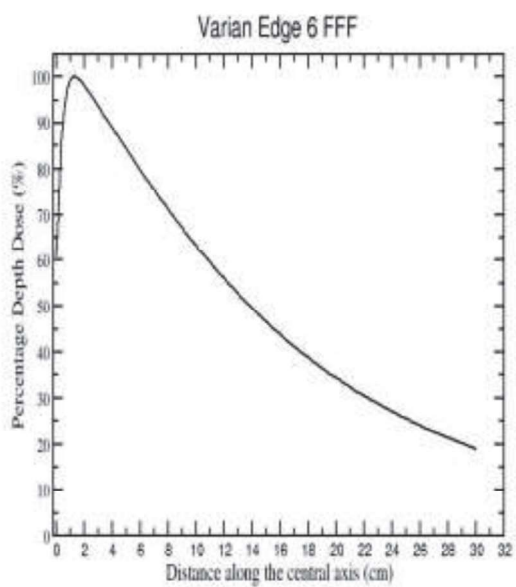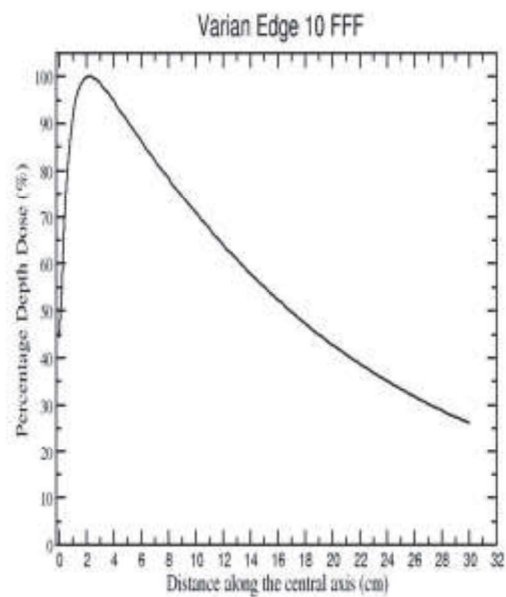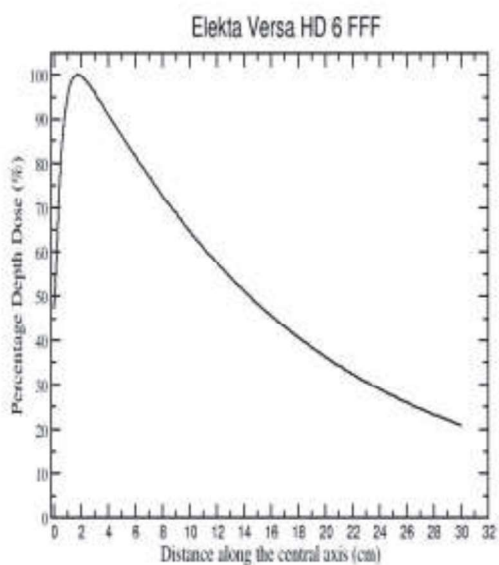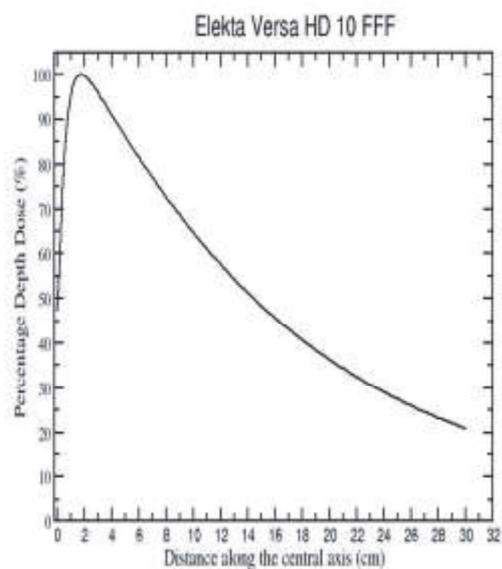
Fig. 5.2 Percentage depth dose for (a) Varian Edge 6 FFF (b) Varian Edge 10 FFF (c) Elekta Versa HD 6 FFF (d) Elekta Versa HD 10 FFF.

5.3.3 Relative Surface dose

In International Electrotechnical Commission (IEC 60601-2-1, 1998) recommended values of relative surface doses for various FF beam energies are shown in Fig. 5.2. Various investigators has already established that the surface dose of FFF beam is higher in comparison to FF beam (Cashmore 2016, Mukesh et al 2016, Ravindra et al 2016).Elevated values of surface doses have been reported for small field sizes with respect to higher field sizes. In our measurement, for field size at 10x10 cm^2 increased surface dose value was observed for FFF beam with respect to FF beam and reverse trend was observed at 20x20 cm^2 field size. Our measurements has also shown the similar trend and listed in Table 5.4 which are also within the prescribed limit of IEC 60601-2-1. Based on the observation of the present study, it is recommended to measure surface doses for field sizes 5x5, 15x15 and 25x25 cm^2, in addition to recommended 10x10 and 20x20 cm^2 field by these protocols.

Table 5.4Relative surface dose values for 6MV and 6FFF, 10MV and 10FFF photon beams of Elekta Versa HD and Varian Edge Medical linear accelerators.

Elekta Versa HD	Relative surface dose			Relative surface dose		
Field Size	6FF	6FFF	Diff (%)	10FF	10FFF	Diff (%)
10x10 cm^2	26.69	28.64	1.95	21.64	24.22	2.58
20x20 cm^2	37.57	35.44	2.13	34.24	31.64	2.6
Varian Edge	Relative surface dose			Relative surface dose		
Field Size	6FF	6FFF	Diff (%)	10FF	10FFF	Diff (%)
10x10 cm^2	49.8	58.4	8.6	33	42.5	9.5
20x20 cm^2	57.5	63.1	5.6	44.2	46.7	2.5

5.3.4 Beam Profile analysis

5.3.4.1Renormalisation factor

Table 5.5 presents the renormalization factors calculated using the derivative method recommended by Fogliata et al (2012, 2015) for the unflattened beams of the investigated Linacs. Values of renormalization factors for 10FFF are found to be relatively more in comparison to 6FFF. There is also a trend of increased value with respect to field size irrespective of the beam energy was found. Values of relative surface dose determined in this work are in close agreement to the values published of Fogliata et al for 6FFF beam of Versa HD except 4.7% for 20x20 cm^2 field. Additionally, it is also observed that the values of renormalization factors are dependent on Linac model.

Table 5.5 Beam profile renormalization values determined for 10FFF & 6FFF photon beams from Elekta Versa HD and Varian Edge.

Energy	Collimator Setting (cm^2)	Profile renormalization values	
		Elekta Versa HD	Varian Edge
10 FFF IN Beam Profile	10x10	121.537	123.542
	15X15	138.811	143.057
	20X20	157.497	164.374
	25x25	177.776	187.758
10 FFF CR Beam Profile	10x10	121.537	123.54
	15X15	138.811	143.06
	20X20	157.467	164.37
	25x25	177.7763	187.76
6FFF IN Beam Profile	10x10	111.295	113.424
	15X15	120.267	123.89
	20X20	130.193	135.648
	25x25	141.232	148.953
6FFF CR Beam Profile	10x10	111.295	113.424
	15X15	120.267	123.89
	20X20	130.193	135.64
	25x25	141.232	148.953

5.3.4.2 Off-axis ratio (OAR)

Measured OAR values are presented in table 5.6 for 10x10 cm^2 field size of the 6FFF and 10FFF photon beams for both IN and CR profiles. It is observed that OAR values are larger for 6FFF beam as compared 10FFF beam. Further it is also noted that OAR values of Varian Edge are higher as compared to the corresponding OAR values of Elekta Versa HD.

Table 5.6 Off Axis Ratio for 6FFF and 10FFF beam energies for Elekta Versa HD and Varian Edge Linacs. (IN:inline, CR: cross line)

Linac	Beam energy & type of profile	OAR at +3 cm	OAR-3 cm
Elekta Versa HD	10 FFF IN	89.5	89.3
	10 FFF CR	88.6	88.9
	6FFF IN	93.6	92.6
	6FFF CR	92.8	92.7
Varian Edge	10 FFF IN	90.7	91.4
	10 FFF CR	91.3	91.8
	6FFF IN	94.4	94.5
	6FFF CR	95	94.9

5.3.4.3 Beam Symmetry

One set of symmetry values for 6FFF and 10 FFF are presented in Table 5.7 as both the protocols demands similar consideration. From the tabulated values, symmetry shows good agreement across the models and among the field sizes and energies. The values of symmetry obtained are well within the acceptable limit.

Table 5.7 Beam symmetry of the investigated Elekta Versa HD and Varian Edge Linacs.
(IN :inline, CR: cross line)

Beam Energy & type of profile	Collimator Setting (cm^2)	Elekta Versa HD	Varian Edge
10FFF IN	10x10	100.88	100.58
	15X15	101.14	101.4
	20X20	101.01	102
	25x25	101.03	102.1
10 FFF CR	10x10	101.03	100.13
	15X15	101.16	100.16
	20X20	101.15	100.24
	25x25	101.28	100.31
6FFF IN	10x10	100.38	100.13
	15X15	100.2	101.48
	20X20	100.5	102.24
	25x25	100.31	102.2
6FFF CR	10x10	101.43	100.18
	15X15	101.23	100.37
	20X20	101.35	100.52
	25x25	101.2	100.61

5.3.4.4 Degree of Unflatness

After generating the profiles it has been observed that the FFF beam profiles for field sizes equal to or greater than 5x5 cm^2 exceeds the conventionally defined flatness tolerance value of ± 3%. Therefore, Degree of Unflatness has been determined by AERB TG recommended method for FFF beam and values are presented in Table 5.8. The values for Degree of Unflatness parameters shows large variations from model to model, however Elekta Versa HD shows relatively less variation among the beam energies in comparison to Varian Edge. Values of $X_{90\%}$, $X_{75\%}$, $X_{60\%}$ are more in case of low energy and less in case of high energy. This is due to the fact that in low energy the lateral scatter

is more in comparison to high energy. Further it has been noted that more variation is in $X_{60\%}$ values irrespective of beam energy.

Table 5.8 Degree of unflatness for the 6FFF & 10FFF photon beam from Elekta Versa HD and Varian Edge Linacs. (IN :inline, CR: cross line). Values of $X_{90\%}$, $X_{75\%}$, $X_{60\%}$ are in mm.

	Collimator Setting (cm²)	Elekta Versa HD			Varian Edge		
		$X_{90\%}$	$X_{75\%}$	$X_{60\%}$	$X_{90\%}$	$X_{75\%}$	$X_{60\%}$
10 FFF IN	10x10	58	91	97	57	90	97
	15X15	61	118	145	61	114	141
	20X20	63	121	181	63	106	178
	25x25	61	124	177	64	120	185
10FFF CR	10x10	56	89	95	58	85	94
	15X15	59	113	142	62	118	141
	20X20	60	118	171	64	110	179
	25x25	62	124	176	65	125	199
6FFF IN	10x10	73.5	94.5	97.5	75	93.5	97
	15X15	82.5	136	146	90	136	144
	20X20	86	160	195	97	167	194
	25x25	89	170	233	101	182	240
6FFF CR	10x10	72	94.5	96.3	75	92	97
	15X15	81	134	144	91	138	145
	20X20	87	159	194	98	172	194
	25x25	88	169	232	104	184	243

5.3.4.5 Unflatness

Values of Unflatness are presented in Table 5.9. A well-defined trend was observed for 6FFF as well as 10FFF beams in both the Linacs. It increases with respect to field size. Minimum deviation was observed between IN and CR profile. Among the Linac models and across the beam energies the Unflatness values varies from 1.22 to 1.70.

Table 5.9 Unflatness values for the 6FFF & 10FFF photon beam from Elekta Versa HD and Varian Edge Linacs. (IN :inline, CR: cross line)

Beam energy & profile	Collimator Setting (cm^2)	Unflatness values	
		Elekta Versa HD	Varian Edge
10FFF IN	10x10	1.222	1.229
	15X15	1.373	1.378
	20X20	1.53	1.562
	25x25	1.691	1.616
10FFF CR	10x10	1.234	1.223
	15X15	1.383	1.347
	20X20	1.539	1.497
	25x25	1.704	1.657
6FFF IN	10x10	1.141	1.133
	15X15	1.236	1.221
	20X20	1.335	1.238
	25x25	1.443	1.327
6FFF CR	10x10	1.155	1.134
	15X15	1.248	1.204
	20X20	1.346	1.286
	25x25	1.454	1.375

5.3.4.6 Field size

In our study, values calculated manually as per AERB TG are presented in Table 5.10 and it is found that the values are within the prescribed limit of conventional FF beam. However, it is observed that careful approaches need to be adopted while carrying out identification of the IP. Using the method recommended by Fogliata et al (2012, 2015) the determined field size values were found to be more close to the collimator setting values.

During completion of this study the IPEM topical report 1: guidance on implementing FFF radiotherapy (Budgell et al 2016) published, which recommended another simpler approach to avoid the dependency of conventional FF to normalize the FFF beam and of course the complexity involved in the previously mentioned methods. As per this report,

the profile of FFF field is divided by profile of fully opened FFF field and then the conventional definition can be applied to this ratio on field size and penumbra. Though IPEM topical report suggests a simpler approach, but is limited to two parameters only and user need to follow other methods to establish further dosimetric parameters.

Table 5.10 Field size of the investigated Elekta Versa HD and Varian Edge Linacs. (IP is h/2 values from the profile and IP_L, IP_R are the IP values in the left and right side from beam central axis. All values are in cm.) (IN:inline, CR: cross line)

Collimator (cm²)	Field Size (IP_L+IP_R) cm	Field Size calculated after renormalization	Collimator (cm²)	Field Size (IP_L+IP_R) cm	Field Size calculated after renormalization
ElektaVersa HD 10FFF IN			**Varian Edge10FFF IN**		
10x10	9.9	9.98	10x10	9.9	9.96
15X15	15.0	14.99	15X15	14.8	14.95
20X20	19.9	19.95	20X20	20.2	20.15
25x25	24.9	25.01	25x25	24.85	24.9
ElektaVersa HD 10FFF CR			**Varian Edge 10FFF CR**		
10x10	9.9	10.0	10x10	9.9	9.96
15X15	14.9	14.99	15X15	14.8	14.95
20X20	20.0	19.95	20X20	20.0	20.05
25x25	25.0	25.01	25x25	25.0	24.98
Elekta Versa HD 6FFF IN			**Varian Edge 6FFF IN**		
10x10	9.95	9.99	10x10	9.9	9.98
15X15	15.0	14.95	15X15	15.0	14.95
20X20	20.0	19.95	20X20	19.9	19.95
25x25	25.0	24.98	25x25	24.9	24.98
Elekta Versa HD 6FFF CR			**Varian Edge 6FFF CR**		
10x10	9.84	9.99	10x10	9.9	9.99
15X15	14.9	14.95	15X15	14.85	14.9
20X20	19.9	19.95	20X20	19.9	20.1
25x25	25.0	24.98	25x25	24.9	24.98

5.3.4.7 Penumbra

Penumbra was analyzed and is presented in the Table 5.11.

Table 5.11 Penumbra of the investigated Elekta Versa HD and Varian Edge Linacs (IN :inline, CR: cross line)

Collimator setting (cm²)	AERB TG		Fogliata et al		Collimator setting (cm²)	AERB TG		Fogliata et al	
	Left	Right	Left	Right		Left	Right	Left	Right
Elekta Versa HD 10FFF IN Beam Profile					**Varian Edge10FFF IN Beam Profile**				
10x10	8	8	8.5	8.5	10x10	8	7	8.6	7.4
15X15	8	8	8.2	8.3	15X15	9	9	9.5	9.8
20X20	8	8	8.2	8.4	20X20	10	9	10.8	9.5
25x25	11	12	11	11.5	25x25	9	10	9.6	10.7
Elekta Versa HD 10FFF CR Beam Profile					**Varian Edge 10FFF CR Beam Profile**				
10x10	6	7	7	6.8	10x10	8	8	8.6	8.7
15X15	9	10	9.3	10.4	15X15	8	8	8.8	9
20X20	7	7	7.5	7.6	20X20	8	9	9	9.2
25x25	12	12	11.8	11.6	25x25	10	10.5	10.8	11
Elekta Versa HD 6FFF IN Beam Profile					**Varian Edge 6FFF IN Beam Profile**				
10x10	5	6	5.4	6.2	10x10	8	8	8.5	8.5
15X15	9	8	9.3	8.6	15X15	9	8	9.6	9.4
20X20	6	7	6.5	7.3	20X20	10	9	10.5	10
25x25	10	10	9.8	9.7	25x25	10	10	10.8	11
Elekta Versa HD 6FFF CR Beam Profile					**Varian Edge 6FFF CR Beam Profile**				
10x10	7.6	7.5	8	8.3	10x10	8	8	8.5	8.4
15X15	10	10	10.3	10.4	15X15	8	9	8.7	9.3
20X20	8	8	8.4	8.3	20X20	9	9	9.5	9.5
25x25	10	10	10.3	10.2	25x25	10	10.5	10.8	11

It is observed that the values of penumbra depend on the profile orientation such as in plane and cross plane. In 6FFF the in plane profile shows a decreased value in comparison with cross plane profiles. However opposite trend has been observed in case of 10FFF for both the Linac models. Considering the Fogliata et al (2012, 2015) method the penumbra values were determined from the renormalized profiles which were found to be higher as compared to AERB TG recommendation for most of the field sizes.

Further it is also noted that the variation in penumbra values of Elekta Versa HD is less in comparison to Varian Edge.

5.3.4.8 Slope and Peak Value

In table 5.12, the slope values for 6FFF and 10FFF beam energies are recorded for different field sizes, at a SSD of 90 cm. Slope values are higher for 10FFF beam energy in comparison to 6FFF and it increases with field size irrespective of beam energy.

Table.5.12 Slope parameter for 6 and 10 FFF beam for different field sizes at 90 cm SSD for Elekta Versa HD and Varian Edge Linacs. (IN : inline, CR: cross line)

Beam Energy & profile	Collimator Setting (cm^2)	Slope parameter			
		Elekta Versa HD Slope		Varian Edge Slope	
		Left	Right	Left	Right
10 FFF IN	10x10	0.648	-0.661	0.673	-0.684
	15X15	0.756	-0.747	0.777	-0.753
	20X20	0.801	-0.799	0.812	-0.802
	25x25	0.826	-0.817	0.856	-0.831
10 FFF CR	10x10	0.699	-0.677	0.623	-0.623
	15X15	0.767	-0.76	0.648	-0.65
	20X20	0.789	-0.801	0.662	-0.667
	25x25	0.805	-0.819	0.666	-0.671
6FFF IN	10x10	0.414	-0.409	0.395	-0.399
	15X15	0.472	-0.469	0.437	-0.428
	20X20	0.5	-0.499	0.446	-0.463
	25x25	0.523	-0.522	0.483	-0.486
6FFF CR	10x10	0.458	-0.426	0.401	-0.396
	15x15	0.487	-0.471	0.423	-0.426
	20x20	0.503	-0.501	0.452	-0.461
	25x25	0.522	-0.526	0.482	-0.491

Further it is recommended by Fogliata et al (2012, 2015) to record the peak position values. It should be ideally located on the central axis representing the intersection point

of the two slopes. This identifies the forward direction of the beam. Table 5.13 represents the peak position values. For 6FFF the peak position deviate more in comparison to 10FFF which is due to the fact that 6FFF produces more flat beam relative to 10FFF.

Table 5.13 Peak Position parameter for 6 and 10 FFF beam for different field sizes at 90 cm SSD for Elekta Versa HD and Varian Edge Linacs. (IN: inline, CR: cross line)

Beam energy & profile	Collimator Setting (cm²)	Peak position (mm)	
		Elekta Versa HD	Varian Edge
10 FFF IN	10x10	0.33	-0.44
	15X15	-0.83	-1
	20X20	-0.05	-1.66
	25x25	0.34	-1.38
10 FFF CR	10x10	-0.51	-0.66
	15X15	0.89	-0.76
	20X20	0.3	-0.67
	25x25	0.65	-0.65
6FFF IN	10x10	0.66	-0.32
	15X15	-0.01	-0.55
	20X20	0.78	-0.85
	25x25	1.36	-0.7
6FFF CR	10x10	-1.08	-0.98
	15X15	0.8	-0.94
	20X20	-0.11	-0.77
	25x25	0.38	-0.7

5.4 Conclusions

FFF beam generated from Linacs were studied with respect to their dosimetric parameters using the protocols introduced by AERB TG and Fogliata et al (2012, 2015) for establishing FFF beam radiotherapy and values were compared. In this work the beam profile consistency were studied over a period of time (in three months and six months interval) by comparing the values with respect to their base line values during commissioning of the units. Profiles were selected for evaluation of dosimetric

parameters after their compliance with base line values. Further, it is worth noting that, AERB TG methodologies for normalization of beam profiles is a relatively simpler approach and could be implemented easily.

From both the manufactured models, it is observed that the energy parameters such as $TPR_{20,10}$ and PDD varies significantly mainly attributing to the technology adopted to generate the beam. Due to the variation in energy, surface dose measurement shows larger deviation. Therefore, it is recommended to measure the surface dose at least for 5x5, 10x10, 15x 15, 20x20, 25x25 cm^2 field sizes as the nature of variation are not consistent. In the beam profile analysis, it is observed that the renormalization factors as recommended by Fogliata et al (2012, 2015) are machine dependent. Therefore, this parameter needs to be evaluated for the particular model. Off Axis Ratio shows good agreement across the profile type. Maximum deviation observed as 1% for IN beam profile of 6FFF of Versa HD, however the CR beam profile shows only 0.1% deviation. In the context of symmetry, both the manufactured models are within the prescribed tolerance limit and in good agreement across the beam profiles. In addition to this as indicated by Fogliata et al (2012, 2015) the slope value is also indirectly represent consistency in symmetry and energy of the beam. Based on the results of this study, it is clear that in case of 10FFF beam energy the slope is steeper in comparison to 6FFF that indicated more forward picked values as the energy increases. Maximum difference between left and right slope is within 0.03. With respect to beam flatnees, the definition certainly needs modification which was already discussed in both the protocols. The values of these alternate parameters $X_{90\%}$, $X_{75\%}$, $X_{60\%}$ (as per AERB task group) show larger deviation from model to model and from low energy beam to high energy beam. This study indicates that measuring only this parameter in the place of flatness of FFF

beam is not sufficient to address the profile shape and consistency. Therefore, parameters such as Unflatness and Peak position need to be measured either by renormalizing the profiles as recommended by Fogilata et al (2012, 2015) or simply following the AERB task group profile analysis method. While analyzing field size and penumbra parameters from the measured profiles, it has been observed that more fine tuned values were observed after renormalization of the profiles by the method recommended by Fogilata et al (2012, 2015) This might be due the fact that the approach for finding the inflexion/renormalization point slightly varies across the protocols.

As these two independent protocols are not adequately addressing the complete nature of beam profiles and many variations were observed, it is therefore required to incorporate the parameters such as Beam Energy, PDD, Field Size, Penumbra, Symmetry, Degree of Unflatteness, value of Unflattenesss, Slope, Peak position, Surface dose and Off Axis Ratio in the FFF beam dosimetry regime.

CHAPTER 6

Measurement and comparison of surface dose and leakage radiation for flattening filter free and flattened photon beams

6.1. Introduction

Surface dose plays a significant role in radiotherapy. Dose received by the basal skin layer can result in various complications such as skin erythema, epilation, dry desquamation, wet desquamation, necrosis etc depending on the magnitude of dose received (Kim et al 1998, Carl and Vestergaard 2000, Ishmael et al 2008). At the same time it is also important that dose to targets which are lying close to the surface are accurately known so that under dosage due to the dose delivery will not occur. Therefore, accurate measurement of dose at the surface is essential for proper treatment of patients. However, accurate measurement of surface dose and the doses at the buildup region is a difficult task. Surface dose is machine dependent and can be affected by many parameters such as field size, SSD, beam energy, materials present in the beam line, type of dosimeter used for its measurement etc. (Kry et al 2012, Ponisch et al 2006, Kragl 2009, Cashmore 2016). The FF is responsible for the majority of contamination electrons reaching the patient surface, its removal is therefore likely to reduce this contribution. However, the filter also acts as a beam hardener by removing low-energy photons from the spectrum. With the filter removed, this low-energy component is allowed to pass through to the patient and will act to increase the surface dose. Energy spectrum and electron contaminations are the two factors, which can change the surface dose in FFF beams. Whether this results in higher or lower skin doses in clinical situations is, therefore, of interest. Because of the steep dose gradient near the surface as well as in the buildup region, careful considerations are required in the selection of detectors for measurement of surface dose. In the present study, the relative surface dose for the photon beams have been studied as per the definition provided by International

127

Electrotechnical Commission (IEC) (IEC-60601-2-1, 2009-2010). The study was carried out for various field sizes such as 5x5, 10x10, 15x15, 20x20 and 25x25 cm^2.

It has already been discussed in the Chapter 5 that introduction of this FFF technology poses several challenges in beam acceptance criteria however TPS commissioning for FFF beams follow the standard procedures as for conventional Linac (Budgell et al 2016). In addition, one of the major advantages of FFF beams is the lower leakage radiation level as comparison to FF beams. IEC has issued regulations and safety standards regarding the radiation leakage measurements. Several requirements were stipulated in IEC. The first criterion relates the radiation leakage through the collimator jaws, i.e. in the area between the useful beam and the maximum useful beam. Its purpose is to limit the dose given to the patient's normal tissue immediately surrounding the treatment volume. A second criterion relates radiation leakage in the patient plane outside the maximum useful field; its purpose is to limit whole body dose in the patient. A third criterion relates the radiation leakage measured at a distance of 1 m from the path of the electron beam as it travels from the gun to the X-ray target; its purpose is to protect personnel, if inadvertently remain in the treatment room during beam 'ON' condition and reduce the requirement of room shielding. Leakage radiation requirements to the patient area and outside the patient area recommended by various standards were reviewed by Devanney et al (1980). The X-ray head leakage may vary with energy in dual energy accelerators, which was reported by Conere et al (1989). Apart from the shielding requirements all around the Linac head, other aspects of head leakage radiation are covered by a number of investigators (Conere et al 1989, Devanney et al 1980, Dixon et al 1977, Huen et al 1979, Kase et al 1986, Nelson et al 1984, Rawlinson et al 177, Taumann 1981, Vander Laarse et al 1988). Recently, Kinsara et al (2016) have reviewed

leakage from a linear accelerator and its side effects on cancer patients emphasizing the leakage radiation from MLC (Multi Leaf Collimator). In the present study, leakage radiation from a Linac was measured as per IEC 60601-2-1 recommendations.

6.2. Medical Linear Accelerators used

Surface dose measurements were carried out for photon beams of nominal energies 6MV and 10 MV generated from Elekta Ltd make Versa HD model and Varian Medical System make True Beam Linac model in FF and FFF mode. For flattened photon beams the FF is in place and for FFF photon beams an open port is used where a thin foil is placed instead of a FF depending on the technology adopted by the manufacturer. We refer to the four photon beams investigated in this study which are6 MV, 6FFF, 10MV and 10FFF for the nominal photon beam energies of 6 and 10 in the presence and absence of FF respectively. The dose rates can go up to 1400 MU/min for 6 MV FFF and 2400 MU/min and 2200 MU/min for 10 MV FFF beams respectively for Varian and Elekta Linacs.

For the leakage radiation measurement, True Beam STx SVC accelerator having capability of producing photon energies of 6 MV, 10 MV, 15 MV, 6FFF, 10FFF and electron beam energies of 6 MeV, 9 MeV, 12 MeV and 15 MeV was used. The maximum field size achieved for this unit is 40 x40 cm^2 and with Multi Leaf Collimator (MLC) it is 40x22 cm^2. The dose rate in FF mode for both 6 MV and 10 MV was 600 MU/min. The dose rate in FFF mode was 1400 MU/min and 2400 MU/min for 6FFF and 10FFF beam energies, respectively.

6.3 Dosimeter and Phantoms used

6.3.1 For surface dose measurement

Dosimeters used for surface dose measurement are plane parallel plate (PP) ionization chamber, EBT3 GafChromic film and Al_2O_3 optically stimulated luminescent (OSL) dosimeter. A solid water phantom of dimension 30x30x30 cm^3 of physical density of 1.04 g/cm^3 having provision for holding the chamber and various thickness of sheets were used in this study. The details of the dosimeters used are as mentioned below:

PP chamber: The plane parallel plate ionization chamber, PTW Germany make Roos Ionization Chamber type 34001, having volume 0.35 cm3 with wall material 1.01 mm PMMA, 0.02 mm graphite and 0.1mm lacquer. Entrance window area density for the chamber is 132 mg/cm^2.

GafChromic EBT3 film: GafChromic EBT3 film (International Specialty Product, NJ, US) has a single active layer of approximately 30 μm thickness. This active layer is sandwiched between two 125 μm thick transparent polyester sheets. It allows scanning on either side instead of smooth polyester substrate matte polyester substrate was used in EBT3 film to prevent Newton's rings formation. EBT3 is more sensitive than older versions of GafChromic films having a dose range of 1 cGy to 40 Gy.

Al_2O_3optically stimulated luminescent dosimeter: Bhabha Atomic Research Centre (BARC), India developed a dosimetric grade α‑Al_2O_3:C phosphor having grain size 75–100 μm which was sandwiched between two thin transparent plastic sheets (Kulkarni et al 2015). The dimension of Al_2O_3 disc is 7 mm diameter and 0.14 mm thickness. Background OSL measurements of all the discs were carried out using in-house developed OSLD badge reader system.

6.3.2 For leakage measurement

A PTW make 0.6cc ion chamber with adequate build up material with a solid water phantom of dimension 30x30x20 cm^3 were used in the leakage measurement. Point of measurement was centered at d_{max} of each beam in SAD setup. The measurements were performed as per the stipulations of IEC (IEC 60601-2-1, 2009-2010).

6.4 Measurement procedure

6.4.1 Measurement of surface dose

The surface dose for any field size is defined as the dose measured at 0.5 mm depth (from the surface) for that field size divided by the dose at d_{max} at a 10x10 cm^2 field size. Surface doses are expressed relative to the dose at dose maximum for the respective energy and field size. The measurements were done with the FF and FFF beams aligned along the central axis with square field sizes of 5x5 cm^2, 10x10 cm^2, 15x15 cm^2, 20x20 cm^2 and 25x25 cm^2 with build-up depths extending from the surface to 2 mm towards the d_{max} and at d_{max}. The surface doses delivered by the FF, and FFF beams were measured using a plane-parallel ionization chamber in solid water phantom. The measurements were done at negative voltage (-300 V) for FF and FFF beams. Based on the commissioning data of the Linacs, the d_{max} were 1.5 and 2.4 cm for 6 MV and 10 MV FF beam and 1.4 and 2.2 cm for 6 MV and10 MV FFF for True Beam and Versa HD respectively at a standard SSD of 100 cm and field size of 10x10 cm^2. Various investigators have reported that near surface, build up dose has a linear increase up to few mm depth much before attending d_{max}. Considering the above fact, to avoid the positional inaccuracy, the PP chamber was placed at 0mm, 1mm and 2 mm depth to find the ionization reading at 0.5mm depth (from the graph). The ionization value was also recorded for d_{max} of the respective field sizes (5x5, 10x10, 15x15, 20x20, 25x25 cm^2) at

SSD of 100 cm with the appropriate buidup and the reference point of measurement was ensured. As the study was mainly aimed at comparison of relative surface dose for FF and FFF beam energies, requisite correction factors were not considered.

EBT3 (Gafchromic) film pieces of dimension were 2x2 cm^2 were irradiated in a 30x30x30 cm^3 solid water phantom. The dose in the surface and build-up region dose were measured with the film sandwiched tightly between the slabs and irradiated while oriented perpendicular to the beam axis at 1 mm and 2 mm depths and at d$_{max}$ of respective field sizes (5x5, 10x10, 15x15, 20x20, 25x25 cm^2) at SSD of 100 cm. The effective point of measurement was defined at 0.15 mm depth (Battum L.J. et al 2008, Devic S et al 2006). For depth of 0 mm, the film was placed on the surface of the phantom with appropriate SSD correction. Each irradiation step delivered 200 MUs. After verifying the dose linearity and unirradiated film was used as the background. All films were scanned 24 h after irradiation. An Epson 10000XL (Epson America, Inc., Long Beach, USA) flatbed document scanner was used to scan the films following the manufacturer scanning protocol and recommendations. Epson software was used for scanning the films in transmission mode with a resolution of 75 dpi and with image enhancements turned off. The images were saved as 48‑bit tag image format files for further analysis. The surface dose of the scanned images was calculated by using OmniPro–I'mRT software (Version 1.6; IBA dosimetry, Germany). Calibration of the films and background OD of the films were carried out only to confirm the irradiation of the films and counter checks as and when required.

The Al$_2$O$_3$ dosimeter discs having response within ±5% were selected for their use in the two element OSLD badge. The dosimeter was wrapped in an aluminium foil of 15 μm

thick to provide light-tight casing. The measurements were carried out using the same solid water phantom which was used for film measurement and the set up was corrected for SSD. To study the dose linearity of Al_2O_3 OSL dosimeter doses of 50 MU, 100 MU and 200 MU were delivered placing the OSLD at the surface of the phantom for a 10 cm x 10 cm field size. Accordingly it was decided to measure the response at 100 MU. For the readout of Al_2O_3OSL dosimeters, the OSL reader system was operated in a continuous wave OSL (CW‑OSL) mode at 20 mW/cm^2 with blue (470 nm) light stimulation.

Extrapolation was made for EBT3 and Al_2O_3 dosimeters because their effective depths of measurement were just above the phantom. The measurements were carried out at 100 cm SSD. The measured surface doses of 6FFF and 10FFF beams were compared with the corresponding nominal flat beam energies 6 MV and 10 MV, respectively.

6.4.2 Measurement of leakage

Leakage measurement points were considered with respect to the area 'M' as indicated in Fig. 6.1 with variable couch angles ranging from 22.5^0 to 337.5^0.
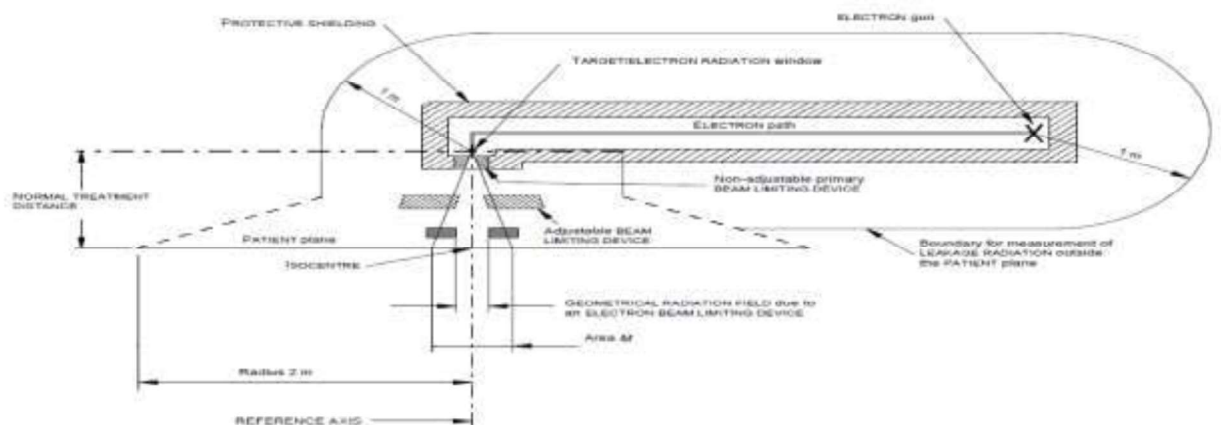
Fig.6.1 Schematic diagram presenting different regions for specifying the radiation leakage.

Radiation levels were measured for each Beam Limiting Devices (BLDs) and other conditions as discussed below.

6.4.2.1 Leakage radiation through X-Collimator: To evaluate the transmission through X-collimator beam limiting device (secondary collimator), ready pack films (Kodak X-Omat V) was placed in the plane normal to the radiation beam axis at the normal treatment distance i.e. at 100 cm by setting X-collimators for minimum field size and Y-collimators for maximum field size (i.e. field size 0x40 cm^2) so that transmission occurred only through the pair of X-collimators and irradiated to a dose equivalent of 2000 MU in SAD set up. The exposed radiographic films were evaluated to locate the point of elevated leakage radiation through the X-collimator in beam ON condition excluding the junction of the jaws. For determination of maximum absorbed dose due to leakage radiation through X-collimator, measurement point was identified where the radiographic film indicated the maximum elevated leakage radiation. Repeated measurements were carried out at that point. For the measurement of absorbed dose due to leakage radiation, ion chamber was irradiated to 200 MU and open field (10x10 cm^2) measurement was taken for 100 MU. Accordingly, the leakage radiation meter readings were tabulated for 100 MU. Similarly other sets of measurement were carried out for determination of average leakage radiation level by performing the measurement at 24 measuring points as indicated in the inner circles of area M at NTD (Figs. 6.2 (a) and (b)), located at different couch angles. Since the maximum square field size (without clipped corner) is 40x40 cm^2, the R_0 becomes 40/2 x$\sqrt{2}$ =28.28 cm.
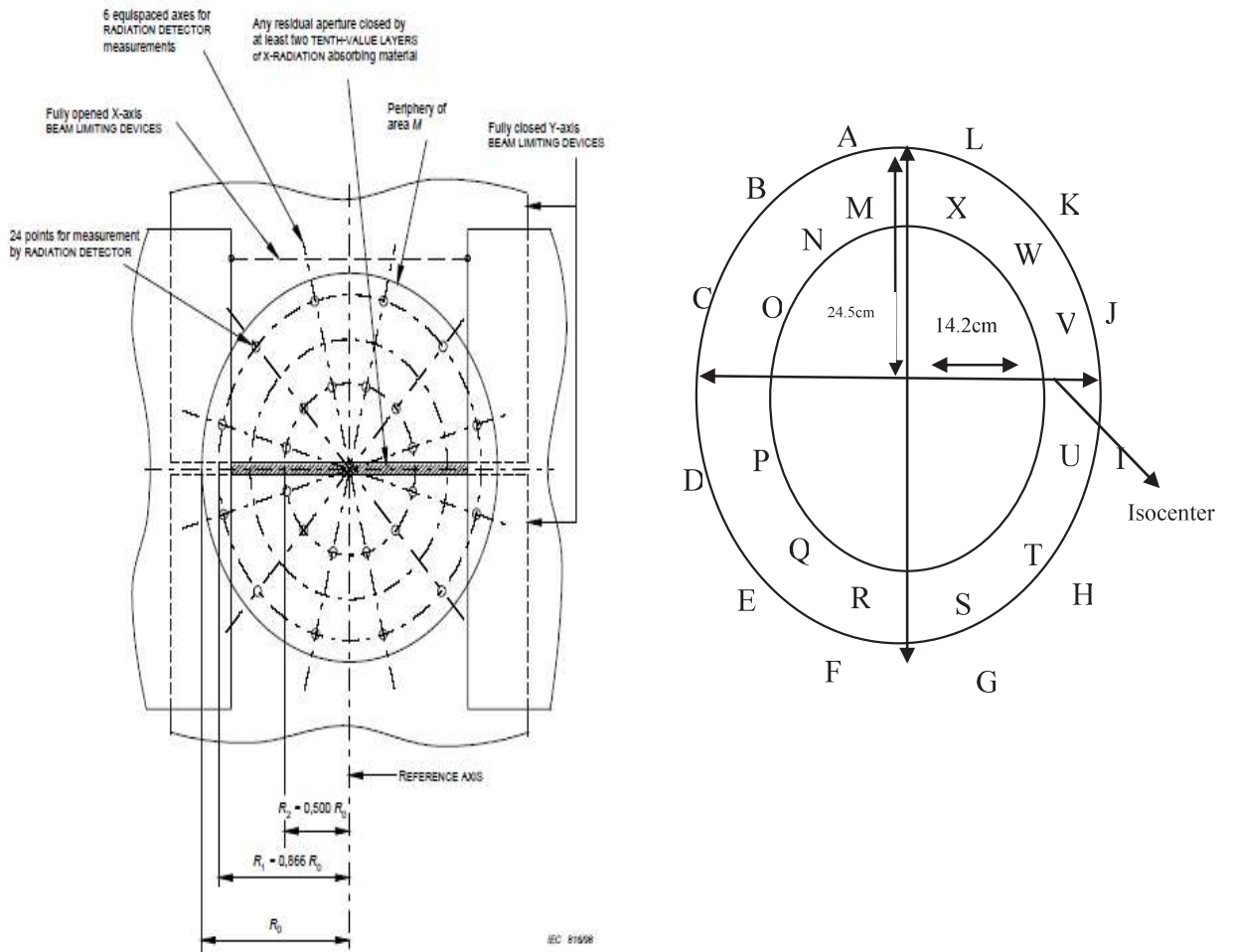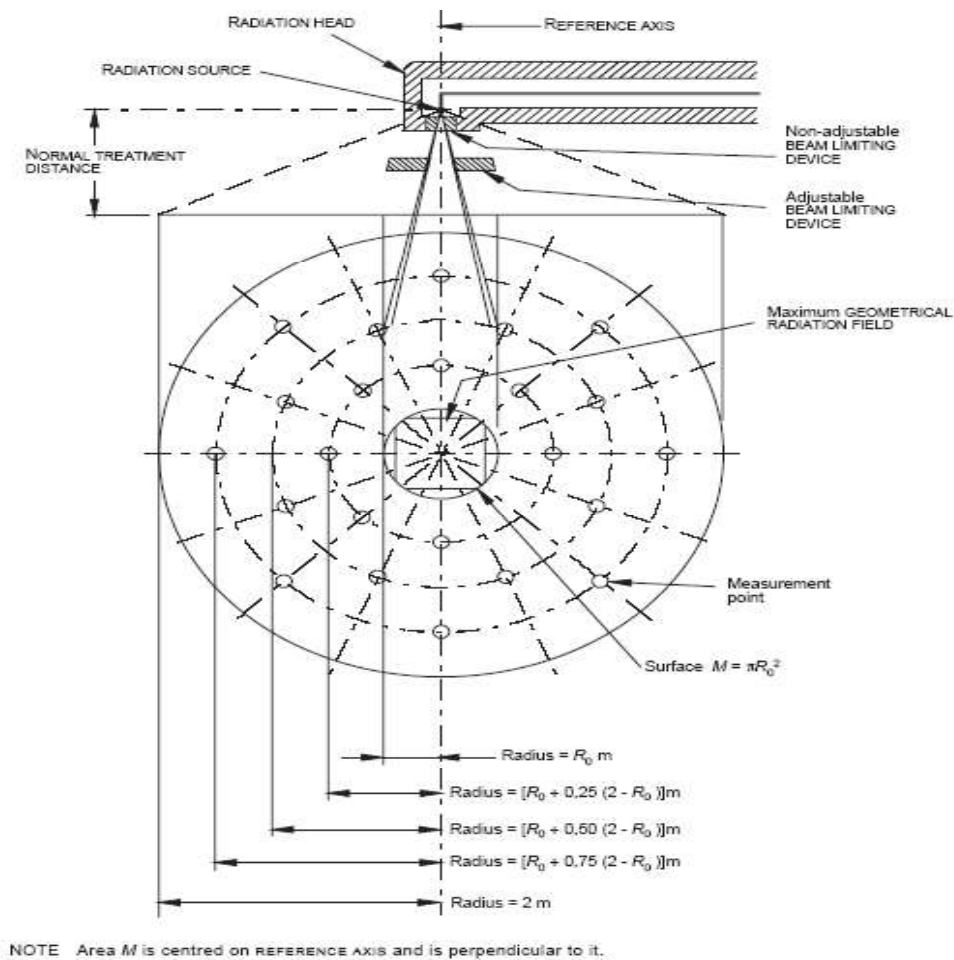
Fig.6.2 Schematic diagram presenting the measurement points for leakage radiation in the patient plane inside the area M (a) as per IEC (b) location and identification of 24 points.

Therefore, the two concentric circles were considered having radii 24.49 cm (approximated to 24.5 cm) and 14.14 cm (approximated to 14.2 cm) and divided into 12 sectors, which provides 24 intersections considered to be the points of measurement. These values were also compared with measured values of open field absorbed dose.

6.4.2.2 Leakage radiation through Y-Collimator: To evaluate the transmission through Y-collimator beam limiting device (secondary collimator), ready packs films (Kodak X-Omat V) was placed in the plane normal to the radiation beam axis at the normal treatment distance i.e. at 100 cm by setting Y-collimators for minimum field size and X-collimators for maximum field size (i.e. field size of 40x0 cm^2) so that transmission occurred only through the pair of Y-collimators and irradiated to a dose equivalent of 2000 MU with SAD set up.

The exposed radiographic films were evaluated to locate the point of elevated leakage radiation through the Y-collimator in beam ON condition excluding the junction of the jaws. For determination of maximum absorbed dose due to leakage radiation through Y-collimator, measurement point was identified where the radiographic film indicated the maximum elevated leakage radiation. Measurements were carried out at that point. For the measurement of absorbed dose due to leakage radiation chamber was irradiated to 200 MU and open field (10x10 cm^2) measurement was taken for 100 MU. Accordingly the leakage radiation meter readings were tabulated for 100 MU. Similarly other sets of measurement were carried out for determination of average leakage radiation level by performing the measurements at 24 measuring points as indicated in the inner circles of area M (see Figs. 6.2 (a) and (b)) at NTD, located at different couch angles. These values were also compared with measured values of open field absorbed dose. Since the maximum square field size (without clipped corner) is 40x40 cm^2, the R_0 becomes 40/2 x$\sqrt{2}$ =28.28 cm. So the two concentric circles were considered having radii 24.49 cm (approximated to 24.5 cm) and 14.14 cm (approximated to 14.2 cm) and divided into 12 sectors, which provides 24 intersections considered to be the points of measurement. These values were also compared with measured values of open field absorbed dose.

**6.4.2.3 Leakage radiation through Multi Leaf Collimator (MLC)**

To evaluate the transmission through MLC beam limiting device (tertiary collimator), ready packs films (Kodak X-Omat V) was placed in the plane normal to the radiation beam axis at the normal treatment distance i.e. at 100 cm by setting X and Y-collimators for maximum field size and MLC for minimum field size so that transmission occurred only through the MLC and irradiated to a dose equivalent of 2000 MU with SAD set up. The exposed radiographic films were evaluated to locate the point of elevated leakage radiation through the MLC in beam ON condition excluding junction MLC leaves. For the determination of maximum absorbed dose due to leakage radiation through MLC, measurement point was identified where the radiographic film indicated the maximum elevated leakage radiation level. Measurement was carried out at that point. For the measurement of absorbed dose due to leakage radiation chamber was irradiated to 200 MU and open field measurement was taken for 100 MU. Accordingly the leakage radiation meter readings were tabulated for 100 MU. Similarly other sets of measurement were carried out for determination of leakage radiation level by performing the measurements at 24 measuring points as indicated in the inner circles of area M (see Figs. 6.2 (a) and (b)) at NTD, located at different couch angles. These values were also compared with measured values of open field absorbed dose. Since the maximum square field size (without clipped corner) is 40x22 cm^2, the R_0 becomes 22.8 cm. So the two concentric circles were considered having radii 19.74 cm (approximated to 19.7 cm) and 11.4 cm and divided into 12 sectors, which provides 24 intersections considered to be the points of measurement.

6.4.2.4 Leakage Radiation outside the Useful Beam in the Patient Plane

Leakage radiation outside the area M (inside the patient plane): An On Board Imaging system was mounted at the gantry of True Beam STx SVC model Linac which was used for leakage radiation determination. At the gantry side with the support of an extension board a maximum clearance level could be attained up to 110 cm from isocenter. Therefore, it was determined for 22 selected measuring points as indicated in the outer circles of area M located at different couch angles within 2 meter diameter circle as shown in Figs. 6.3(a) and (b).

(a)
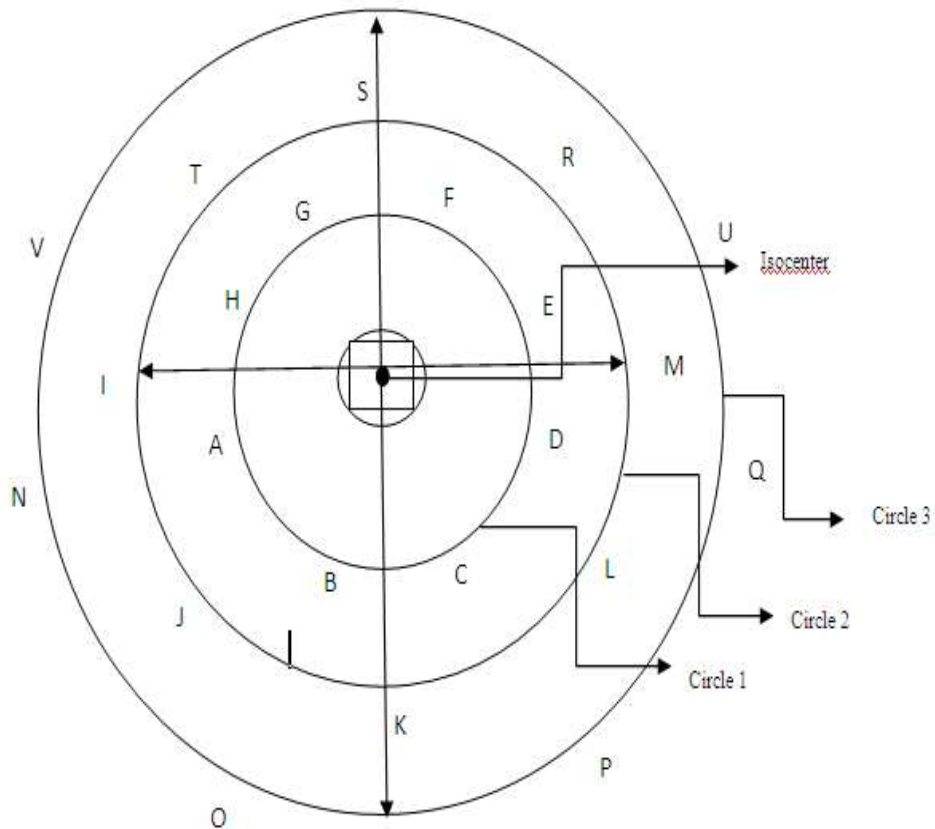
(b)

Fig.6.3 Schematic diagram presenting the measurement points for leakage radiation in the patient plane outside the area M (a) As per IEC, 2010 (b) location and identification of points.

During the measurement all BLDs were fully closed. To evaluate the leakage radiation in the patient plane within 2 m radius from the reference axis excluding the useful beam (area M), 22 measurement points were considered as per IEC (IEC, 2010). As determined earlier, the radius R_0 is 28.28 cm. So, three distances from the central axis with respect to R_0 are 71.21 cm, 114.14 cm and 157.07 cm. In this study, we have considered the circles of radius 71 cm, 114 cm and 157 cm. But due to limited clearance at gantry side, the radius was considered as 71 cm and 100 cm excluding the three extreme points.

Leakage Radiation outside the area M (outside the patient plane): To evaluate the transmission through the head including the path of electron, Kodak X-Omat V ready pack films were wrapped around the accelerator head. The field was set to 0x0 cm^{2}i.e.all BLDs were fully closed so that no scattering radiation reach to the films and the accelerator was switched on to deliver a dose equivalent to 2400 MU at isocenter in order to obtain a good optical density and 800 MUs were delivered for subsequent measurements. The exposed radiographic films were evaluated to locate the point of maximum leakage radiation through the accelerator head. Further, to cross verify for the maximum radiation leakage point at 1 metre from the accelerator, it was decided to use a pressurized ion chamber based Fluke Biomedical, USA make 450R survey meter. Then different suitable gantry angles were set to expose the ion chamber with appropriate buildup. Arrangements were made to keep the chamber central axis parallel to the gantry axis. The 10x10 cm^2 open field reading was recorded at d$_{max}$ for each energy.

In order to measure the average leakage radiation level, it was decided to measure at 3 points left to the couch, 3 points right to the couch and one point at the extreme end of the couch except within the volume formed by a plane of radius 2 m, centered on and orthogonal to the reference axis at the isocenter as shown in Fig. 6.4.
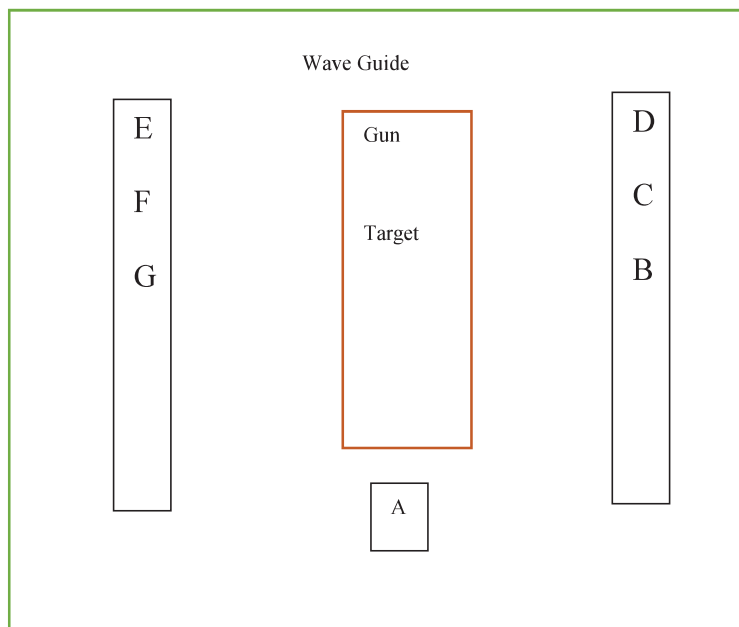
Fig. 6.4 Schematic diagram showing the points outside the patient plane

6.5 Results and Discussion

6.5.1 Results of Surface dose

The measurement of dose near to the surface is difficult as it depends on the accuracy of the measurement as well as the type of the detector used. The measured values found in this study were considered relative to the same unit rather absolute values. In the present study, similar trend was demonstrated by all the detectors used which are presented in Table 6.1 (for PP ionisation chamber), Table 6.2 (for EBT3 Gafchromic film) and Table 6.3 (Al_2O_3 OSL dosimeter). This may be due to the increase in number of scattered electrons in the air and collimator.

Table 6.1 Relative surface dose presented for Elekta Versa HD and Varian True beam Linacs using an parallel plate ionisation chamber.

Field Size (cm²)	Relative surface dose (Versa HD)				Relative surface dose (True Beam)			
	6 MV	6FFF	10 MV	10FFF	6 MV	6FFF	10 MV	10FFF
5X5	33.42	37.64	24.83	29.83	38.61	49.65	27.38	32.77
10X10	37.71	40.17	29.84	33.9	43.19	52.77	33.14	36.84
15X15	42.03	42.84	35.57	37.12	47.82	55.70	37.62	40.21
20x20	45.99	44.53	40.72	39.92	52.36	58.15	41.74	43.81
25X25	49.31	47.42	45.42	42.58	56.51	60.37	45.89	47.71

Table 6.2 Relative surface dose presented for Elekta Versa HD and Varian True beam Linacs using EBT3 GafChromic film.

| Field Size (cm²)	Relative surface dose (Elekta Versa HD)				Relative surface dose (Varian True Beam)			
	6 MV	6FFF	10 MV	10FFF	6 MV	6FFF	10 MV	10FFF
5X5	9.37	13.69	7.39	10.09	13.00	24.30	9.45	18.14
10X10	17.08	18.52	12.18	16.14	17.10	26.40	13.24	21.20
15X15	19.87	19.46	16.76	19.67	21.9	32.7	18.13	26.80
20x20	24.82	23.28	24.04	22.07	29.40	37.2	23.16	31.95
25X25	28.85	27.15	29.33	26.50	31.60	37.58	28.52	34.86

Table 6.3 Relative surface dose presented for Elekta Versa HD and Varian True beam Linacs using Al_2O_3 OSL dosimeter.

Field Size (cm^2)	Relative surface dose (Versa HD)				Relative surface dose (True Beam)			
	6 MV	6FFF	10 MV	10FFF	6 MV	6FFF	10 MV	10FFF
5X5	33.25	41.52	28.51	35.24	38.42	47.21	30.22	44.23
10X10	42.83	44.82	29.03	37.53	47.23	52.13	39.11	43.55
15X15	48.03	48.87	33.48	41.82	51.22	54.89	45.39	50.21
20x20	57.82	52.49	42.58	40.50	58.36	59.78	49.11	52.48
25X25	62.84	55.69	50.56	42.53	59.32	60.23	57.23	58.63

The relative surface dose was observed to be greater for the FFF beam as compared to the flattened beam for both the photon beam energies 6 and 10 MV in case of Varian True beam Linac. However, for Elekta Versa HD, the trend was similar up to 15x15 cm^2 field size and after which the relative surface dose for 6 MV increases as compared to 6FFF and the same has been observed for 10 MV and 10 FFF around 20x20 cm^2 field size. True beam gives higher surface dose than Versa HD for all the field sizes, more in 6 MV than 10 MV beam energy which can be identified in Figures 6.5 – 6.7 obtained using EBT3 Film, PP chamber and Al_2O_3 OSLD. The True Beam data obtained using the PP chamber are comparable with the values published by Hrbacek et al (2011), Wang et al (2012) and Fogliata et al (2015). Sigamani et al (2016) used EBT2 film for the surface dose measurement for Varian TrueBeam Linac. The results of the present study were in agreement with Sigamani et al (2016) values (with in 1 %) for EBT3 film. It may be noted that EBT2 and EBT3 films have similar composition with minor structural changes. It was observed that, both PP chamber and OSL Al_2O_3 dosimeters shows higher surface dose. However, the high spatial resolution and low spectral sensitivity provided by Gafchromic films make them relatively suitable for measurement of surface dose. Further, it was found that the trend of relative changes among Versa HD and True beam remains same in the 10 MV range.
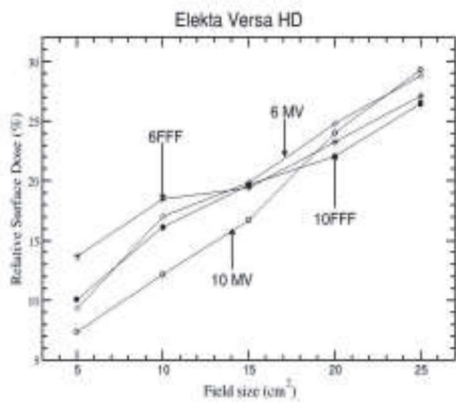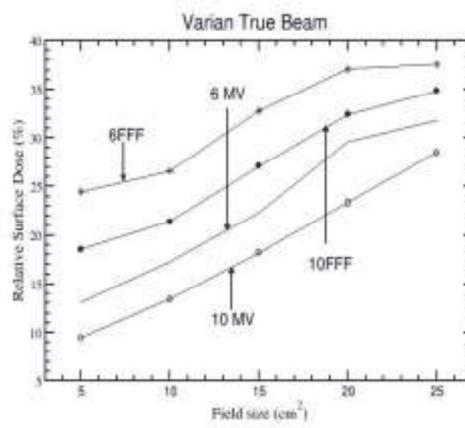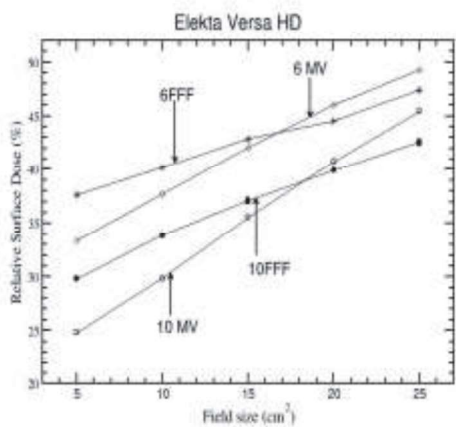
(a)   (b)
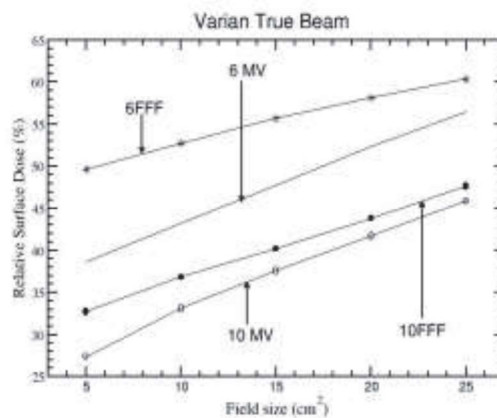
Fig. 6.5 Relative Surface Dose measured using EBT3 films for (a) Elekta Versa HD (b) Varian True beam Linacs.

(a)   (b)

Fig. 6.6 Relative Surface Dose measured using PP chamber for (a) Elekta Versa HD (b) Varian True beam Linacs.
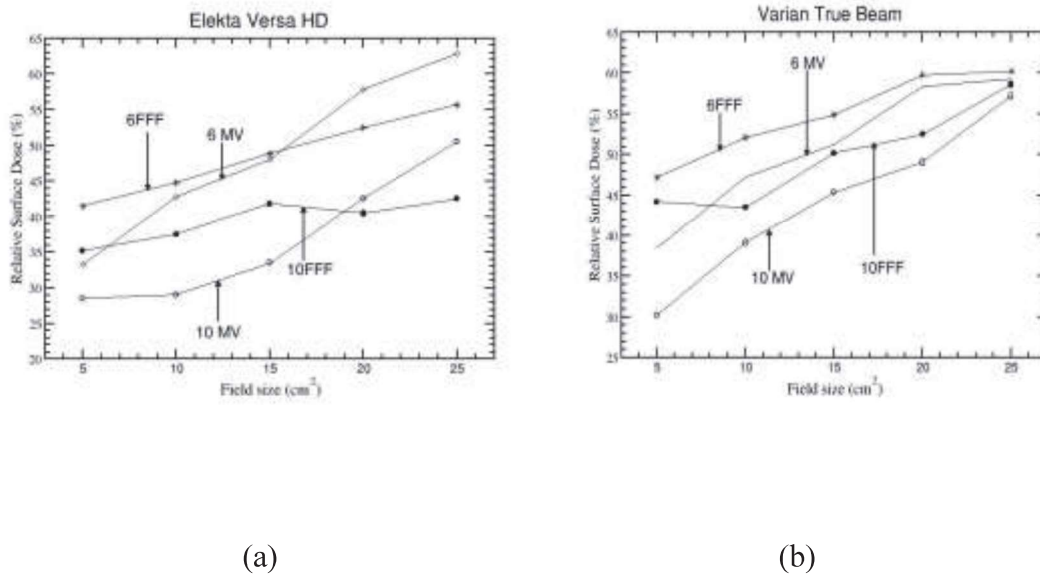
(a)   (b)

Fig. 6.7 Relative Surface Dose measured using Al_2O_3 OSLD for (a) Elekta Versa HD (b) Varian True beam Linacs.

6.5.2 Results of leakage radiation

6.5.2.1 Leakage radiation through the X, Y collimator and MLC: Average values of absorbed dose due to leakage radiation of 6 MV, 6FFF, 10 MV and 10FFF for True Beam STx SVC for X-Jaw transmission, Y-Jaw transmission are presented in Table 6.4 and Table 6.5 respectively. As MLC is placed as a tertiary collimator in this Linac, the leakage radiation due to MLC transmission is considered with respect to the maximum permissible limit which is 5% of the useful open field absorbed dose and is presented Table 6.6. The maximum values of absorbed dose due to leakage radiation of 6 MV, 6FFF, 10 MV and 10 FFF for True Beam STx SVC for X-Jaw transmission, Y-Jaw transmission and MLC transmission using films are presented in Table 6.7.

Table 6.4 Average values of leakage radiation of photon beam energies 6 MV, 6FFF, 10MV and 10FFFfor True Beam STx SVC for X-Jaw transmission.

Energy			6 MV		6 FFF		10 MV		10 FFF	
Avg. Meter Readings (nC/100 MU)	Dose rate (MU/min)		600		1400		600		2400	
	Position	Couch Angle	MR(nC)	Transmission (%)	MR (nC)	Transmission (%)	MR (nC)	Transmission (%)	MR (nC)	Transmission (%)
	Open Field (10x10 cm^2)	0.0	18.59 18.59 18.60	Avg.=18.59	18.53 18.52 18.54	Avg.=18.53	19.36 19.36 19.37	Avg.=19.36	18.9 18.9 18.9	Avg.=18.9
	A	22.5	0.033	0.18	0.015	0.08	0.042	0.22	0.015	0.08
	B	45	0.032	0.17	0.016	0.09	0.043	0.22	0.016	0.08
	C	67.5	0.033	0.18	0.017	0.09	0.044	0.23	0.015	0.08
	D	292.5	0.035	0.19	0.015	0.08	0.042	0.22	0.015	0.08
	E	315	0.031	0.17	0.014	0.08	0.041	0.21	0.017	0.09
	F	337.5	0.032	0.17	0.015	0.08	0.045	0.23	0.015	0.08
	G	22.5	0.033	0.18	0.017	0.09	0.043	0.22	0.014	0.07
	H	45	0.034	0.18	0.015	0.08	0.044	0.23	0.016	0.08
	I	67.5	0.030	0.16	0.016	0.09	0.045	0.23	0.015	0.08
	J	292.5	0.032	0.17	0.015	0.08	0.044	0.23	0.016	0.08
	K	315	0.033	0.18	0.015	0.08	0.043	0.22	0.015	0.08
	L	337.5	0.031	0.17	0.016	0.09	0.042	0.22	0.015	0.08
	M	22.5	0.055	0.30	0.036	0.19	0.068	0.35	0.039	0.21
	N	45	0.053	0.29	0.037	0.20	0.069	0.36	0.04	0.21
	O	67.5	0.055	0.30	0.035	0.19	0.068	0.35	0.039	0.21
	P	292.5	0.054	0.29	0.036	0.19	0.067	0.35	0.038	0.20
	Q	315	0.052	0.28	0.038	0.21	0.069	0.36	0.039	0.21
	R	337.5	0.053	0.29	0.039	0.21	0.070	0.36	0.04	0.21
	S	22.5	0.054	0.29	0.039	0.21	0.071	0.37	0.041	0.22
	T	45	0.055	0.30	0.038	0.21	0.072	0.37	0.042	0.22
	U	67.5	0.059	0.32	0.037	0.20	0.073	0.38	0.043	0.23
	V	292.5	0.057	0.31	0.035	0.19	0.071	0.37	0.044	0.23
	W	315	0.056	0.30	0.036	0.19	0.075	0.39	0.044	0.23
	X	337.5	0.057	0.31	0.039	0.21	0.076	0.39	0.045	0.24
Average	leakage	radiation (%)	**0.24**		**0.14**		**0.29**		**0.15**	

Table 6.5 Average values of leakage radiation of photon beam energies 6 MV, 6FFF, 10MV and 10FFFfor True Beam STx SVC forY-Jaw transmission.

Energy			6 MV		6 FFF		10 MV		10 FFF	
Avg. MR (nC/100 MU)	Dose rate (MU/min)		600		1400		600		2400	
	Position	Couch Angle	MR(nC)	Transmission (%)	MR (nC)	Transmission (%)	MR (nC)	Transmission (%)	MR (nC)	Transmission (%)
	Open Field (10x10 cm²)	0.0	18.59 18.59 18.60	Avg.=18.59	18.53 18.52 18.54	Avg.=18.53	19.36 19.36 19.37	Avg.=19.36	18.9 18.9 18.9	Avg.=18.9
	A	22.5	0.029	0.16	0.014	0.08	0.031	0.16	0.014	0.07
	B	45	0.028	0.15	0.012	0.06	0.032	0.17	0.015	0.08
	C	67.5	0.026	0.14	0.015	0.08	0.033	0.17	0.013	0.07
	D	292.5	0.029	0.16	0.014	0.08	0.033	0.17	0.013	0.07
	E	315	0.028	0.15	0.012	0.06	0.031	0.16	0.015	0.08
	F	337.5	0.027	0.15	0.012	0.06	0.032	0.17	0.014	0.07
	G	22.5	0.028	0.15	0.015	0.08	0.031	0.16	0.013	0.07
	H	45	0.029	0.16	0.014	0.08	0.032	0.17	0.015	0.08
	I	67.5	0.028	0.15	0.015	0.08	0.034	0.18	0.015	0.08
	J	292.5	0.027	0.15	0.013	0.07	0.032	0.17	0.014	0.07
	K	315	0.029	0.16	0.012	0.06	0.031	0.16	0.015	0.08
	L	337.5	0.028	0.15	0.015	0.08	0.032	0.17	0.013	0.07
	M	22.5	0.045	0.24	0.03	0.16	0.057	0.29	0.037	0.20
	N	45	0.043	0.23	0.031	0.17	0.058	0.30	0.035	0.19
	O	67.5	0.044	0.24	0.029	0.16	0.058	0.30	0.036	0.19
	P	292.5	0.045	0.24	0.032	0.17	0.056	0.29	0.035	0.19
	Q	315	0.044	0.24	0.03	0.16	0.058	0.30	0.037	0.20
	R	337.5	0.045	0.24	0.031	0.17	0.057	0.29	0.038	0.20
	S	22.5	0.044	0.24	0.032	0.17	0.058	0.30	0.039	0.21
	T	45	0.046	0.25	0.031	0.17	0.061	0.32	0.038	0.20
	U	67.5	0.047	0.25	0.03	0.16	0.062	0.32	0.042	0.22
	V	292.5	0.048	0.26	0.032	0.17	0.063	0.33	0.041	0.22
	W	315	0.049	0.26	0.032	0.17	0.062	0.32	0.042	0.22
	X	337.5	0.048	0.26	0.034	0.18	0.063	0.33	0.044	0.23
Average	leakage	radiation (%)	**0.20**		**0.12**		**0.24**		**0.14**	

Table 6.6 Values of leakage radiation of photon beam energies 6 MV, 6FFF, 10 MV and 10FFF for True Beam STx SVC for MLC transmission.

Energy			6 MV		6 FFF		10 MV		10 FFF	
	Dose rate (MU/min)		600		1400		600		2400	
Avg. MR (nC/100 MU)	Position	Couch Angle	MR (nC)	Transmission (%)	MR (nC)	Transmission (%)	MR (nC)	Transmission (%)	MR (nC)	Transmission (%)
	Open Field (10x10 cm²)	0	18.59 18.59 18.60	Avg.=18.59	18.53 18.52 18.54	Avg.=18.53	19.36 19.36 19.37	Avg.=19.36	18.9 18.9 18.9	Avg.=18.9
	A	22.5	0.21	1.13	0.14	0.76	0.25	1.29	0.18	0.95
	B	45	0.21	1.13	0.15	0.81	0.24	1.24	0.21	1.11
	C	67.5	0.19	1.02	0.14	0.76	0.21	1.08	0.19	1.01
	D	292.5	0.19	1.02	0.15	0.81	0.22	1.14	0.19	1.01
	E	315	0.20	1.08	0.17	0.92	0.23	1.19	0.18	0.95
	F	337.5	0.21	1.13	0.14	0.76	0.23	1.19	0.18	0.95
	G	22.5	0.21	1.13	0.15	0.81	0.21	1.08	0.19	1.01
	H	45	0.19	1.02	0.16	0.86	0.23	1.19	0.20	1.06
	I	67.5	0.19	1.02	0.15	0.81	0.24	1.24	0.19	1.01
	J	292.5	0.19	1.02	0.15	0.81	0.22	1.14	0.19	1.01
	K	315	0.20	1.08	0.16	0.86	0.23	1.19	0.20	1.06
	L	337.5	0.21	1.13	0.15	0.81	0.23	1.19	0.17	0.90
	M	22.5	0.25	1.34	0.19	1.03	0.26	1.34	0.25	1.32
	N	45	0.24	1.29	0.21	1.13	0.25	1.29	0.25	1.32
	O	67.5	0.25	1.34	0.21	1.13	0.28	1.45	0.25	1.32
	P	292.5	0.24	1.29	0.22	1.19	0.26	1.34	0.25	1.32
	Q	315	0.27	1.45	0.23	1.24	0.28	1.45	0.26	1.38
	R	337.5	0.26	1.40	0.22	1.19	0.29	1.50	0.26	1.38
	S	22.5	0.26	1.40	0.21	1.13	0.29	1.50	0.25	1.32
	T	45	0.28	1.51	0.20	1.08	0.30	1.55	0.26	1.38
	U	67.5	0.28	1.51	0.22	1.19	0.31	1.60	0.27	1.43
	V	292.5	0.27	1.45	0.22	1.19	0.30	1.55	0.25	1.32
	W	315	0.28	1.51	0.21	1.13	0.29	1.50	0.28	1.48
	X	337.5	0.27	1.45	0.22	1.19	0.29	1.50	0.27	1.43
Average	leakage	radiation (%)		1.24		0.98		1.32		1.18

Table 6.7 Maximum values of leakage radiation of photon beam energies 6 MV, 6FFF, 10MV and 10FFF for True Beam STx SVC for X-jaw, Y-jaw and MLC transmission.

Energy		6 MV	6 FFF	10 MV	10 FFF
	Dose rate (MU/min)	600	1400	600	2400
Avg. Meter Readings in nC/100 MU	Open Field (10x10 cm^2)	Avg.=18.59	Avg.=18.53	Avg.=19.36	Avg.=18.9
	Point selected from radiograph		Meter Readings (nC)		
X Jaw	Measurement 1	0.06	0.039	0.076	0.047
	Measurement 2	0.063	0.041	0.079	0.045
	Measurement 3	0.064	0.04	0.077	0.046
Average lekage radiation	w.r.t open field (%)	0.34	0.22	0.4	0.24
Y Jaw	Measurement 1	0.051	0.033	0.063	0.042
	Measurement 2	0.05	0.034	0.062	0.044
	Measurement 3	0.051	0.035	0.063	0.045
Avg leakage radiation	w.r.t open field (%)	0.27	0.18	0.32	0.23
MLC	Measurement 1	0.28	0.23	0.32	0.29
	Measurement 2	0.28	0.25	0.31	0.28
	Measurement 3	0.28	0.25	0.32	0.29
Avg leakage radiation	w.r.t open field (%)	1.51	1.31	1.64	1.52

As per IEC the leakage radiation through the collimators need to be compared with the maximum absorbed dose measured on the reference axis at NTD in a open 10 cm x 10 cm radiation field and expressed in percentage and each BLD excluding MLC shall attenuate X-ray radiation such that anywhere in the area M, excepting the rectangular radiation field, the absorbed dose due to leakage radiation dose not exceed 2% of the maximum absorbed dose measured on the reference axis at NTD in a 10 cm x 10 cm radiation field. The maximum absorbed dose due to leakage radiation in 6 MV and 10 MV were found be greater than the corresponding 6FFF and 10FFF beams for X-jaw and Y-jaw. However the relative variation of 10 MV with 10FFF was more as compared to the variation between 6 MV and 6FFF. All these values are within the specified tolerance limit of 2%. Further, as per IEC for radiation fields of any size, the average absorbed

dose, due to leakage radiation through the collimators, in the useful beam (area M), shall not exceed 0.75% of the maximum absorbed dose on the reference axis at NTD. The average absorbed dose due to leakage radiation showed the similar trend shown for maximum absorbed dose due to leakage radiation for both X-jaw and Y-jaw and found to be with the specified tolerance limit.

As stipulated in IEC the absorbed dose due to leakage radiation through the parts of a multi-element BLD that project into the rectangular radiation field formed by the automatically adjustable BLDs referred i.e. MLC shall not exceed 5% of the maximum absorbed dose measured on the reference axis at NTD in a 10 cm x 10 cm radiation field. The maximum absorbed dose due to leakage radiation in 6 MV and 10 MV were found be greater than the corresponding 6FFF and 10FFF beams for MLC. The measured values are within the specified tolerance limit.

6.5.2.2 Leakage Radiation outside the Useful Beam

Leakage radiation outside the area M (inside the patient plane): Values of this parameter is presented in the Table 6.8. The average meter reading obtained were compared with that for the open field 10x10 cm^2 field size meter reading. In order to obtain sufficient chamber signal 800 MUs were delivered for this measurement both for open field and closed field.

As stipulated in IEC, the Linac shall be provided with protective shielding that attenuates ionizing radiation so that, in a plane circular surface of radius 2 m centered on and orthogonal to the reference axis at the isocentre and orthogonal to the reference axis at the isocentre, and excluding the area M, the absorbed dose due to leakage radiation, excluding neutron shall not exceed a maximum of 0.2% and an average of 0.1% of the

maximum absorbed dose measured at the center of the plane in a 10x10 cm^2 radiation field. In this study, it was found that the maximum and average leakage radiation in the patient plane excluding the area M was found to be within the tolerance limit of 0.2 % and 0.1 % respectively. Further, it is also noted that the absorbed dose due to leakage radiation is more in case of flattened beam in comparisons to the FFF beam.

Table 6.8 Measured values of Leakage radiation in the patient plane excluding area M.

Energy		6 MV		6 FFF		10 MV		10 FFF	
Dose rate (MU/min)		600		1400		600		2400	
Avg. Meter Readings in nC/800 MU	Position	Avg MR (nC)	Transmission (%)	Avg MR (nC)	Transmission (%)	Avg MR (nC)	Transmission (%)	Avg MR (nC)	Transmission (%)
	Open Field (10x10 cm^2)	149		148		155		151	
	A	0.006	0.0040	0.003	0.0020	0.009	0.0058	0.003	0.0020
	B	0.002	0.0013	0.001	0.0007	0.008	0.0052	0.009	0.0060
	C	0.002	0.0013	0.001	0.0007	0.012	0.0077	0.005	0.0033
	D	0.0012	0.0008	0.002	0.0014	0.011	0.0071	0.003	0.0020
	E	0.005	0.0034	0.002	0.0014	0.004	0.0026	0.002	0.0013
	F	0.004	0.0027	0.003	0.0020	0.009	0.0058	0.003	0.0020
	G	0.003	0.0020	0.002	0.0014	0.005	0.0032	0.003	0.0020
	H	0.005	0.0034	0.001	0.0007	0.009	0.0058	0.005	0.0033
	I	0.005	0.0034	0.001	0.0007	0.008	0.0052	0.005	0.0033
	J	0.003	0.0020	0.002	0.0014	0.009	0.0058	0.007	0.0046
	K	0.004	0.0027	0.003	0.0020	0.009	0.0058	0.005	0.0033
	L	0.006	0.0040	0.002	0.0014	0.012	0.0077	0.006	0.0040
	M	0.005	0.0034	0.003	0.0020	0.006	0.0039	0.008	0.0053
	N	0.005	0.0034	0.001	0.0007	0.005	0.0032	0.004	0.0026
	O	0.005	0.0034	0.001	0.0007	0.006	0.0039	0.004	0.0026
	P	0.004	0.0027	0.002	0.0014	0.009	0.0058	0.004	0.0026
	Q	0.004	0.0027	0.001	0.0007	0.009	0.0058	0.004	0.0026
	R	0.004	0.0027	0.002	0.0014	0.009	0.0058	0.007	0.0046
	S	0.004	0.0027	0.003	0.0020	0.009	0.0058	0.005	0.0033
	T	0.006	0.0040	0.002	0.0014	0.012	0.0077	0.006	0.0040
	U	0.005	0.0034	0.001	0.0007	0.006	0.0039	0.004	0.0026
	V	0.004	0.0027	0.001	0.0007	0.009	0.0058	0.004	0.0026
			0.0028		**0.0012**		**0.0054**		**0.0032**

Leakage radiation outside the area M (outside the patient plane): Value of this parameter are presented in the Table 6.9.

Table 6.9 Measured values of Leakage radiation outside the patient plane excluding the area M.

Energy		6 MV		6 FFF		10 MV		10 FFF	
	Dose rate (MU/min)	600		1400		600		2400	
Avg. Meter Readings in nC/800 MU	Position	Avg MR (nC)	Transmission (%)	Avg MR (nC)	Transmission (%)	Avg MR (nC)	Transmission (%)	Avg MR (nC)	Transmission (%)
	Open Field (10x10 cm^2)	149		148		155		151	
	A	0.009	0.0060	0.007	0.0047	0.008	0.0052	0.006	0.0040
	B	0.008	0.0054	0.008	0.0054	0.008	0.0053	0.004	0.0026
	C	0.005	0.0034	0.004	0.0027	0.007	0.0046	0.005	0.0032
	D	0.004	0.0027	0.003	0.0020	0.006	0.0040	0.004	0.0026
	E	0.004	0.0027	0.004	0.0027	0.007	0.0046	0.005	0.0032
	F	0.006	0.0040	0.003	0.0020	0.005	0.0033	0.004	0.0026
	G	0.005	0.0034	0.002	0.0014	0.006	0.0040	0.004	0.0026
Avg.	Leakage(%)		**0.0039**		**0.0030**		**0.0044**		**0.0030**

The average value of all the measurements at the seven points (Fig. 6.4) for both FF and FFF beams shows that the leakage radiation in FFF mode is lesser than that in FF mode. The maximum value was recorded at the point from the scanned films where the radiography films showed an elevated radiation level. It was carried out for 10 MV beam energy only. After identification of that point repeated measurement were carried out at the point and the value found to be 0.008 %. From this study, it was found that the maximum and average leakage radiation level were within the tolerance limit of 0.2 % and 0.1 % respectively.

Conclusions:

FFF beam change the dosimetric characteristics of photon beams by softening the energy spectra compared to FF beam, thus changing the surface doses. Our study compares the surface dose for two different Linac model from two different manufacturer. It is found that the variation in surface dose in Versa HD Linac is less in comparison to TrueBeam Linac. Within the clinical range of field size the relative surface dose from Versa HD unit initially increases till the field size close to 15 x 15 cm^2 ~ 20 x 20 cm^2 and then decreases which does not holds good for True Beam Linac. Therefore, careful evaluation of surface dose is required and the stability of this parameter need to be periodically checked with respect to the values obtained during commissioning. Surface dose varies with field size for both the cases i.e. for FFF and FF beam. Therefore, instead of measuring the surface dose for a recommended field size (AERB TG, 2015) of 20x20 cm^2, the measurement should be carried out other lower and higher field sizes. The relative variation for 6 MV and 6FFF in case of True Beam is found to be more in comparison to 10 MV and 10FFF. However, opposite trend has been observed in case of Versa HD unit. All the detectors have demonstrated similar trend for this relative surface dose measurement.

Regarding absorbed dose due to leakage radiation in FF and FFF beam, our study shows that absorbed dose due to leakage radiation is lower for FFF beam in comparison to FF beam for all the conditions stipulated in IEC. All the results obtained from this study found well within the tolerance limit specified in IEC.

Chapter 7

Summery, Conclusion and Future work

7.1. Summery and Conclusion

Significant benefits were noted due to introduction of FFF radiotherapy beam in terms of high dose rate, lesser leakage radiation & head scatter and lesser surface dose, etc. However, dosimetric parameters of the Linac in the absence of FF have been changed to a great extent. Therefore, the beam acceptance protocol put several challenges while commissioning the C-Arm Linacs producing FFF beam. In the current scenario it has been observed that the use of Linac in FFF mode has been increased.

Feasibility study for use of indigenously developed Linac (Siddharth) in FFF mode was carried out using Monte Carlo-based EGSnrc code system. In this study, Monte Carlo caculated results are benchmarked with the results obtained from measurements. It was observed that the dosimetric parameters are within the permissible limit for the FFF beam. Considering the requirement of an enhancer plate in the place of FF, the investigation on optimum thickness and material of the desired enhancer plate were also carried out. It was found that 3 mm Al in combination with 1 mm Cu is the optimum material and thickness required for the enhancer plate.

Shielding requirements of a Linac bunker operated in FF and FFF mode was compared with that of a Linac bunker operated for FF beam only. It is found that overall the barrier thickness for a Linac operated in FF mode is higher about 20 % to that of a Linac operated in both FF and FFF. Hence, the lower consumption of shielding material and space for new treatment vaults housing the Linacs with FFF and FF modes may reduce the building cost, whereas for existing facilities, one might take the benefits in terms of increased weekly workload. As per the recommendations of Budgell et al (2016) a full assessment of expected workload and type of treatment should be carried out and time

averaged dose rates should be used rather than instantaneous dose rates in radiation protection calculations. Although, the shielding requirement study (for this thesis work) for FFF beam producing Linac in Indian Senario was initiated much before the above said publication, the same recommendations has been followed and the results were demonstrated in our study.

Various dosimetric parameters recommended by different protocols i.e. by Fogliata et al (2012 and 2015) and AERB task group (Sahani et al 2014) were studied in detail. It was observed that the results of dosimetric parameters evaluated using the protocols differ significantly. Though the values are compared with respect to FF beam and with respect to the values determined during the commissioning of the Linac, unavailability of a rational specified tolerance limit for the parameters, attract concerns on implementing the protocols. Many methods, such as profile normalization, determination of IP, etc. adopted by these protocols are cumbersome. However, in this study values are determined for Varian Edge and Elekta Versa HD units. Based on the results, new formalisms were suggested which needs to be incorporated in the FFF beam dosimetry.

Surface dose and leakage radiation were measured using different dosimeters. The key benefit of filter removal with respect to the reduction of absorbed dose due to leakage radiation from the treatment head and beam limiting devices were investigated. The relative surface dose has been studied using various detectors and the measured values are compared with FF beam surface dose. It was demonstrated that the surface dose varies at large from model to model and relative variation in FF and FFF mode are also different across the models.

7.2 Future Work:

The scope for future work includes:

1. Further studies need to be carried out based on the recommendations of Budgell et al (2016) , Ponich et al (2006) and Fogliata et al (2012 and 2015) and AERB TG (Sahani et al 2014) on various dosimetric parameters for indigenously developed Linac and should be compared with commercially available Linacs.

2. Keeping in view, the requirement of enhancer plate thickness and material, various different materials can be investigated to optimize the beam steering requirement, providing sufficient signal to the servo plate, prevention of direct incidence of electron beam in case of target rupture and optimizing in reduction of surface dose. Further, Monte Carlo –calculated need to be carried out to bench mark the data with measurement.

3. The study on structural shielding requirement can be extended for 10 MV and also for 6 MV without considering the contribution from FF beam for both the cases. Recently, due to introduction of a helical structure Linac "Halcyon" from Varian Medical System, the need has arisen to study the shielding requirements for this kind of helical Linac due the adopted technology is different from C-Arm Linacs. In addition to the workload calculation based on the MU delivered for different clinical cases, consideration of IMRT factor in the shielding calculation need to be investigated.

4. Though FFF radiotherapy beam has been fully investigated before its clinical implementation, there are still certain ambiguity in the beam acceptance criteria persists. This is typically in the context of tolerance limit of the recommended parameters by the available protocols. It is worth noting that many of these parameters are evaluated with respect to FF beam available in that particular Linac, however this might not be the case all the time as standalone FFF Linac has been introduced (www.varian.com/halcyon) and

may be C-arm FFF standalone Linac will be made available in future. Therefore, it must be taken into account while prescribing the limits on dosimetric parameters that the Elekta linacs are energy-matched with the respective beam whereas Varian linacs have a lower effective energy. Therefore, machine specific study and comparative studies on the same FFF beam produced from various Linac need to be carried out.

5. Though, this study demonstrated the behavior of relative surface dose for FF and FFF beam produced from Elekta and Varian Linacs, but for clinical cases further study required for proper estimation of the surface dose (skin dose). As the estimation of surface dose already established for FF beam by using correction factors recommended by Velkley (Velkley et al 1975), Mellenberg (Mellenberg et al 1990) and Gerbi (Gerbi et al 1990), the applicability of these correction factors need to be studied for FFF beam. Because of high dose rate in FFF mode, dose rate dependent chambers may need correction factors to achieve precision in dosimetry (Xiao et al 2015). The technology adopted by the manufacturers fixed different electron energy for the photon beam production. For example, Varian Medical System uses the same incident electron energy and Elekta Ltd uses higher incident electron energy in the production of FFF beam in comparison to FF beam. Therefore, characteristics of FFF beam produced by varying the incident electron energy need to be studied in order to establish various properties of photon beam as a function of incident electron beam energy.

6. Further, considering the clinical need, FFF beam has been well adopted in IMRT, SRS/SRT, VMAT etc. wherein high dose rate plays very important role. But the radiobiology of such high dose rate delivery has not yet established. Future studies required in this direction.

References

Adler J R, Chang S D, Murphy M J, Doty J, Geis P and Hancock S L 1997 The Cyberknife: a frameless robotic system for radiosurgery *Stereotact. Funct. Neurosurg.* **69**124-8

AERB Annual Report **2007** (www.aerb.gov.in)

AERB Annual Report **2017** (www.aerb.gov.in)

Agostinelli S, Allison J, Amako K, Apostolakis J, Araujo H, Arce P et al 2003 Geant4—a simulation toolkit *Nucl. Instrum. Methods Phys. Res. A* **506** 250-303

Andreo P 1991 Monte Carlo techniques in medical radiation physics *Phys. Med. Biol.***36** 861-920

Andreo P, Burns D T, Hohlfeld H, Huq M S, Kanai T, Laitano F, Smyth V, Vynckier S 2000 IAEA Technical Report Series No. 398 (International Atomic Energy Agency, Vienna)

Ankit K, Neeraj S, Shiru S, Satyajit P, Abhijit M, Lalit A M 2017 Monte Carlo study of a flattening filter-free 6 MV photon beam using the BEAMnrc code *Biomed. Res.***28** 1566-73.

Attix F H 1986 Introduction to Radiological Physics and Radiation Dosimetry New York Wiley U.S.A.

Barnett G C, West C M, Dunning A M, Elliott R M, Coles C E, Pharoah P D, Burnet N G 2009 Normal tissue reactions to radiotherapy: towards tailoring treatment dose by genotype *Nat. Rev. Cancer***9** 134-142

Baro J, Sempau J, Fernandez-Varea J M and Salvat F 1995 PENELOPE: an algorithm for Monte Carlo simulation of the penetration and energy loss of electrons and positrons in matter   Nucl. Instrum. Methods Phys. Res. B 100 31-46

Barton M B, Gebski V, Manderson C, Langlands A O 1995 Radiation Therapy: are we getting value for money? *Clin. Oncol.* **7** 287-92

Baskar R, Lee A K, Yeol R, Yeoh W 2012 Cancer and Radiation Therapy: Current Advances and Future Directions *Int. J. Med. Sciences* **9** 193-199

Battum L J, Hoffman D, Piersma H, Heukelom S 2008 Accurate Dosimetry with Gafchromic EBT Film of a 6 MV Photon Beam in Water: What Level Is Achievable? *Med. Phy.*, **35** 704-716, 2008

Begg A C, Stewart F A, Vens C 2011 Strategies to improve radio-therapy with targeted drugs. *Nat. Rev. Cancer***11** 239-253

Berger M J1963 Monte Carlo Calculation of the penetration and diffusion of fast charged particles in *Methods in Computational Physics* edited by Alder B, Fernbach S and Rotenberg M Academic Pres New York**1**135-215

Berger M. J, Hubbell J.H., XCOM, Photon cross sections on a personal computer. Report No.NBSIR87–3597. Gaithersburg, MD: NIST; 1987. Available from: http://physics.nist.gov/PhysRefData/Xcom/html/xcom1.html

Bernier J, Hall E J, Giaccia A 2004 Radiation oncology: a century of achievements *Nature* **4** 737-747

Bielajew A F and Rogers D W O 1987 PRESTA: The Parameter Reduced Electron-Step Transport Algorithm for electron Monte Carlo transport Nucl. Instrum. Methods Phys. Res. B18 165-181

Bielajew A.F. 2001 Fundamentals of the Monte Carlo method for neutral and charged particle transport (The University of Michigan, 2001)

Bielajew A F 2000 Fundamentals of the Monte Carlo method for neutral and charged particle transport. The University of Michigan U.S.A

Brahme A, Kraepelien T and Svensson H 1980 Electron and photon beams from a 50 MeV racetrack microtron *Acta. Radiol. Oncol.* **19** 305-319

Brahme A and Andreo P 1986 Dosimetry and quality specification of high energy photon beams *Acta. Radiol. Oncol.* **25** 213-23

Brien P F, Gillies B A, Schwartz M, Young CandDavey P 1991 Radiosurgery with unflattened 6-MV photon beams *Med. Phys.* **18** 519-21

Briesmeister J F (ed) 1988 MCNP-A General Monte Carlo N-Particle Transport Code Version 4A LA-12625-M (Los Alomos, NM: Los Alamos National Laboratory)

Briesmeister J F (ed) 1997 MCNP-A General Monte Carlo N-Particle Transport Code Version 4B LA-12625-M (Los Alamos, NM: Los Alamos National Laboratory)

Budgell G, Brown K, Cashmore J, Duane S, Frame J, Hardy M, Patnter D and Thomas R 2016 IPEM topical report 1: guidance on implementing flattening filter free (FFF) radiotherapy *Phys. Med. Biol.* **61** 8360-8394

Carl J and Vestergaard A 2000 Skin damage probabilities using fixation materials in high- energy   photon beams *Radiothe. Oncol.* **55** 191-8

Cashmore J 2006 The characterization of unflattened photon beams from a 6 MV linear accelerator *Phys. Med. Biol.* **53** 1933-46

Cashmore J 2008 The characterisation of unflattened photon beams from a 6MV linear accelerator *Phys. Med. Biol.* **53** 1933-1946

Cashmore J 2016 Surface dose variations in 6 and 10 MV flattened and flattening filter-free (FFF) photon beams *J. App. Cli. Med. Phy.* **17** 293-307

Castrillón S V and Henríquez F C 2009 Comparison of IPSM 1990 photon dosimetry code of practice with IAEA TRS-398 and AAPM TG-51 *J. Appl. Clin. Med. Phys.* **10** 136-146   doi:10.1120/jacmp.v10i1.2810.

Conere T, Weatherburn H and Wassen B 1989 An Interesting Radiation Protection Finding around a Linear Accelerator *Br. J. Radiol.* **62** 1033

Dalaryd M, Kragl G, Ceberg C, Georg D, McClean B, af Wetterstedt S, Wieslander E and Knöös T 2010 A Monte Carlo study of a flattening filter-free linear accelerator verified with measurements *Phys. Med. Biol.* **55** 7333-44

Delaney G, Jacob S, Featherstone C, Barton M 2005 The role of radiotherapy in cancer treatment: estimating optimal utilization from a review of evidence-based clinical guidelines *Cancer* **104** 1129-1137

DeMarco J J, Solberg T D, Wallace R E and Smathers J B 1995 A verification of Monte Carlo code MCNP for thick target bremsstrahlung calculation *Med. Phys.* **22** 11-16

Devanney J A 1980 Radiological Safety of Accelerators, a Comparison of Performance Standards *Nuc. Sci.***30** 1583-1587

Devic S, Seuntjens J, Abdel-Rahman W, Evans M, Olivares M, Podgorsak E B, Vuong T, Soares CG 2006 Accurate skin dose measurements using radiochromic film in clinical applications *Med. Phy.***33** 1116–1124

Dixon R L, Ekstrand K E and Huff W J 1977 Beam Characteristics of the Varian 6 MV Clinac 6X accelerator *Inter. J. Rad. Onco. Bio. Phys.* **2** 585-590

Eatmon S 1996 Cancer: An Overview in Principles and Practice of Radiation Therapy - Introduction to Radiation Therapy Washington C M and Leaver D T (eds.), Mosby Year Book Inc., New York, USA.

Eckhardt R 1987 Stan Ulam, John von Neumann and the Monte Carlo method Los Alamos Science, Special Issue **15** 131-41

Emiliano Spezi and Geraint Lewis 2008 An overview of Monte Carlo treatment planning for radiotherapy *Rad. Prot. Dosi.* 1-7

Ferrari A, Sala PR, Fassò A and Ranft J 2005 FLUKA: A Multi-Particle Transport Code. Technical Report CERN-2005-10, INFN/TC 05/11, SLAC-R-773, CERN, INFN, SLAC.

Fishman G S 1996 Monte Carlo: concepts, algorithms, and applications (Springer Series inOperations Research and Financial Engineering) Springer

Fogliata A, Garcia R, Knoos T, Nicolini G, Clivio A, Vanetti E, Khamphan C and Cozzi L 2012 Definition of parameters for quality assurance offlattening filter free (FFF) photon beams in radiation therapy *Med. Phys.* **39** 6455-64

Fogliata A, Fleckenstein J, Schneider F, Pachoud M and Ghandour S 2015 Flattening filter free beams from TrueBeam and Versa HD units: Evaluation of the parameters for quality assurance *Med. Phys.* **43** 205-12

Followill D S, Taior R C, Tello V M and Hanson W F 19998 An empirical relationship for determining photon beam quality in TG-21 from a ratio of percent depth doses *Med. Phys.* **25** 1202-05

Fu W, Dai J, Hu Y, Han D and Song Y 2004 Delivery time comparison for intensity modulated radiation therapy with/without flattening filter: a planning study *Phys. Med. Biol.* **49** 1535-1547

Georg D, Knoos T and McClean B 2011 Current status and future perspective of flattening filter free photon beams *Med. Phys.* **38** 1280-93

Gerbi B J and Khan F M 1990 Measurement of dose in the buildup region using fixed-separation plane-parallel ionization chamber *Med. Phys.* **17** 17-26

Gerig L, Soubra M and Salhani D 1994 Beam characteristics of the Therapax DXT300 orthovoltage therapy unit *Phys. Med. Biol.* **39** 1377-92

Greene D and Williams P C 1997 Linear Accelerators for Radiation Therapy, Institute of Physics Publishing Bristol

Gupta T and Anand N C 2012 Image-guided radiation therapy: Physician's perspectives. *J. Med. Phy.* **37** 174-82

Hounsell A R and Wilkinson J M 1999 Electron contamination and build-up doses in conformal radiotherapy fields *Phys. Med. Biol.* **44** 43-55

Halbleib J 1988 Structure and Operation of the ITS code system in Monte Carlo Transport of Electrons and Photons edited by Jenkins TM, NelsonW R and Rindi A, Nahum A E and Rogers D W O Plenum Press, New York, 249-262

Hrbacek J, Lang S, and Klöck S 2011 Commissioning of photon beams of a flattening filter-free linear accelerator and the accuracy of beam modeling using an anisotropic analytical algorithm *Int. J. Radiat. Oncol. Biol. Phys.* **80** 1228–1237

Huang Y, Siochi A and John E B 2012 Dosimetric properties of a beam quality-matched 6 MV unflattened photon beam *J. Appl. Clin. Med. Phys.* **13** 71-81

Huen A, Findley D O and Skov D D 1979 Attenuation in Lipowitz's Metal of Xrays Produced at 2,4, 10 and 18 MV and Gamma Rays from Cobalt-60 *Med. Phys.* **6** 147- 148

IAEA Safety Report Series No. 47 2006 Radiation Protection in the Design of Radiotherapy Facilities. ISBN- 92: 0-100505-9.

IEC 60601-2-1 1998 MEDICAL ELECTRICAL EQUIPMENT - Part 2-1: Particular requirements for the safety of electron accelerators in the range 1 MeV to 50 MeV. International Electrotechnical Commission (IEC): CEI / IEC 60601-2-1.

IEC 60601-2-1 2010 (3rd edition) MEDICAL ELECTRICAL EQUIPMENT - Part 2-1: Particular requirements for the safety of electron accelerators in the range 1 MeV to 50MeV International Electrotechnical Commission (IEC): CEI / IEC 60601-2-1

IEC60976 2008 MEDICAL ELECTRICAL EQUIPMENT –Medical electron accelerators – Functional performance characteristics

IPEM Report No. 75 1997 The Design of Radiotherapy Treatment Room Facilities, Institute of Physics And Engineering in Medicine, York

Ishmael P E, Shvydka D, Pearson D, Gopalakrishnan M, Feldmeier J J 2008 Surface and build-up region dose analysis for clinical radiotherapy photon beams *Appl. Radiat. Isot.* **66** 1438-42

Izewska J 1993 Shaping of photon beams from electron linear accelerators in radiation therapy *Med. Phys.* **20** 171-7

Jackson S M 1970 The clinical application of electron beam therapy with energies up to 10 MeV *Br. J. Radiol.* **43** 431-44

Jackson S P and Bartek J 2009 The DNA-damage response in human biology and disease. *Nature* **461** 1071-1078

Javedan K, Feygelman V, Zhang R R, Moros E G, Correa C R, Trotti A, Li W and Zhang G G 2014 Monte Carlo comparison of superficial dose between flattening filter free and flattened beams *Phys. Med.* **30** 503-508

Jeraj R, Mackie T R, Balog J, Olivera G, Pearson D, Kapatoes J, Ruchala K and Reckwerdt P 2004 Radiation characteristics of helical tomotherapy *Med. Phys.* **31** 396-404

Johns H E and Cunningham J R 1983 *The Physics of Radiology,* 4th ed. (Thomas C C Publisher Ltd. Springfield IL)

Julia J, Kragl G and Dietmar G 2014 Impact of a flattening filter free linear accelerator on structural shielding design *Z. Med. Phys.* **24** 38-48

Kase K R and Svensson G K 1986 Head Scatter Data for Several Linear Accelerators 4-18 MV *Med. Phys.* **13** 530-532

Karlsson M, Svensson H, Nyström H and Stenberg J 1988 The 50 MeV Racetrack accelerator :A new approach to beam shaping and modulation. Proc. Symp. On Dosimetry in Radiotherapy (Vienna, 1988)(IAEA-SM-298/68)(Vienna: IAEA)vol. 2 307-20

Karzmark C J 1987 Total Skin Electron Therapy: Technique and Dosimetry AAPM Report No. 23 Published by the American Institute of Physics, Inc. New York

Kawrakow I, Mainegra-Hing E, Rogers DW O, Tessier F and Walters BR B 2010 The EGSnrc Code System: Monte Carlo simulation of electron and photon transport. NRCC Report PIRS–701. Ottawa, ON: National Research Council of Canada. Available from: http://www.irs.inms.nrc.ca/EGSnrc/pirs701.pdf

Keall P J, Siebers J V, Arnfield M, Kim J O and Mohan R 2001 Monte Carlo dose calculations for dynamic IMRT treatments *Phys. Med. Biol.* **46** 929-41

Khan F M 2010 *The Physics of Radiation Therapy*, 4th ed. (Lippincott Williams & Wilkins, Baltimore MD)

Klein E E, Esthappan J and Li Z 2003 Surface and buildup dose characteristics for 6, 10, and 18 MV photons from an Elekta Precise linear accelerator *J. Appl. Clin. Med. Phys.* **4** 1-7

Kim S, Liu C R, Zhu T C and Palta J R 1998 Photon beam skin dose analyses for differentclinical setups *Med. Phys.* **25** 860-66

Kinsaran A, El-Gizawy A, Banoqitah E and Xuewei M 2016 Review of Leakage from a Linear Accelerator and Its Side Effects on Cancer Patients *J Nucl Med Radiat Ther* , **7:3** DOI: 10.4172/2155-9619.1000288

Knöös T and McClean B 2007 Dose calculations for external photon and electron beam therapy 9th Biennial ESTRO meeting. Barcelona, Spain

Kragl G, Wetterstedt S, Knausl B, Lind M and McCavana P 2009 Dosimetric characteristics of 6 and 10 MV unflattened photon beams *Radiother. Oncol.* **93** 141-6

Kragl G, Baier F, Lutz S, Albrich D, Dalaryd M, Kroupa B, Wiezorek T, Knöös T and Georg D 2011 Flattening filter free beams in SBRT and IMRT: dosimetric assessment of peripheral doses *Z. Med. Phys.* **21** 91-101

Kry S F, Titt U, Pönisch F, Vassiliev O N, Salehpour M, Gillin M and Mohan R 2007 Reduced Neutron Production Through Use of a Flattening-Filter-Free Accelerator *Int. J. Radiat. Oncol. Biol. Phys.* **68** 1260-1264

Kry S F, Howell R M, Polf J, Mohan R and Vassiliev O N 2009 Treatment vault shielding for a flattening filter‑free medical linear accelerator *Phys. Med. Biol.* **54** 1265‑73

Kry S F, Smith S A, Weathers R and Stovall M 2012 Skin dose during radiotherapy: a summary and general estimation technique J. *Appl. Clin. Med. Phys.* **13** 20-34

Kushwaha H S and Srinivasan P 2009 Applications of Monte Carlo Methods in Nuclear Science and Engineering ISBN: 978-81-8372-047-2

Lamb A, Blake S 1998 Investigation and modelling of the surface dose from linear Accelerator produced 6 and 10MV photon beams *Phys. Med. Biol.* **43** 1133-1146

Li Allen X, Lijun Ma, Shahid Naqvi, Rompin Shih and Cedric Yu Monte Carlo dose verification for intensity-modulated arc therapy *Phys. Med. Biol.* **46** 2269-2282

Lind M, Knoos T, Ceberg C, Wieslander E, McClean B, and D. Georg 2009 Photon beam characteristics at the Monitor chamber level in a flattening filter free linac: A Monte Carlo study *Radiother. Oncol.* **92** S57

Livingston M S and Blewett John P 1962 Particle Accelerators- McGraw Hill Publishers

Ma C M and Rogers D W O 2004 BEAMDP as a General-Purpose Utility. NRC Rep. 2004; PIRS 509e Rev A.

Mackie T R1990 Applications of the Monte Carlo Method in Radiotherapy Vol. III of Dosimetry of Ionizing Radiation edited Kase K, Bjarngard B E and. AttixF H (Academic Press, New York) 541-620

Mackie T R, Holmes T, Swerdloff S, Reckwerdt P, Deasy J O, Yang J, Paliwal B and Kinsella T 1993 Tomotherapy: a new concept for the delivery of dynamic conformal radiotherapy *Med. Phys.* **20** 1709-19

Mellenberg D E 1990 Determination of build-up region over response corrections for a Markus type chamber *Med. Phys.* **17** 1041-4

Metropolis N 1987 The beginning of the Monte Carlo method, Los Alamos Science (1987 Special Issue dedicated to Stanislaw Ulam) 125-130

Mohan R 1997 Why Monte Carlo? XII Int. Conf. on the Use of Computers in RadiationTherapy (Salt Lake City, Utah, May 1997) 16-18

Morgan G, Ward R and Barton M 2004 The contribution of cytotoxic chemotherapy to 5-year survival in adult malignancies *Clin. Onc.* **16** 549-60

Mukesh N. M, Srimanta P, Ranjith C P, Saravana K G and Rishabh D 2016 Dosimetric properties of equivalent-quality flattening filter-free (FFF) and flattened photon beams of Versa HD linear accelerator *J. Appl. Cli. Med. Phys.* **17** 358-370

NCRP Report No. 151 2005 Structural shielding design and evaluation for megavoltage X-ray and gamma-ray radiotherapy facilities. National Council on Radiation Protection and Measurements (NCRP) ISBN-13: 978-0-929600-87-1

Nelson W R and LaRiviere P D 1984 Primary and Leakage Radiation Calculations at 6, 10, and 25 MeV *Health Phys.* **47** 811-818

Nelson W R, Hirayama H and RogersD W O 1985The EGS4 Code System, Report SLAC–265, Stanford Linear Accelerator Center, Stanford, California

Nilsson B and Sorcini B 1989 Surface dose measurements in clinical photon beams *Acta. Oncol.* **28** 537‑42

Nilsson B and Brahme A 1986 Electron contamination from photon beam collimators *Radiother. Oncol.* **5** 235-244

O'Brien P F, Gillies B A, Schwartz M, Young C and Davey P 1991 Radiosurgery with unflattened 6-MV photon beams *Med. Phys.* **18** 519 -21

Papoulis A and Pillai SU 1965 Probability Theory, Random Variables and Stochastic Processes 4th Edition (Publisher: Mcgraw Higher Ed)

Ponisch F, Titt U, Vassiliev O N, Kry S F and Mohan R 2006 Properties of unflattened photon beams shaped by a multileaf collimator *Med. Phys.* **33** 1738-46

Petti P L, Goodman M S, Gabriel T A and Mohan R 1983 Investigation of buildup dose from electron contamination of clinical photon beams *Med. Phys.* **10** 18-24

Podgorsak E B, Metcalfe P and VAN DYK J 1999 Medical accelerators ‑ The Modern Technology in Radiation Oncology: A Compendium for Medical Physicists and Radiation Oncologists (VAN DYK, J., Ed.), Medical Physics Publishing, Madison, WI   349–435

Podgorsak E B 2005 *Radiation Oncology Physics: A Handbook for Teachers and Students* International Atomic Energy Agency, Vienna

Rath G K 2002 Radiation Therapy in the Management of Cancer, Fifty years of Cancer Control in India – National Cancer Control Programme DGHS, MH&FW, Government of India

Ravindra S, Gourav G, Ganesh P and Senthil K 2016 Commissioning of TrueBeamTM Medical Linear Accelerator: Quantitative and Qualitative Dosimetric Analysis and   Comparison of Flattening Filter (FF) and Flattening Filter Free (FFF) Beam *Int. J. Med.   Phys. Clin. Eng. and Rad. Onco.* **5** 51-69

Rawlinson J A and Johns H E 1977 Letter Concerning Treatment Machine Leakage *Med. Phys.* **4** 456-457

Reco C and Clifton Ling C 2008 Broadening the scope of image-guided radiotherapy (IGRT). *Acta Oncol.* **47** 1193-200

Ringborg U, Bergqvist D, Brorsson B, Cavallin-Ståhl E, Ceberg J 2003 The Swedish Council on Technology Assessment in Health Care: systematic overview of radiotherapy   for cancer including a prospective survey of radiotherapy practice in Sweden 2001-summary and conclusions *Acta. Oncol.* **42** 357-365

Rogers D W O, Walters B, Kawrakow I 2016 BEAMnrc users manual. PIRS 509(A)rev ; Ottawa, ON: National Research Council of Canada: 2016

Rogers DWO 2006 Fifty years of Monte Carlo simulations in medical physics *Phys. Med. Biol.*   **51** 287-301

Rogers D W O *2002* Monte Carlo techniques in radiotherapy Phys**.** *Canada* **58** 63-70

Rogers DWO, Kawrakow I, Seuntjens JP, Walters BRB and Mainegra-Hing E 2010 NRC User Codes for EGSnrc. NRCC Report PIRS-702 (revB). Ottawa, ON: National Research Council of Canada. Available from: http://www.irs.inms.nrc.ca/EGSnrc/pirs702.pdf

Rogers D W O and Bielajew A F 1990 Monte Carlo techniques of electron and photon transport for radiation dosimetry in *The Dosimetry of Ionizing Radiation* Vol III edited by Kase K R, Bjarngard B E and Attix F H San Diego, CA: Academic Press 427-539

Rogers D W O 1984 Low energy electron transport with EGS*Nucl. Inst. Meth.***227**535-48

Rogers D W O and Bielajew A F 1986 Differences in Electron Depth Dose Curves Calculated with EGS and ETRAN and Improved Energy Range Relationships *Med. Phys.***13** 687-94

Sahani G, Sharma S D, Dash Sharma P K, Deshpande D D, Negi P S, Sathianarayanan V K and Rath G K 2014 Acceptance criteria for flattening filter-free photon beams from standard medical electron accelerator: AERB task group recommendation *J. Med. Phys.***4**206-11

Seltzer SM 1988 An Overview of ETRAN Monte Carlo Methods in Monte Carlo Transport of Electrons and Photons edited by Jenkins TM, NelsonWR andRindi A Ettore Majorana International Science Series, vol38. Springer, Boston, MA

Stephen F K, Rebecca M H, Jerimy P, Radhe M and Vassiliev O N 2009 Treatment vault shielding for a flattening filter-free medical linear accelerator *Phys. Med. Biol.* **54** 1265-73

Sheikh-Bagheri D, Rogers D W O, Ross C K and Seuntjens J P 2000 Comparison of measured and Monte Carlo-calculated dose distributions from the NRC linac *Med. Phys.***27** 2256-66

Sipila P 1994 Quality assurance of treatment planning systems: Radiation Dose in Radiotherapy from Prescription to Delivery IAEA-TECDOC-734, IAEA, Vienna 341-34

Sigamani A, Nambiraj A, Yadav G, Giribabu A,Srinivasan K, Gurusamy V, Kothanda R, Kaviarasu K, Rajesh T 2016 Surface dose measurements andcomparison of unflattened and flattened photon beams *J. Med. Phys.* **41** 85-91

Sigamani A and Nambiraj A 2017 Comparision of surface dose delivered by 7 MV-unflattened and 6 MV-flattened photon beams Reports of practical *Oncology and Radiotherapy* **22** 243-250

Stathakis S, Esquivel C, Gutierrez A, Buckey C R, and Papanikolaou N 2009 Treatment planning and delivery of IMRT using 6 and 18 MV photon beams without flattening filter *Appl. Radiat. Isot.* **67** 1629-37

Subhalaxmi M, Dixit P K, Selvam T P, Yavalkar S S, Deshpande D D 2018 Monte Carlo investigation of photon beam characteristics and itsvariation with incident electron beam parameters for indigenous medicallinear accelerator *J. Med. Phys.* **43** 1-8

Svensson H 1984 1st international symposium on quality assurance in radiation therapy. Int. *J. Radiat. Oncol. Biol. Phys.* **10** 59-65

Taumann L 1981 The Treatment Head Design for Medical Linear Accelerators, IEEE Trans *Nuc. Sci.* **28** 1893-1898

Teh B S, Woo S Y and Butler E B 1999 Intensity Modulated Radiation Therapy (IMRT): A New Promising Technology in Radiation Oncology *The Oncologist* **4** 433-42

Titt U, Vassilliev O N, Ponisch F, Dong L, Liu H and Mohan R 2006 A flattening filter free photon treatment concept evaluation with Monte Carlo *Med. Phys.***33** 1595-602

Tyner E, McClean B, McCavana P, and af Wetterstedt S 2009 Experimental investigation of the response of an a-Si EPID to an unflattened photon beam from an Elekta Precise linear accelerator *Med. Phys.***36** 1318-29

Ugur A, Nazmiye D K, Canan K and Hatice B 2016 Surface and Buildup Region Dose Measurements with Markus Parallel-Plate Ionization Chamber, GafChromic EBT3 Film, and MOSFET Detector for High-Energy Photon Beams *Advances in High Energy Physics* 1-10

Vassiliev O N, Titt U, Ponisch F, Kry S F, Mohan R and Gillin M T 2006a Dosimetric properties of photon beams from a flattening filter free clinical accelerator *Phys. Med. Biol.* **51**1907-17

Vassiliev O N, Titt U, Kry S F, Ponisch F, Gillin M T and Mohan R 2006b Monte Carlo study of photon fields from a flattening filter free clinical accelerator *Med. Phys.***33** 820-7

Velkley D E, Manson D J, Purdy J A and Oliver G D 1975 Build-up region of megavoltage photon radiation sources *Med. Phys.***2**14-9

Van der Laarse R, Bminvis I A D and FaridNooman M 1988 Wall Scattering Effects in Electron Beam Collimation *Acta. Radiol. Onco1.* **18** 113-124

Walters B, Kawrakow I and Rogers D W O 2016 DOSXYZnrc Users Manual, Ionizing Radiation Standards National Research Council of Canada.

Walters B R B, Kawrakow I and Rogers DWO 2002 History by history statistical estimators in the BEAM code system *Med. Phys.* **29** 2745-52

Wang Y, Mohammad K K, Joseph Y T and Stephen B E 2012 Surface Dose Investigation of the Flattening Filter-Free Photon Beams *Int. J. Rda. Oncol. Biol. Phy.* **83** 281-285

Webb S 2003 The physical basis of IMRT and inverse planning *Br. J. Radiol.* **76** 678-89

Wilson RR 1952 Monte Carlo of shower production *Phys. Rev.* **86** 261-9

Xiao Y, Kry S, Popple R, Yorke E, Papanikolaou N, Stathakis S, Xia P, Huq S, Bayouth J, Galvin J, Yin F F 2015 Flattening filter-free accelerators: a report from the AAPM Therapy Emerging Technology Assessment Work Group *J. Appl. Clin. Med. Phy.* **16** 12-39

Zanini A, Durisi E, Fasolo F, Ongaro C, Visca L, Nastasi U, Burn K W, Scielzo G, Adler J O, Annand J R and Rosner G 2004 Monte Carlo simulation of the photoneutron field in linac radiotherapy treatments with different collimation systems *Phys. Med. Biol.* **49** 571-82

Zhu T C and Bjärngard B E 1994 The head-scatter factor for small field sizes *Med. Phys.* **21** 65-68

Zhu T C and Bjarngard B E 1995 The fraction of photons undergoing head scatter in X-ray beams *Phys. Med. Biol.* **40** 1127-34

Structural Shielding Design of a 6 MV Flattening Filter Free Linear Accelerator: Indian Scenario

Bibekananda Mishra, T. Palani Selvam[1], P. K. Dash Sharma

Radiological Safety Division, Atomic Energy Regulatory Board, Niyamak Bhavan, [1]Radiological Physics and Advisory Division, Health Safety and Environmental Group, Bhabha Atomic Research Centre, Mumbai, Maharashtra, India

Abstract

Detailed structural shielding of primary and secondary barriers for a 6 MV medical linear accelerator (LINAC) operated with flattening filter (FF) and flattening filter free (FFF) modes are calculated. The calculations have been carried out by two methods, one using the approach given in National Council on Radiation Protection (NCRP) Report No. 151 and the other based on the monitor units (MUs) delivered in clinical practice. Radiation survey of the installations was also carried out. NCRP approach suggests that the primary and secondary barrier thicknesses are higher by 24% and 26%. respectively, for a LINAC operated in FF mode to that of a LINAC operated in both FF and FFF modes with an assumption that only 20% of the workload is shared in FFF mode. Primary and secondary barrier thicknesses calculated from MUs delivered on clinical practice method also show the same trend and are higher by 20% and 19%, respectively, for a LINAC operated in FF mode to that of a LINAC operated in both FF and FFF modes. Overall, the barrier thickness for a LINAC operated in FF mode is higher about 20% to that of a LINAC operated in both FF and FFF modes.

Keywords: Flattening filter, flattening filter free, medical linear accelerator, monitor units, primary barrier, secondary barrier

INTRODUCTION

Standard medical linear accelerators (LINACs) used in radiotherapy are equipped with a flattening filter (FF). The FF is designed to produce uniform dose distribution across the field in a homogeneous medium. Recently, there has been an increasing interest in operating medical LINAC without FF. A FF free (FFF) LINAC is basically a standard LINAC with the FF removed from the beam line. The main advantages of removing the FF are increased dose rate in addition to reduced scatter and leakage radiation inside and outside the target volume.[1-5] These benefits result from removal of attenuation of the primary beam, reduction of the scatter radiation originating from the FF, and reduction of leakage radiation due to decrease in beam energy. Reduction of the head scatter also improves dosimetry of the FFF beams due to reduction of output variation with field size and field size-dependent parameters.[6-8] FFF LINAC has been investigated in detail and is used in radiotherapy treatments including advanced modalities such as intensity-modulated radiation therapy treatments and stereotactic radiosurgery.[9-13] As expected, there are differences in the beam characteristics of LINAC operated in FFF mode to

that of LINAC with the FF mode. FFF LINAC beam is softer, for example, the central axis percent depth dose in water for a 6 MV FFF beam resembles a 4 MV FF beam.[14] In addition, the lateral dose profile is peaked on the central axis, and less integral target current is required to generate the same dose to the tumor.[15,16] As a result, the shielding parameters, such as the tenth-value layers (TVLs) and scatter fractions, calculated for flattened beams, may not be appropriate for shielding evaluations for unflattened beams.[17-19] Since FFF beam is used for advanced modalities requiring higher monitor units (MUs) to be delivered, it must be determined whether shielding needs to be enhanced or reduced to use an FFF machine in comparison to vault of FF machine.

Considering the LINACs with FFF beam available in India and their growth, this study was carried out to find the impact

Address for correspondence: Mr. Bibekananda Mishra,
Radiological Safety Division, Atomic Energy Regulatory Board,
Mumbai - 400 094, Maharashtra, India.
E-mail: m.bibek@gmail.com

Comparison of measured and Monte Carlo calculated dose distributions from indigenously developed 6 MV flattening filter free medical linear accelerator

Bibekananda Mishra[1], Subhalaxmi Mishra[2], T Palani Selvam[2], ST Chavan[3], SN Pethe[3],
[1] Radiological Safety Division, Atomic Energy Regulatory Board; Homi Bhabha National Institute, Mumbai, Maharashtra, India
[2] Homi Bhabha National Institute; Radiological Physics and Advisory Division, Health, Safety and Environment Group, Bhabha Atomic Research Centre, Mumbai, Maharashtra, India
[3] Medical Electronics Division-1, Society for Applied Microwave Electronics Engineering and Research, Mumbai, Maharashtra, India

Correspondence Address:
Mr. Bibekananda Mishra
Radiological Safety Division, Atomic Energy Regulatory Board, Mumbai - 400 094, Maharashtra
India

Abstract

Purpose: Monte Carlo simulation was carried out for a 6 MV flattening filter-free (FFF) indigenously developed linear accelerator (linac) using the BEAMnrc user-code of the EGSnrc code system. The model was benchmarked against the measurements. A Gaussian distributed electron beam of kinetic energy 6.2 MeV with full-width half maximum of 1 mm was used in this study. **Methods:** The simulation of indigenously developed linac unit has been carried out by using the Monte Carlo-based BEAMnrc user-code of the EGSnrc code system. Using the simulated model, depth and lateral dose profiles were studied using the DOSXYZnrc user-code. The calculated dose data were compared against the measurements using an RFA dosimertic system made by PTW, Germany (water tank MP3-M and 0.125 cm^3 ion chamber). **Results:** The BEAMDP code was used to analyze photon fluence spectra, mean energy distribution, and electron contamination fluence spectra. Percentage depth dose (PDD) and beam profiles (along both X and Y directions) were calculated for the field sizes 5 cm × 5 cm - 25 cm × 25 cm. The dose difference between the calculated and measured PDD and profile values were under 1%, except for the penumbra region where the maximum deviation was found to be around 3%. **Conclusions:** A Monte Carlo model of indigenous FFF linac (6 MV) has been developed and benchmarked against the measured data.

Full Text

Introduction

Conventional medical linear accelerators (linac) are equipped with a flattening filter (FF) which is primarily designed to produce a flat beam profile at a given depth by compensating for the nonuniformity of photon fluence across the field. However, FF decreases the output considerably and produces quality changes within the primary beam by scattering and absorption of primary photons.[1] The requirement to have a flattened beam profile for treatment delivery is not necessary when a certain type of advanced modality treatments such as intensity-modulated radiation therapy (IMRT) or intensity-modulated arc therapies is used. In IMRT, the patient dose distribution can instead be shaped by the multileaf collimator (MLC) to create the desired clinical effect. In principle, the FF can be removed, and the leaf sequences can be adjusted accordingly to produce fluence distributions similar to those of a beam with an FF. The removal of FF with its associated attenuation from X-ray beam path increases dose rate.[2] The other possible effect is substantial reduction in head scatter, as the FF is the major source of scattered photons. FF-free (FFF) beams in radiotherapy thus have the advantage of shorter treatment delivery time and lower out-of-field dose compared to conventional flattened beams.[3] For small field sizes, unflattened fields have dose profiles similar to those of a flattened beam. This, along with the higher dose rate in FFF mode, will increase the efficiency when delivering stereotactic radiosurgery.[4],[5],[6] For larger clinical targets, the desired photon fluence could be modulated using the MLC and movable jaws allowing FFF beams to be a useful approach for the delivery of radiotherapy treatments.[7],[8],[9],[10],[11] Further, the vault design for FFF linac has shown lesser shielding requirements in comparison to FF linac.[12]

SAMEER (Society for Applied Microwave Electronics Engineering and Research), Mumbai, India has developed an indigenous linac unit named as "SIDDHARTH" which is capable of delivering cost-effective radiotherapy treatment in India. Presently, the linac unit is being used clinically at various hospitals in India in FF mode with photons of energies 4 and 6 MV. Recently, Subhalaxmi et al. have reported the dosimetric characteristics of this unit using Monte Carlo method as well as by measurement.[13] However, due to the increase in interest of operating the linac in FFF mode, the feasibility study has been carried out for the same unit in FFF mode. The objective of this study is to evaluate the dosimetric characteristics of indigenously developed linac in FFF mode using Monte Carlo method and verify the results with the measured data. It may be noted that the measured data were generated in linac service mode to find the feasibility for clinical use of this linac in FFF mode.

Monte Carlo method has become a powerful tool in radiotherapy dose calculations, and many studies have been performed using this method for studying beam characteristics of linac.[14],[15],[16],[17],[18] Several Monte Carlo studies of FFF treatment machines have been published.[19],[20],[21],[22],[23] In this study, Monte Carlo simulation of indigenously developed linac unit of photon energy 6 MV in FFF mode was carried out, and the data were verified with measurement for its clinical use. For this purpose, the user-codes BEAMnrc [24] DOSXYZnrc [25] of the EGSnrc code system [26] were used to study its dosimetric characteristics. The calculated dose data were then compared with the measured data. The BEAMDP [27] (BEAM Data Processor) user-code of the EGSnrc code system was used to analyze the phase-space files and to extract the spectra of particles such as photons and electrons reaching the plane at the source to surface distance (SSD) of 100 cm. This study reports the percentage depth dose (PDD), TPR 20/10, beam profiles, surface dose, build-up dose, mean energy, photon fluence, and contaminant electron fluence spectra for the 6 MV FFF beam.

Materials and Methods

Monte Carlo simulation

Simulation of medical linear accelerator using BEAMnrc code

The geometry of indigenously developed linac was simulated using the BEAMnrc [24] user-code of EGSnrc [26] code system based on the detailed design specification provided by the vendor. Different components of the linac head such as target, primary collimator, monitor chamber, and secondary collimator were accurately modeled. [Figure 1] shows the linac modeled in the present study. In this simulation, Z-axis is taken along the beam axis, and the origin is taken at the front face of the target.{Figure 1}

1
2

Beam characteristics analysis of unflattened X-Rays from standard Medical Linear Accelerator: A comparison of protocols

3
4

Bibekananda Mishra[1,4], S D Sharma[2,4], A. Dinesh[3], T. Palani Selvam[2,4], A Pichandi[3]

[1]Radiological Safety Division, Atomic Energy Regulatory Board, Mumbai, India

[2]Radiological Physics and Advisory Division, Bhabha Atomic Research Centre, Mumbai, India.

[3]Health care Global enterprise, Bangalore, India.

[4]Homi Bhabha National Institute, Training School Complex, Anushaktinagar, Mumbai, India

5
6
7
8
9

Abstract

10

The dosimetric parameters of Medical electron Linear Accelerator (Linac) generated flattening filter free (FFF) photon beams differ from the flattened beams. FFF beams are not standard in terms of the parameters describing the beam characteristics. Hence, it is not possible to use the parameters in the same way as they are commonly used for established flattened beams. Several investigators had proposed new parameters for FFF beam description. The purpose of the present work was to study the dosimertic characteristics of the FFF beams generated by the commercially available Linacs of two manufacturers (Edge of Varian Medical System and Versa HD of Elekta Medical System) as per the recommendations of AERB Task Group and the results were compared with the published data. It is observed that $TPR2_{0,10}$ and PDD varies significantly attributing to the technology adopted to generate the beam. Due to this variation in energy, surface dose shows larger deviation. The beam profile analysis indicates that the renormalization factors are machine dependent and needs to be evaluated for the given model of Linac.

11
12
13
14
15
16
17
18
19
20
21
22

23
24

1

Shielding consideration of Flattening Filter Free Medical Accelerators

Bibekananda Mishra[1], T. Palani Selvam[2], P.K. Dash Sharma[1]
[1]Radiological Safety Division, Atomic Energy Regulatory Board-400 094
[2]Radiological Physics & Advisory Division, Bhabha Atomic Research Centre, Mumbai- 00094
e-mail: m.bibek@gmail.com

Aim: Recently several accelerator manufacturer have introduced Flattening Filter Free beam (FFF) Medical Accelerators (linac). These linacs are used in cancer treatment at various radiotherapy centers. The beam energy produced from these linacs are 6 MV and 10 MV. The aim of this study is to calculate the primary wall shielding requirement for a 6MV FFF beam accelerator as per NCRP report 151.

Materials and Methods: The significant difference between the FFF and Flatten Beam (FB) is higher dose rate varying in the range of 1400 to 2400 MU per minute. Reduced head scatter due to removal of the flattening filter from the beam path have also been reported by various investigators. Standard convension used for the linac bunker are primary wall where dircetly the beam is facing to the wall, secondary wall where the scatter and leakage radiation are the contributers. As per the stipulations of NCRP-151[1], in order to calculate the wall thickness, it is necessary to estimate the workload (W). W is defined asfollows;

W= {Dose (in cGy) delivered per patient x number of patients x number of days per week}/PDD(10). Radiation level at any point outside the buner wall is calculated using reduction factor which is as follows;

$$RF = \frac{WUT}{Pd^2}$$

where

P   is the permissible/ allowed dose limit per week outside the barrier (cSv. Week-1)
W   is the workload in cGy.week-1 at 1m
U   is the use factor or fraction of time that the beam is likely to be incident on the barrier; or the fraction of time that the area outside the barrier is likely to be occupied
d   is the distance from the source to the outside of the barrier in 'm'

The thickness of the barrier can then be determined using tenth value layers (TVLs) based on energy of the X-ray of the treatment unit and the type of material.

The number (n) of TVLs required is given by n = no. of TVLs = log(RF) . In this study we used the published values of TVL[2] for FFF beam energy. The percentage depth dose at 10 cm depth was refered from the litereture qutaed value which is 63.4%[3]. Number patients treated in a FFF enabled linac were considered from the technique used to deliver the radiation dose in FFF mode. They are mainly IMRT, SRS, SRT and Modulated Arc therapy. These data were collected from various radiotherapy ceneter located in India. For primary barriers, the values of U and T are 0.25 and 1respectively. Concreate is the shielding material considered having density 2.35g/cm^{3}.

Flattening Filter Free beam acceptance study of high energy X-Ray beam generated from Medical Linear Accelerator using AERB protocol.

Bibekananda Mishra

Radiological Safety Division, Atomic Energy Regulatory Board-400 094
Mumbai, India - 400 094
e-mail: m.bibek@gmail.com

Aim: Flattening Filter Free beam (FFF) generated from commercial Medical Accelerators are in clinical use at various radiotherapy facilities. Currently, there are two manufacturer namely Varian Medical System and Elekta Ltd. are manufacturing 6 MV and 10 MV FFF X-Ray beams with dose rate varying in the range of 1400 to 2400 MU per minute. The aim of this study is to analyse the beam profiles and other parameters of Varian TrueBeam SVC with FFF and Elekta Versa HD accelerators as per the recommendation of Task Group (TG) constituted by Atomic Energy Regulatory Board (AERB), Mumbai.

Materials and Methods: AERB TG recommends measuring beam quality, Off Axis Ratio, Depth of dose maximum, percentage depth dose at 10 cm, Symmetry, lateral separation between inflection points at 90%, 75% and 60% dose levels, field size and penumbra for a 20 x 20 cm^2 field size and values are compared to their baseline results. In this study, some measurements were also carriedout for 10x10 cm^2 field size. The above said parameteres were generated using PTW MP3 Radiation Field Analyser (RFA) and 0.125 cm³ ionization chamber (PTW make Semiflex). The measurements were performed with 2 mm resolution for both PDD and beam profiles. PTW software MEPHYSTO mcc (Version 3.3) was used to calculate the dosimetric parameters. The profiles were ploted in a graph sheet and infletion points were identifies. Accordingly, Relative Dose Value (RDV) was ploted. Then the field size and penumbra ware estimated using the protocol.

Results and Discussion:
Values determined from the measurements are tabulated in Table-1. It is observed that the TrueBeam SVC produces lower energy, lower d_{max}, lower PDD, higher surface dose difference in comparison to Versa HD. Lateral separation at dose value of 90%, 75% and 60% shows more deviation in 6MV energy range of Versa HD in comparision to TrueBeam SVC and comparable results were observed in 10MV. Penumbra values are more in TrueBeam SVC than in Versa HD.

Conclusions:
From this study it is observed that due to different engineering difference in the manufactured models variation in different parameters is large. However, these values are well within the stipulated tolerance limit with respect to their baseline values.

Reference:
Sahani G, Sharma SD, Dash Sharma PK et al. Acceptance criteria for flattening filter-free photon beams from standard medical electron accelerator: AERB task group recommendation. J. Med. Phys.2014;39:206-11.

Measurement and analysis of surface dose for flattening filter free medical accelerator using advanced markus chamber.

Bibekananda Mishra[1] **,** A. Pichandi [2], S. D. Sharma[3,4],T. Palani Selvam[3,4], P.K. Dash Sharma[1]

[1]Radiological Safety Division, Atomic Energy Regulatory Board-400 094

[2]Health Care Global Enterprises, Bangalore

[3]Radiological Physics & Advisory DivisionBhabha Atomic Research Centre, Mumbai - 400 094

[4]Homibhabha National Institute, Anushaktinagar, Mumbai-400 094 e-mail: m.bibek@gmail.com

Introduction: Surface dose plays significant role in radiotherapy. Doses received by the basal skin layer can result skin erythema, epilation, necrosis etc depending on the magnitude of doses received.[1] Hence, accurate measurement of dose at the surface is essential for treatment of patients. Surface dose is machine dependent and can be affected by many parameters such as field size, source-to-surface distance (SSD), beam energy, type of dosimeter used for its measurement etc.[2]

Purpose: Recently, flattening filter-free (FFF) medical linear accelerator (linac) has been introduced. With the filter removed, this low-energy component is allowed to pass through to the patient and increases the surface dose. Energy spectrum and electron contamination are the two factors, which can change the surface dose in FFF. In this study, the relative surface dose has been studied for two different linac models in FF and FFF mode for 6 MV beam energy considering the fact that 6 MV is the beam of choice for various clinical cases.

Materials and Methods: Measurements are carried out for photon beam of nominal energy 6 MV generated from Elekta- Versa HD model and Varian-TrueBeam Linac model in FF and FFF mode. The plane parallel plate chamber, PTW Germany make Advanced Markus Ionization chamber type 34045, having volume 0.02 cm3 with a thin flat window thickness of 0.03 mm mm was used.

The surface dose for any field size is defined as the dose measured at 0.5 cm depth (from the surface) for that field size divided by the dose at d_{max} at a 10×10 cm2 field size[3]. The measurements were done for field sizes of 5x5 cm^2 to 25x25 cm^2, with

increment of $5 cm^2$ with build-up depths extending from the surface to 2 mm towards the d_{max} and at d_{max}. As the window thickness of the chamber is very less in comparison to other chambers the positional accuracy is considerable. The PP chamber was placed at 0, 1 and 2 mm depth to interpolate the ionization reading at 0.5mm depth. The ionization value was also recorded for d_{max} of respective field sizes at 100 cm Source to Surface Distance (SSD).

Results and Discussion:

The relative surface dose was observed to be greater for the FFF beam as compared to the flattened beam for the photon beam energy 6 MV in case of True beam Linac. However, for Versa HD, the trend was similar up to 15x15 cm2 field size and after which the relative surface dose increases as compared to 6FFF. TrueBeam gives higher surface dose than Versa HD for all the field sizes. Table 1 and Figure 1 presents the details.

Conclusions:

FFF beam change the dosimetric characteristics of photon beam compared to FF beams, thus changing surface doses. Our study compares the surface dose for two different Linac model from two different manufacturer. It is found that the variation in surface dose in Versa HD Linac is less in comparison to TrueBeam Linac.

References:

1. Carl J. et al. Skin damage probabilities using fixation materials in high-energy photon beams. Radiothe. Oncol. 2000; 55:191-8.

2. Kry SF et al. Skin dose during radiotherapy: a summary and general estimation technique. J Appl. Clin. Med. Phys. 2012; 13(3):20-34.

3. International Electrotechnical Commission (IEC) 60601-2-1

List of Figures

List of Tables

Glossary

3D-CRT   Three-dimensional conformal radiotherapy

ADL   Absorbed dose due to leakage radiation

AERB   Atomic energy regulatory board

AFC   Automatic frequency control

BARC   Bhabha Atomic Research Center

BLD   Beam Limiting Devices

CM   Component Module

CR   Cross plane

CT   Computed tomography

CW-OSL   Continuous Wave OSL

d_{max}   Depth of maximum dose

DNA   Deoxyribo nucleic acid

EGSnrc   Electron-Gamma Shower developed by National Research Council of Canada

FF   Flattening filter

FFF   Flattening filter free

GUI   Graphical user interface

HVL   Half value layer

IAEA   International Atomic Energy Agency

IDR   Instantaneous dose rate

IEC   International Electrotechnical commission

IGRT   Image guided radiotherapy

IMAT   Intensity modulated arc therapy

IN	In plane
IP	Inflection point
IPEM	Institute of Physics and Engineering in Medicine
Linac	Medical Linear accelerator
MC	Monte Carlo
MLC	Multi leaf collimator
MU	Monitor unit
NTD	Normal Treatment Distance
OAR	Off axis ratio
ODI	Optical distance indicator
OSL	Optically stimulated luminescence
PDD	Percentage depth dose
PRESTA	Parameter reduced electron-step transport algorithm
QI	Quality index
RDV	Reference dose value
RF	Reduction factor
RNG	Random number generator
RSD	Relative surface dose
SAMEER	Society for applied microwave electronics engineering and research
SAD	Source to axis distance
SRT	Stereotactic radiotherapy
SRS	Stereotactic radio surgery
SSD	Source to surface distance
SVC	Small Vault Configuration

TBI   Total body irradiation

TG   Task Group

TPS   Treatment planning system

TRS   Technical report series

TVL   Tenth Value layer

VRT   Variance Reduction Techniques

Z   Atomic number